METHODOLOGY TO DIVERT ELECTRICAL ENERGY FROM THE EDDY

CURRENT MAGNETIC RESISTANCE DEVICE OF A HYBRID

GENERATOR USED IN FITNESS MACHINES TO A

GRID TIE INVERTER

BY

JOSEPH DOMENICK CIPOLLINA

BS, Clarkson University, 2009

THESIS

Submitted in partial fulfillment of the requirements for
the degree of Master of Science in Electrical Engineering
in the Graduate School of
Binghamton University
State University of New York
2012

Accepted in partial fulfillment of the requirements for
the degree of Master of Science in Electrical Engineering
in the Graduate School of
Binghamton University
State University of New York
2012

May 9, 2012

Professor Charles R. Westgate, Chair
Department of Electrical and Computer Engineering, Binghamton University

Professor Stephen A. Zahorian, Member
Department of Electrical and Computer Engineering, Binghamton University

Professor Alok C. Rastogi, Member
Department of Electrical and Computer Engineering, Binghamton University

ABSTRACT

A method is developed and described to effectively divert electrical energy to the grid from fitness machines using hybrid generators with eddy current magnetic resistance. The circuit developed to perform this task consists of a buck rectifier and buck converter. The circuit is cost-effective since it does not require alterations of the fitness machine's original printed circuit board and uses the original generator and battery of the machine. Hybrid generators can be found in a large range of recent self-powered fitness machines across different manufacturers and types. Simulations were run with Simulink from MathWorks and LTspiceIV to find element values suitable for experimental testing of the circuit. Testing reveals that an efficiency of 75% is achieved in DC power conversion. With the removal of the eddy current braking device, physical resistance that the user feels is reduced and allows for the user to produce energy with ease.

ACKNOWLEDGMENTS

I would like to acknowledge the support and guidance of Professor Charles Roger Westgate throughout my graduate studies. For the support of the people who I worked closely with on the Human Power Plant project. To my family who helped me aspire and friends who became like family. To my teachers and fellow students who taught me so much. Thank You.

Table of Contents

List of Figures

Chapter 1:   Introduction

The motivation for this research was to generate electricity at the State University of New York at Cortland (SUNY Cortland) by converting the kinetic energy from fitness machines into electrical energy and to use the energy savings for members of the community as noted below. SUNY Cortland looks at this option as a way to motivate students, faculty, and others to exercise and to make a contribution. The research began with a study of what was commercially available before beginning designs. It was found that the payback period for current commercial devices was too long for any investment, and improvement in the payback period would be studied.

1.1   State University of New York Collaboration

The State University of New York at Cortland was selected as the location for implementation because of their large facilities and educational focus on fitness. Their contribution includes the use of their fitness machines for implementation and the support of the students, faculty, and staff. Professor Jeff Bauer was the lead faculty member from the university.

State University of New York at Brockport also contributed with the assistance of Christopher Bauer, a computer science major. Christopher Bauer developed the software and system that would log information such as the energy contributions from each user. The user would be recognized by the use of magnetic swipe card identification such as a college ID card.

The State University of New York at Binghamton through the Electrical and Computer Engineering Department explored methods for retrofitting exercise machines already owned or that could be purchased by SUNY Cortland for use in generating energy.

The goal in this collaboration is to increase the utilization of the fitness machines by adding a competitive aspect. Fraternities, sororities, clubs and other organizations could compete in generating energy over a given period of time. In addition, for increasing utilization a projection of the project is to have a percentage of the energy go to low income housing for lighting.

1.2   Historical

The idea of using human power to practically generate electrical power can be found in patents as early as 1901. The patent, US685685, was filed in 1899 as a way to generate power for telephones using a level pulled by the user [1]. Uses of hand cranks or stationary bicycles connected to a generator are some of the early inventions. Within the last decade companies have been providing fitness centers options to convert or buy exercise machines that produce an excess of energy to offset grid usage.

1.3   Commercial Options

There are many commercially available options and ReRev, Team Dynamo, and The Green Revolution that have become well known.

1.3.1   ReRev

The company leading the development of retrofitting fitness machines to offset gym power usage is ReRev. Their product is designed specifically for fitness machines with resistive loading. Two machines that meet this requirement are Precor elliptical

machines and Woodway EcoMill treadmills [2]. The EcoMill is a rare treadmill that is self powered and does not need to be plugged into the grid [3]. The Precor elliptical machine is a stride fitness machine and can be found at almost any gym in large numbers. According to the ReRev website, their systems have been adopted in a number of major universities, including University of Florida and University of North Texas [4].

As a commercial product, a cost analysis can be done to evaluate the value of human powered devices. To perform this evaluation, assumptions are made in power output of an average person working out, utilization of the machine, cost of electricity, and cost of a given system. It is suggested that an average person during a workout could produce 100 watts on average. Information on the payback periods was given but not finally calculated. The savings produced in energy from a single machine was given to be 18 dollars annually. This was found by assuming 100 watts of power when utilizing the machine 5 hours a day, 365 days a year, and commercial energy cost at 10 cents a kilowatt-hour [5].

The ReRev system was found to have a base cost of approximately $10,000 as a result of the inverter used. The inverter is capable of use with up to 25 machines. The cost of retrofitting each machine varied, but an example was given of a 10 to 15 machine system costing 13 to 14 thousand dollars, including the inverter [2]. The most conservative cost analysis of the system per machine would occur with a system having 25 machines to fully utilize the inverter as the inverter is over 50% of the cost.

Approximating the cost of retrofitting 25 machines is achievable with the given information by taking out the cost of the inverter and finding that just retrofitting 10 to 15 machines cost 3 to 4 thousand dollars. Using the average of these two ranges gives us the

cost of just retrofitting 12.5 machines is 3,500 dollars. Given that the most conservative cost analysis of the system occurs with 25 machines, the system would cost 17,000 dollars. This approximates the cost per machine is 680 dollars.

The payback period for current systems is thus decades for costs ranging from several hundred dollars to a thousand dollars per machine. The wide range of costs and payback periods arises because costs can vary greatly with the facility and machines used in the system [5]. For the lowest cost of 680 dollars per machine, the payback period would be over 37 years.

As the equipment is not rated for a lifetime of 37 years, the investment cannot be justified by the offset power production. There are other considerations such as possible savings in HVAC or increased memberships but these are not easily estimated. The limitation of what fitness machines can be retrofitted with commercially available systems further reduces their effectiveness.

1.3.2   Human Dynamo and the Green Revolution

The companies Human Dynamo and the Green Revolution have taken a different approach by retrofitting stationary bicycles and expanding the fitness machines available for retrofitting. Although they both work with stationary bicycles, Human Dynamo choose to produce their own fitness machines to retrofit and the Green Revolution retrofit stationary bicycles from the company, Spinning [5].

Human Dynamo has focused on developing stationary bicycles to be used in producing energy and one of their first products is Team Dynamo, which includes four upright bicycles attached to the same drive shaft and generator [6]. The four bicycles

being used together can produce been 200 – 400 watts of power at a time [7].This output corresponds to 50 to 100 watts per bicycle.

1.4   SUNY Cortland System

As one of the main goals of SUNY Cortland is to increase machine utilization by retrofitting, it would be necessary to retrofit as many machines as possible. The methods to generate and dissipate energy vary with the type of fitness machines and manufacturer.

1.4.1   Fitness Machines Available

To identify the scope of research, any machines that were not self-powered were not included in the research. Table 1 lists these machines considered during research with their manufacturer, model, machine type, quantity, and physical resistance device.

Manufacturer	MFR Model	Machine Type	Quantity	Physical Resistance Device
Octane	pro3700	Elliptical	6	Hybrid
Precor	c776i	Stepper	2	Hybrid
Precor	amt100i	Adaptive Motion Trainer	4	Hybrid
Precor	efx576i	Elliptical	7	Resistor
Precor	efx576i*	Elliptical	4	Resistor
Precor	efx546	Elliptical	2	Resistor
Precor	846i	Recumbent Bike	2	Hybrid
Cybex	530r	Recumbent Bike	1	Hybrid
Cybex	530c	Upright Bike	6	Hybrid

Table 1 - Fitness Machines Considered for Retrofitting at SUNY Cortland (*Older Machine)

1.4.2   Applied Commercial Options

All options could be utilized if new machines were purchased. When retrofitting current machines from Table 1, SUNY Cortland's only option is ReRev for the elliptical machines, because Human Dynamo produces their own machines and the Green Revolution only retrofit bicycles from the company Spinning. SUNY Cortland thus would only be able to utilize 13 machines with ReRev's system as they are the only self-powered Precor elliptical machines in the facility. As described earlier in Section 1.3.1

the most efficient use of the ReRev system would use 25 machines, so purchasing more

Precor Elliptical machines would help with overall efficiency.

1.4.3   Researched Option

The fitness machines determined to be self-powered that are not covered by the

ReRev system use a hybrid generator to produce physical resistance for the user. The

hybrid generator utilizes both a generator and eddy current braking, instead of a generator

and a load resistor to produce user resistance [8].   Thus the design of another conversion

system would allow the use of 21 more fitness machines in producing energy without

purchasing new machines. The circuit and method for the researched option is further

discussed in the later sections.

1.5   Potential Energy Production

As a percentage of the energy produced is projected to be given to low income

housing for lighting it is necessary to estimate the energy production. To estimate the

energy production it is necessary to make assumptions in utilization and power output.

1.5.1   Assumptions and Calculations in Energy Production

An average person can output between 50 to 150 watts of power over an hour [5].

A conservative assumption of 50 watts should be used as a percentage of the power

generated by a user is consumed by the fitness machines and some machines have been

produced to reduce power flow though electronics but still maintain a the same physical

resistance [9]. The daily individual energy production is 250 watt hours using the same

assumption of utilization of 5 hours a day as the IEEE Spectrum Article [5]. Applying

this to the 21 fitness machines with hybrid generators gives 5.25 kWh daily. With the

same utilization, the 13 Precor Elliptical machines would produce together 6.5 kWh

daily. Both systems could potentially produce 11.75 kWh a day. Retrofitting the fitness machines with hybrid generators would potentially increase the energy production by 80% from using only the machines compatible with the ReRev system.

1.5.2   Energy Equivalence

Turning kilowatt hours into an equivalent amount of light hours requires a clarification between incandescent bulbs and compact fluorescent lights (CFLs). A 23-28 watt CFL produces the same amount of light as a 100 watt incandescent bulb [10]. This information shows that CFL would last about to 4 times as long as an incandescent bulb.

The energy output found in Section 1.5.1 of 11.75 kWh a day could illuminate a single CFL for 470 light hours. With the assumption that there are 8 lights per household on for 8 hours of the day, this energy could give light to 7 households each day.

1.5.3   Energy Credits

To deliver this energy to low income housing a system using energy credits would need to be arranged with New York State Electric and Gas (NYSEG). If the machine's output is connected to the facility it is unlikely that the power generated would turn the meter backwards as the power output of these machines is low compared to the power use of the university building. The energy would then need to be recorded at the inverter and reported on a monthly basis.

It is also possible to have the energy produced by the machines to be directly connected to the grid and bypass the facility. Yet this would likely require additional wiring and increase the cost of the overall system.

1.6   Overview

The remainder of the thesis is divided up into four chapters, where the technical review, Chapter 2, goes into technical detail on the Precor elliptical machines, used by ReRev, and the hybrid generator with data collected and analyzed during normal operation. Chapter 3, Simulation and Design, describes the simulations done on Simulink and LTSpiceIV along with the sizing of element components for circuits implemented. Implementation, Chapter 4, contains the data that was collected and initial conclusions from piecewise testing and on-site testing. Conclusions and further research, Chapter 5, describes in detail the conclusions made from the data along with suggestions for further research to improve the project.

Chapter 2:   Technical Review

While examining the machines available at SUNY Cortland it became apparent that the focus of the study should identify a new system that would be most beneficial to the University for retrofitting. The initial goals were to assess what would minimize the amount of alteration required for the original fitness machines and to determine where the reduction of alterations would be seen as a positive outcome. This study would necessarily encompass cost as the use of devices with the original machines would reduce the need for additional devices to be purchased.

2.1   Scope of Research

There were many machines at SUNY Cortland to assess in terms of retrofitting. The scope of the fitness machines were first reduced by only considering cardio machines since these machines already had generators or motors inside. Cardio machines were defined as fitness machines that are meant to increase a user's heart rate. This definition included the following types of machines: stationary bicycles, elliptical, adaptive motion trainer (AMT), stepper, arc trainer and treadmills. Some of these types have sub-categories, such as upright and recumbent stationary bicycles or standing and seated elliptical machines. When reviewing the internal devices for physical resistance of the machines, differences in sub-categories did not represent a significant change in the device characterization. For example, in an upright stationary bicycle the internal devices were similar to a recumbent stationary bicycle from the same manufacturer.

Treadmills were removed from the scope of the research as most functioned by moving a platform at a speed that the user matches. The fitness machine achieves this by taking power from the grid to power a motor and run a track. The commercial exception to this is the EcoMill that is self-powered and does not require external electrical power [3]. As the facility at SUNY Cortland did not have this machine available it was not included in the scope of research.

The four arc trainers available at SUNY Cortland are models 610A and 600A manufactured by Cybex. From an examination of both machines and reviewing material from Cybex, only models 625 or higher include a generator while others use power from the grid to produce physical resistance. All models use eddy current braking, but only the specified models include generators [11]. As Cybex arc trainer models 625 or higher do use a hybrid generator, a combination of generator and eddy current braking, it could be possible to implement the tested method. Since these machines are not available at SUNY Cortland they fall outside the scope of this thesis.

The machine types remaining in the scope at SUNY Cortland are the stationary bicycle, elliptical, AMT and stepper. Some of these types of machines at SUNY Cortland had entertainment devices, such as the Expresso stationary bicycles with an interactive monitor, which causes a larger use of energy than production by the user [12]. This net use of energy removes the Expresso stationary bicycles scope of research. The fitness machines with their manufacture, model, and type that were considered for retrofitting in this research can be found in Table 1. A rule of thumb that could be applied quickly is that if the machine requires external electrical power to operate, then it would be outside the scope of research. If a fitness facility wanted to retrofit these machines already

outside the scope of research at this time, a generator could replace the physical resistance device already installed in the machine. The original physical resistance device could be friction braking or eddy current braking powered by the grid. Yet, retrofitting these fitness machines would require more alterations and likely increase the cost per watt.

2.2   Physical Resistance Devices within the Scope of Research

As described in Section 1.3.1, the system from ReRev was only able to work with Precor elliptical machines and the EcoMill. The Precor elliptical machine, specifically EFX546, uses a generator with load resistors while other types of machines and manufactures used hybrid generators, combination generator and eddy current braking.

2.2.1   Generator with Load Resistor Concepts

The block diagram of the Precor elliptical machine, EFX546, was identified by examining the fitness machine and can be seen in Figure 1. A picture of the same fitness machine without the enclosure and with labeling is shown in Figure 2. The two load resistors are connected in parallel to have an equivalent resistance of 10 ohms. The six phase generator utilizes permanent magnet alternate current (PMAC). The cast iron disk labeled as the six phase generator has permanent magnets fastened on the inside near the armature. When the founder of the company ReRev, Hudson Harr, examined these fitness machines he designed a method that removes the load resistors and redirects the power to the grid [5]. When measuring the voltage across the load resisters it was found that the power going to the load resistors was voltage controlled.

The waveform seen from an analog oscilloscope is shown in Figure 3 and the primary attributes during different user settings is shown in Table 2. The data shown in

11

Section 2.2.2, builds on the general concept that an increase in the user input of resistance level increases the voltage across the resistor. Since the load is purely resistive, the increase in voltage would cause an increase in current following ohm's law shown below.

$$V = IR \tag{1}$$

Where V is the voltage, I is the current, and R is the resistance. This current is supplied by the PMAC generator in the Precor elliptical machine. An increase of current flowing through the generator causes an increase of torque required to keep the generator running at the same speed. The relationship between torque and current of a PMAC generator is the same as a PMAC motor, and this relationship is linear.

$$T = k_T \hat{I}_s \tag{2} [13]$$

Where T is the torque on the generator (the physical resistance felt by the user), $\hat{I}_s$ is the current in the stator, and k_T the machine torque constant. The stator is the same as the armature in this case because the stator has flowing current. The machine torque constant is related to number of windings in the stator, number of poles, radius of the generator, length of the conductor and peak flux density [13]. As the name implies, the variables that are related to the machine torque constant are constant after physical production.
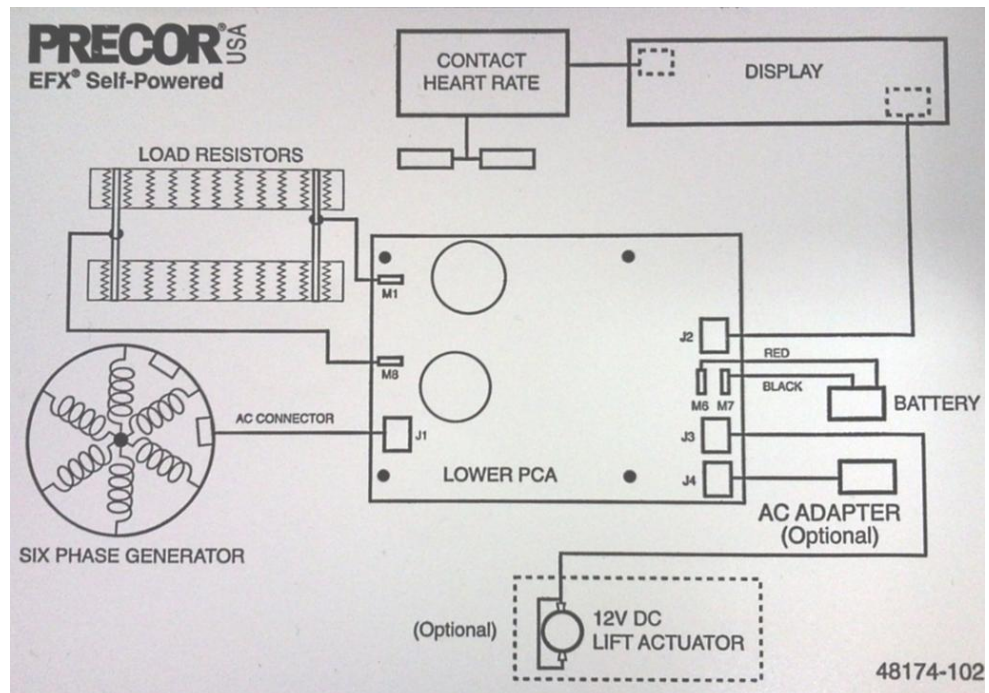
Figure 1 - Precor Elliptical EFX546 Block diagram
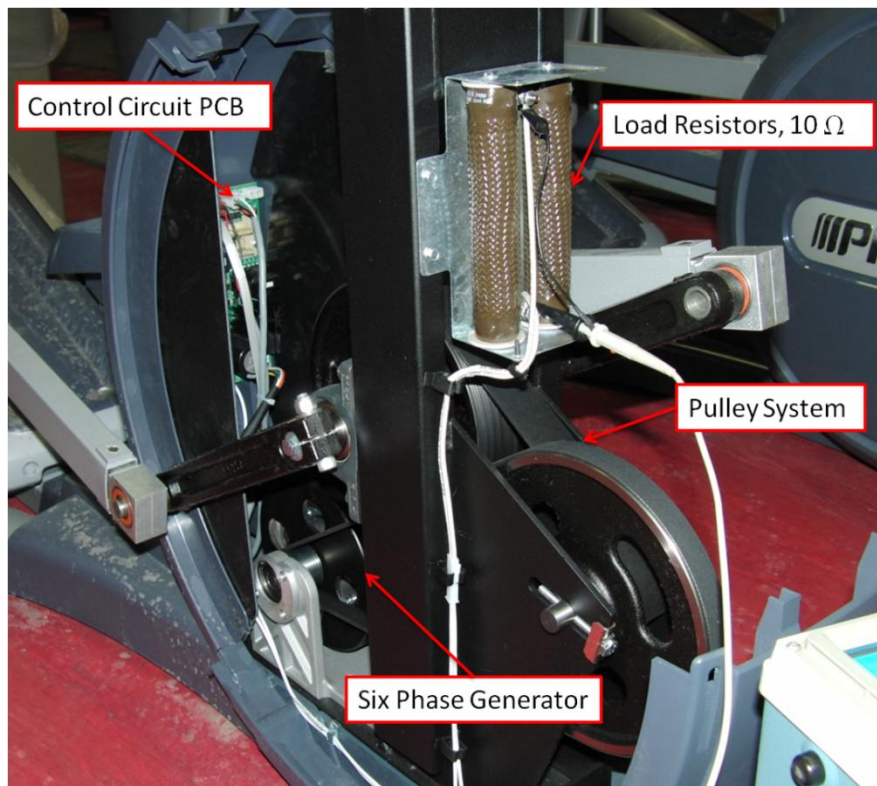
Figure 2 - Labeled Picture of Precor EXF546 without enclosure

2.2.2 Generator with Load Resistor Data

The reconstructed waveform shown in Figure 3 is given for the specific case of a user maintaining their strides per minute (SPM) at 152 and a resistance level of 10. The periodic signal can be described by the equation below for each individual period.

$$V = V_L + (V_H - V_L)e^{-t/10us} \tag{3}$$

Where V is the voltage across the load resistor, V_L is the DC offset voltage, V_H is the peak voltage and t is the time within the period restarting after 32 microseconds. The signal has a period of 32 microseconds and a DC offset voltage that varies per the user input. This equation was developed by using the equation for discharging a capacitor with a time constant of 10us to fit the data.

The average voltage, Vavg, in Figure 3 and Table 2 was found using Equation 3, above, with 32 points for the time domain of 1 to 32 microseconds with an interval of 1 microsecond. The average power, Pavg, was found using the equation below for power calculation with a purely resistive load.

$$Pavg = {V_{avg}^2}/{R} \tag{4}$$

Where R is the resistance, which is 10 ohms for all cases with the Precor elliptical fitness machines. The resistance level (Res Level) set by the user can go as high as 20, but this level is difficult for a user to keep at a steady SPM because of the torque required. It was possible to reach almost 100 watts of power even with a resistance level of 12 when moving at a fast pace of 152 SPM. The MATLAB code used to create the plot in Figure 3 can be found in Section A.10.

14
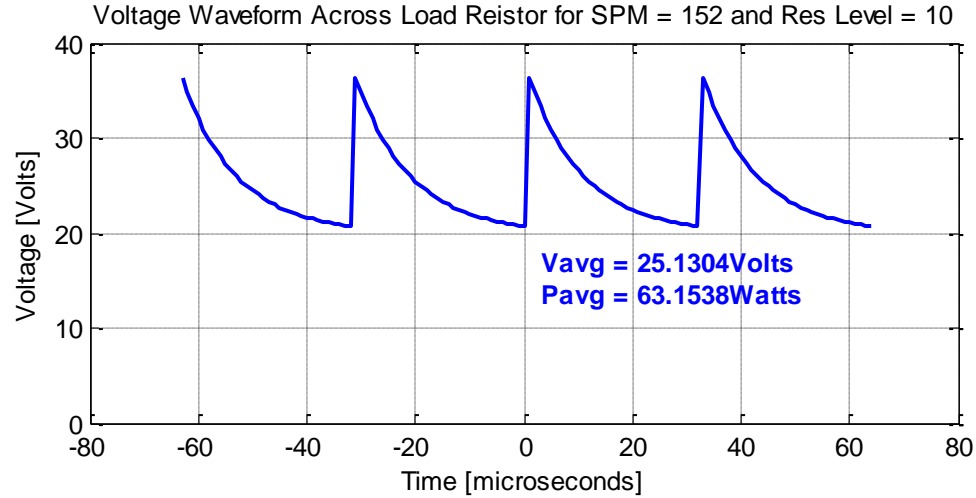
Figure 3 - Reconstructed Voltage Waveform Across Load Resistor

SPM:	110 SPM				134 SPM				152 SPM			
Res Level	V_L (V)	V_H (V)	Vavg (V)	Pavg (W)	V_L (V)	V_H (V)	Vavg (V)	Pavg (W)	V_L (V)	V_H (V)	Vavg (V)	Pavg (W)
1	0	2	0.6	0.0	0	2	0.6	0.0	0	2	0.6	0.0
2	3	7	4.1	1.7	4	8	5.1	2.6	5	9	6.1	3.8
3	5	11	6.7	4.5	5	11	6.7	4.5	7	18	10.1	10.3
4	7	13	8.7	7.6	7	15	9.3	8.6	9	19	11.9	14.0
5	9	16	11.0	12.1	10	17	12.0	14.4	11	20	13.6	18.4
6	11	19	13.3	17.6	12	20	14.3	20.4	14	23	16.6	27.5
7	14	23	16.6	27.5	14	20	15.7	24.7	15	26	18.1	32.9
8	15	25	17.9	31.9	15	27	18.4	33.9	16	30	20.0	40.0
9	16	28	19.4	37.7	18	33	22.3	49.6	18	35	22.9	52.2
10	19	32	22.7	51.6	20	35	24.3	59.0	20	38	25.1	63.2
11	19	35	23.6	55.5	21				23	40	27.9	77.6
12	22	37	26.3	69.1	23				25	45	30.7	94.2

Table 2 - Precor Elliptical Voltage Waveform Primary Attributes

2.2.3 Fitness Machines Using a Hybrid Generator

The block diagram for the Precor recumbent stationary bicycle, C846, was identified while examining the fitness machine as seen in Figure 4, and describes most fitness machines using the hybrid generator. A picture of the same fitness machine without the enclosure and with labeling of the components is shown in Figure 5. The three phase generator and electro-magnet makes up the hybrid generator.

15
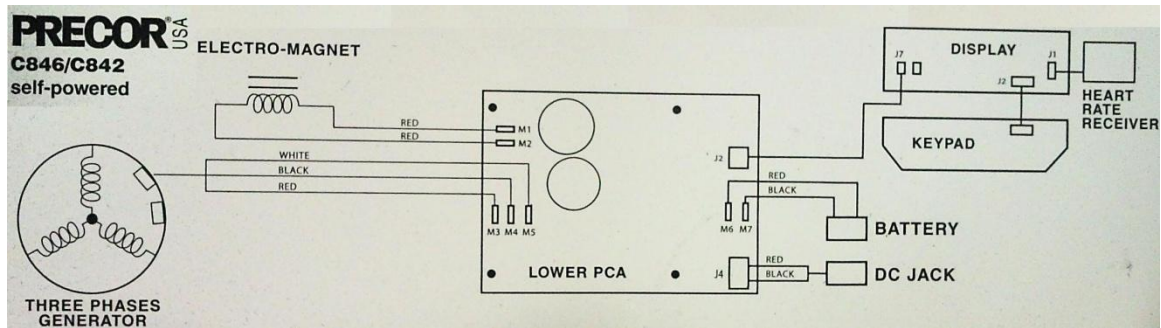
Figure 4 - Precor Recumbent Stationary Bicycle C846 Block Diagram
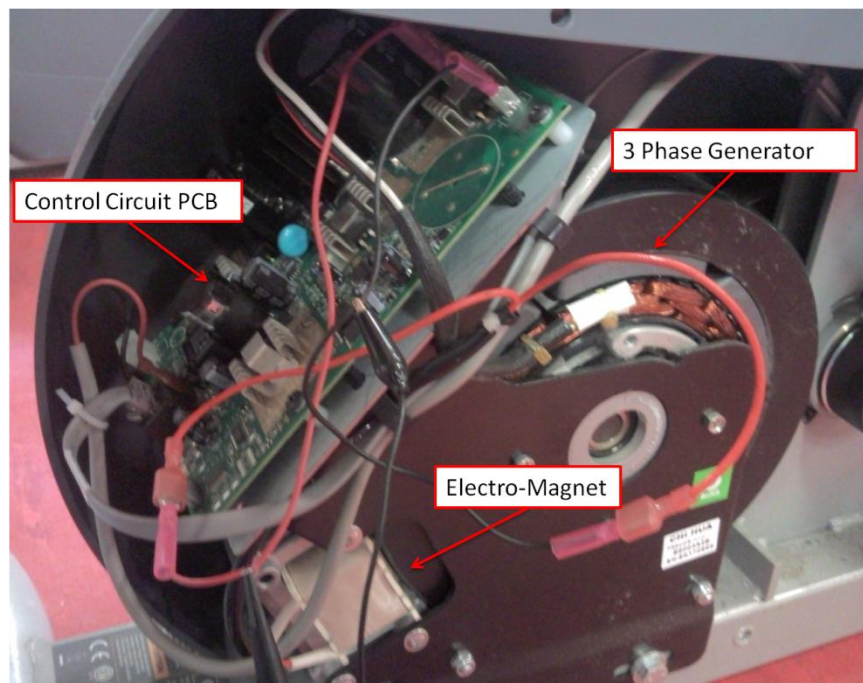
Figure 5 - Labeled Precor Recumbent Stationary Bicycle C846 without Enclosure

When examining the other fitness machines still in the scope of research, it was

found that they all used a hybrid generator. Both Precor and Octane was found to

outsource the production of the hybrid generator to the same manufacturer by examining

the labeling on the device. This can be seen with Figure 5 and Figure 6. Precor reuses this

same device within different types of machines as can be seen in Figure 5 and Figure 7.

The Cybex recumbent stationary bicycle, 530R, has a similar hybrid generator as Precor

and Octane, which can be seen in Figure 8.
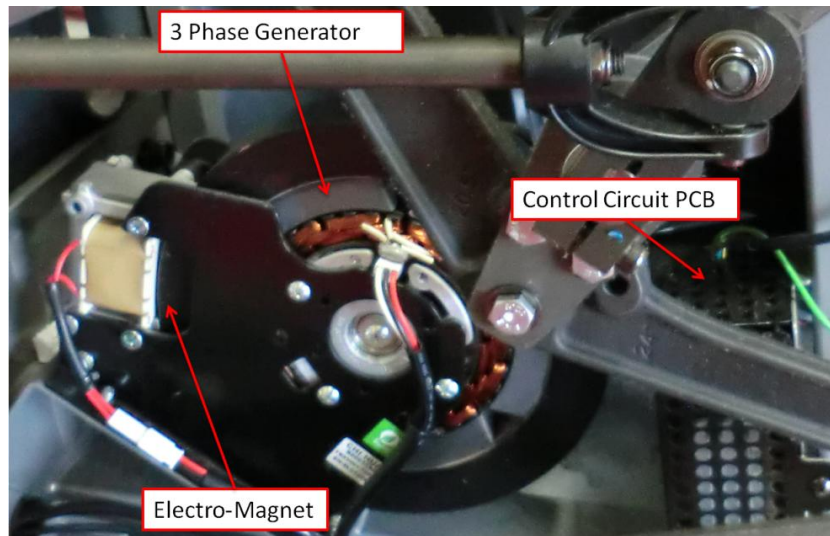
Figure 6 - Labeled Octane Elliptical Pro37000 without Enclosure
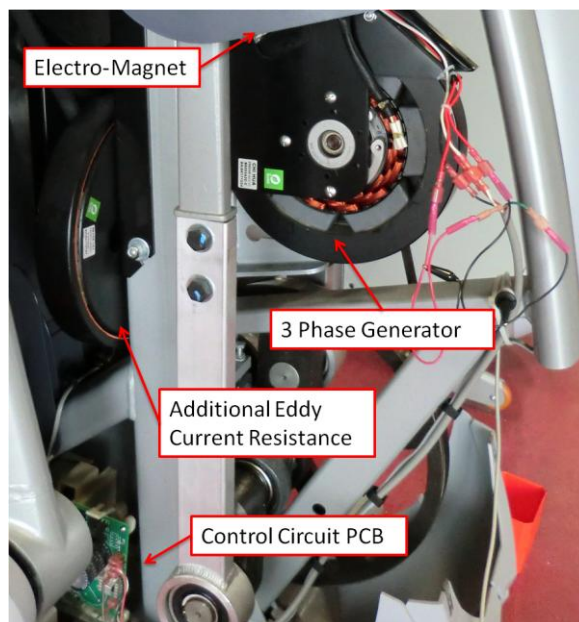
Figure 7 - Labeled Precor AMT100i without Enclosure
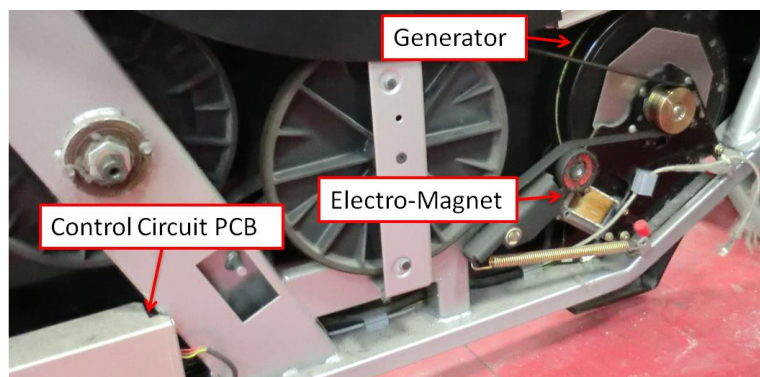
Figure 8 - Labeled Cybex Recumbent Stationary Bicycle 530R without Enclosure

2.2.4 Hybrid Generator Concepts

The use of hybrid generators, involving a combination eddy current braking with a generator was confirmed by Chuck Rosenow from Octane Fitness [8]. The purpose of the device was to decrease cost in manufacturing and reduce the required volume within the machine. The hybrid generator incorporates a PMAC generator to produce power for the machine to be self-sufficient and eliminates the need for the fitness machine to be plugged in. In addition to the PMAC generator, the rotor is made up of permanent magnets and a large cast iron disk to provide a fly wheel for smooth movement. Fastened near the outside of the fly wheel is an inductive core that creates eddy currents within the fly wheel to provide braking when in motion. This method of physical resistance allows for a smaller package and lower cost, by reducing the current flowing though the stator of the generator and allowing a smaller gauge wire to be used. The eddy current braking resistance is controlled by an adjustable DC power supply [9]. The original block diagram and basic circuit schematics for the overall system can be found in Section A.1. The basic circuit schematic from the patent is shown in Figure 9 for easy reference. The circuit labeled 8, is the adjustable DC power supply for the eddy current inductor and shows the topography of a buck converter. The adjustable DC power supply is powered by the circuit labeled 6, which is the commutating and wave filtering circuit that rectifies the AC power from the PMAC generator to DC. Both the buck topography and rectifying will be supported by the data in Section 2.2.5 as the user changes speed or resistance levels.

18
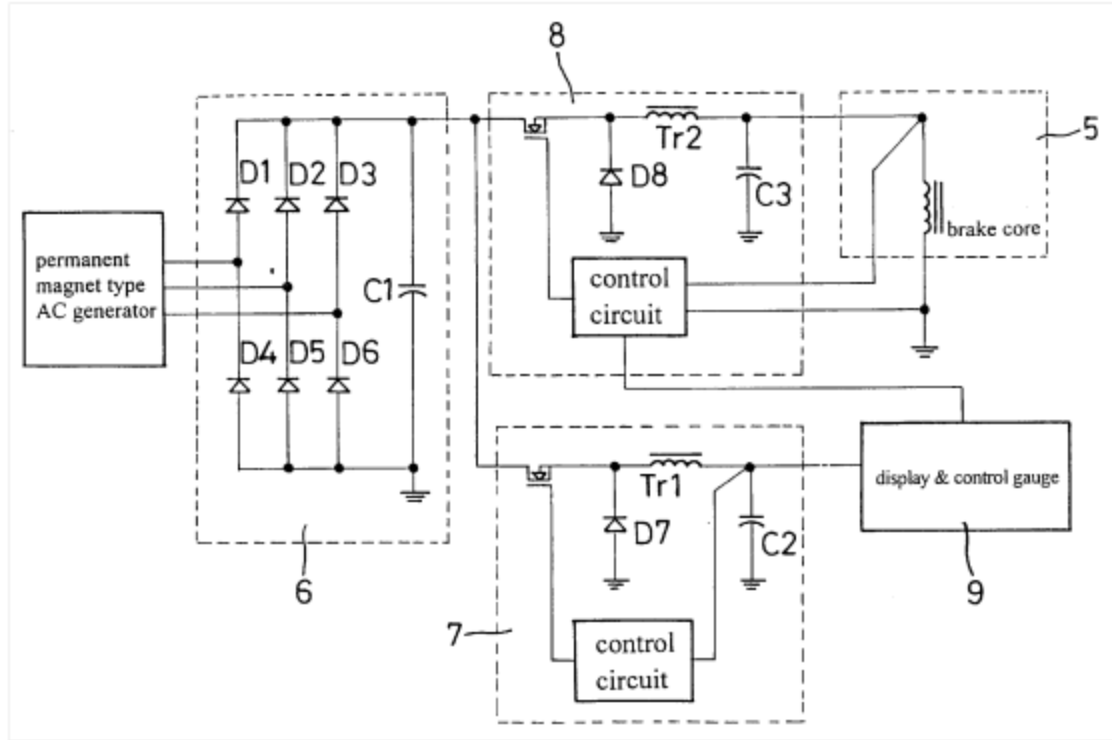
Figure 9 - Basic Circuit Schematic of the Hybrid Generator [9]

2.2.5   Hybrid Generator Data

As the purpose of the tested circuit is to divert the energy from the eddy current inductor to the grid, it was necessary to first find the voltage, current, and power going to the inductor during normal operation. This was for the purpose of design of and comparison to the tested circuit during implementation. Ideally the tested circuit would mimic the inductor and have the same power output to the inverter. To have the tested circuit mimic the inductor a similar inductance would be necessary. Table 3 gives the inductance of the electromagnets in the machines within the scope of research.

Freq (Hz)	Upright - Cybex Cyclone 530C		Recumbent - Precor 846i		Elliptical - Octane Pro 3700		AMT - Precor 100i	
	Parallel		Parallel		Parallel		Parallel	
	L (mH)	Q	L (mH)	Q	L (mH)	Q	L (mH)	Q
1k	415	2.4	262	3.1	345	3.3	300	2.3

Table 3 - Fitness Machine Inductor Measurements

Data represented in Figures 11 - 22 are from the Precor recumbent stationary

bicycle, C846, under normal operation and changes with the user inputs of rotations per

minute (PRM) or resistance level (Res Level). The resistance levels on the machine could

go between 1 and 25. The maximum speed recorded was 108 RPM and the slowest

maintainable speed was 30 RPM. The significant results of all cases recorded are shown

in Table 4 and Table 5. As shown in Figure 10, the data was measured by breaking the

connection between the adjustable DC power supply and eddy current inductor. The

voltage was measured across the inductor and the current was measured with a 50

milliohm precision resistor in series with the inductor to the common ground.

The upper plots in Figures 11 - 22 are the voltage measured with channel 1. The

middle plots are the current measured with channel 2 zoomed out. The bottom plots are

the current measured with channel 2 zoomed in when necessary.
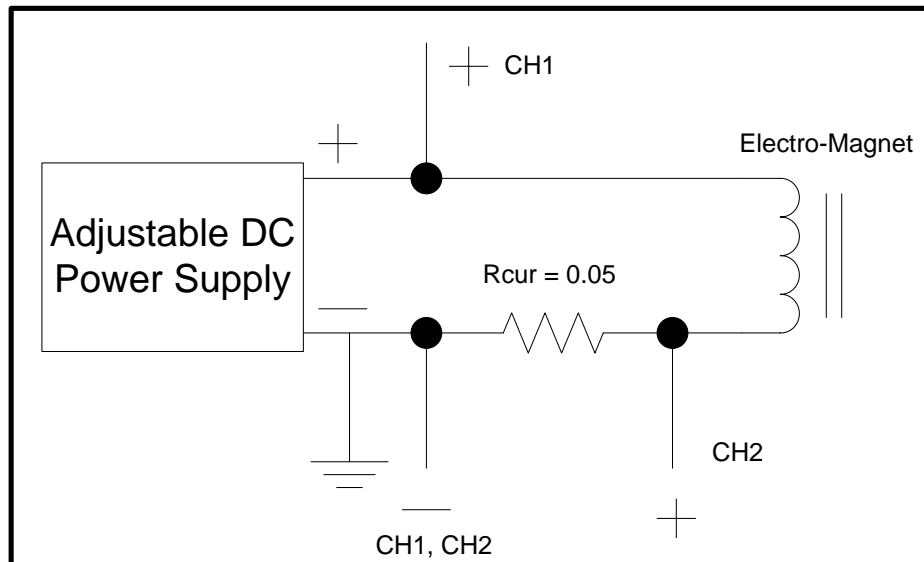
Figure 10 - Voltage and Current Measurement Method
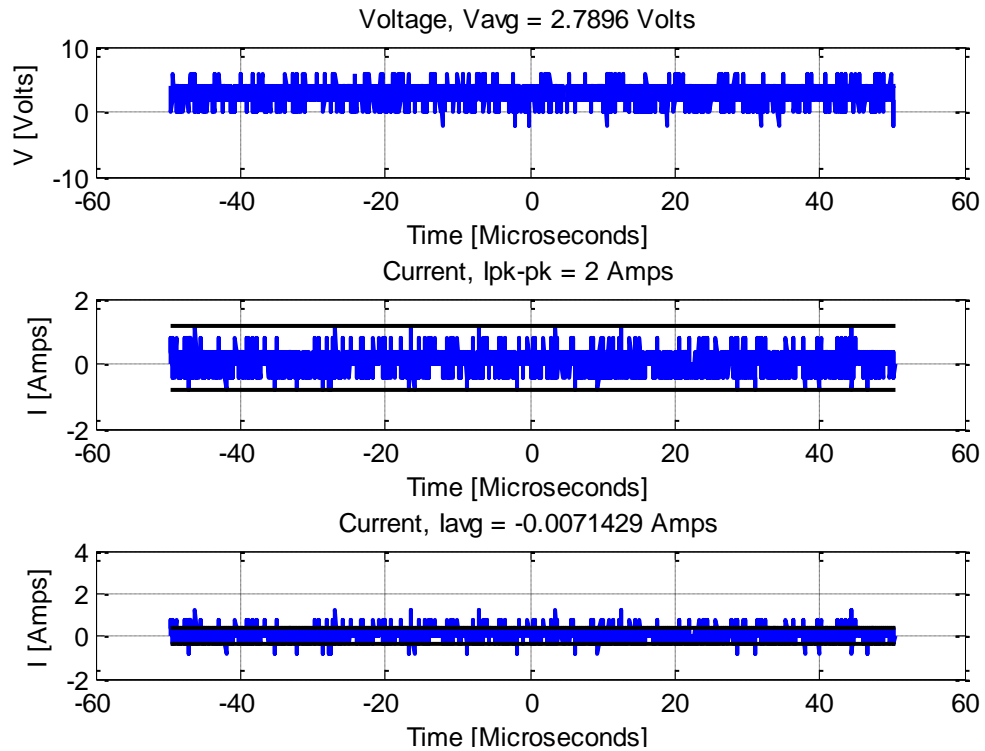
Figure 11 - Normal Operation at 50 RPM and a Res Level of 1
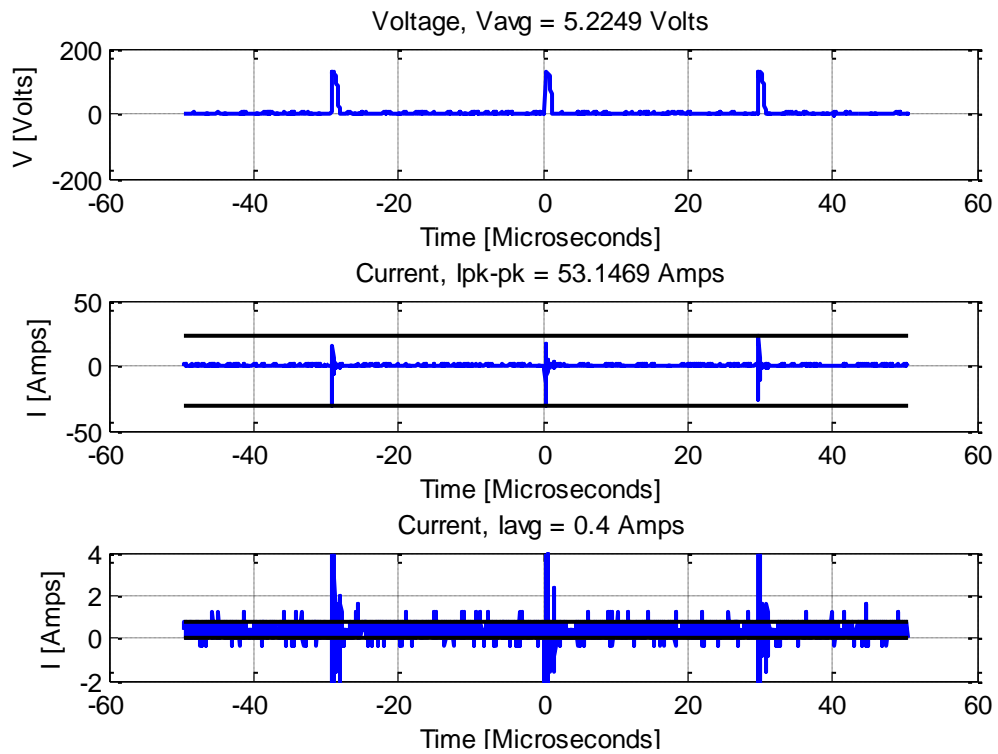
Figure 12 - Normal Operation at 50 RPM and a Res Level of 2

Voltage, Vavg = 7.6081 Volts

Current, Ipk-pk = 53.1469 Amps

Current, Iavg = 0.61429 Amps
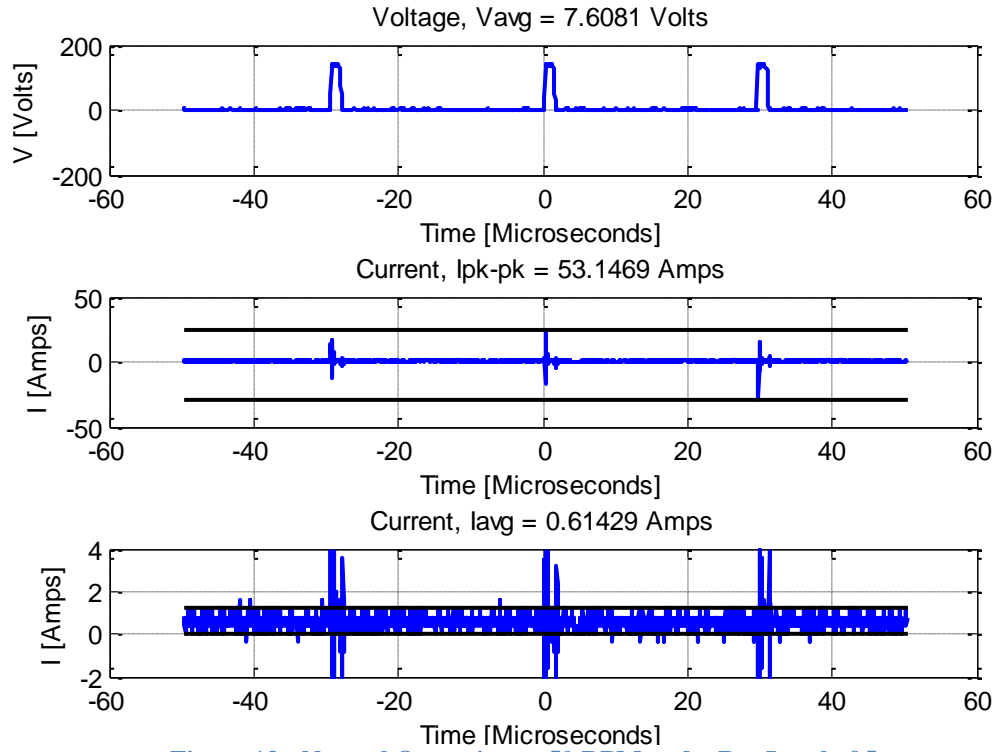
Figure 13 - Normal Operation at 50 RPM and a Res Level of 5

Voltage, Vavg = 10.9987 Volts

Current, Ipk-pk = 49.6 Amps

Current, Iavg = 0.80714 Amps
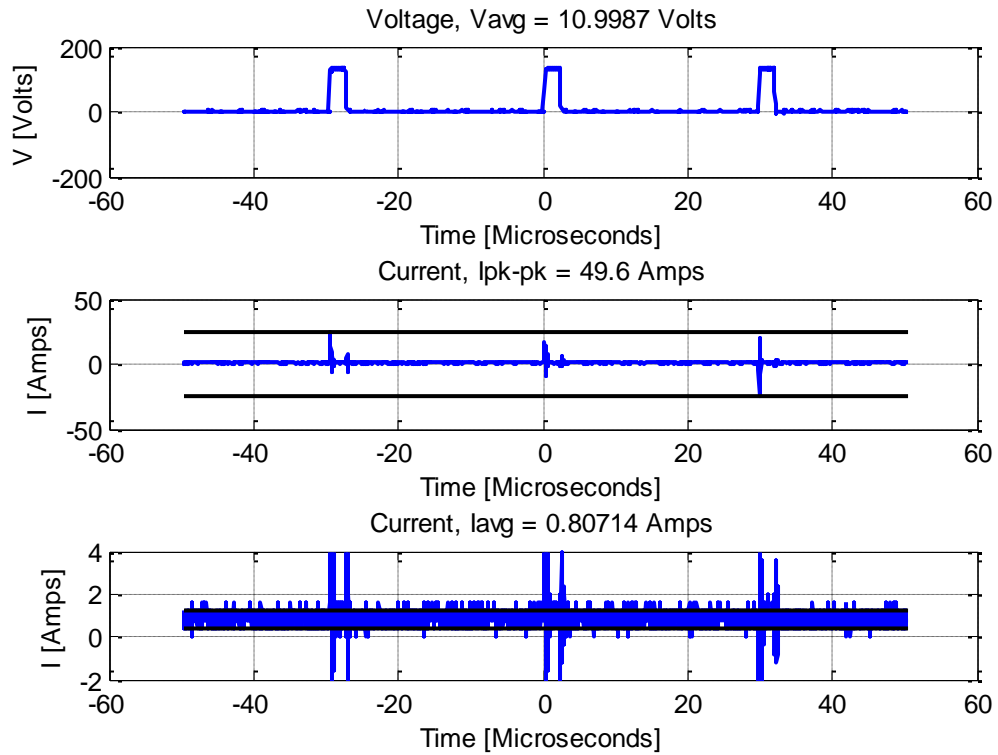
Figure 14 - Normal Operation at 50 RPM and a Res Level of 10

22

Voltage, Vavg = 14.0215 Volts

Current, Ipk-pk = 61.6 Amps

Current, Iavg = 1.1929 Amps
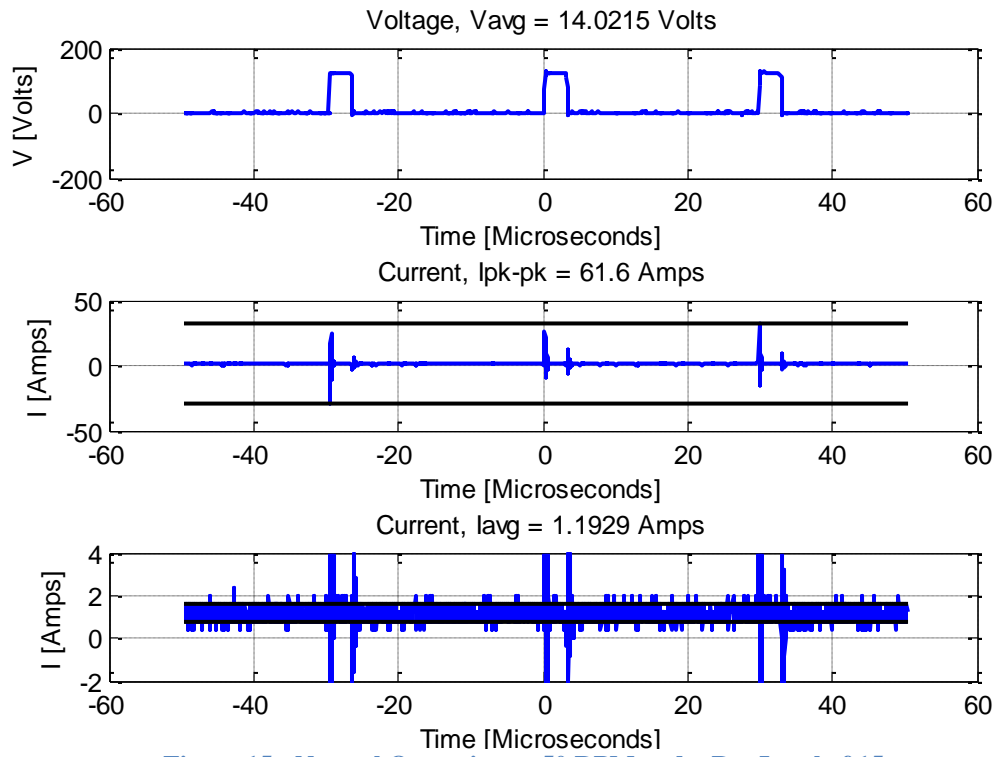
Figure 15 - Normal Operation at 50 RPM and a Res Level of 15

Voltage, Vavg = 18.3908 Volts

Current, Ipk-pk = 56.4 Amps

Current, Iavg = 1.6 Amps
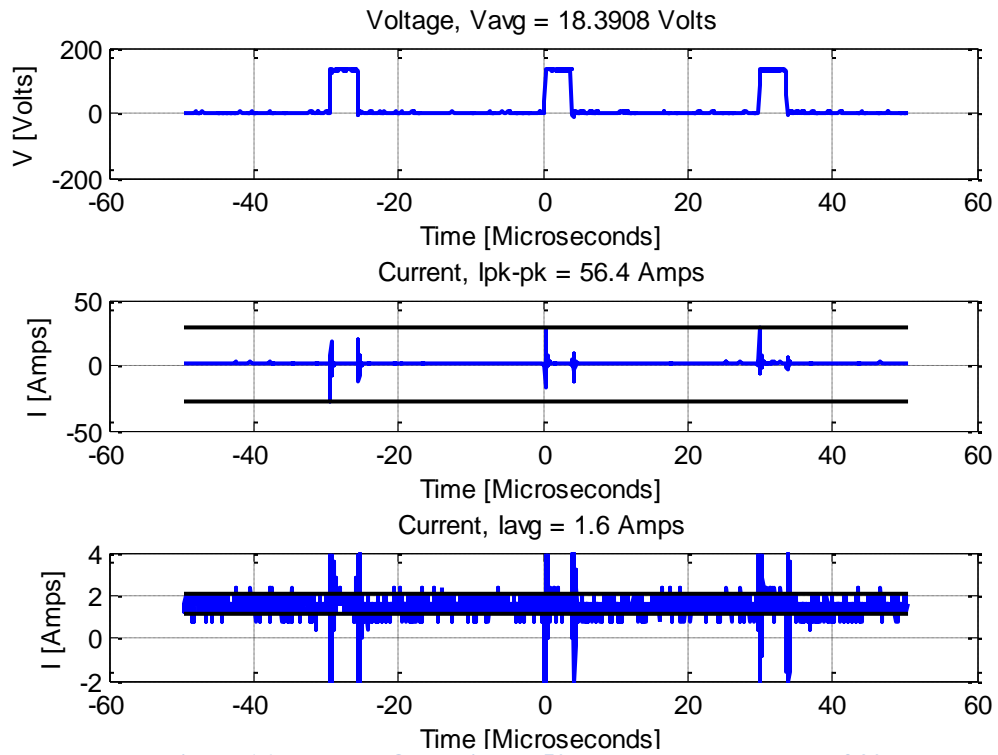
Figure 16 - Normal Operation at 50 RPM and a Res Level of 20
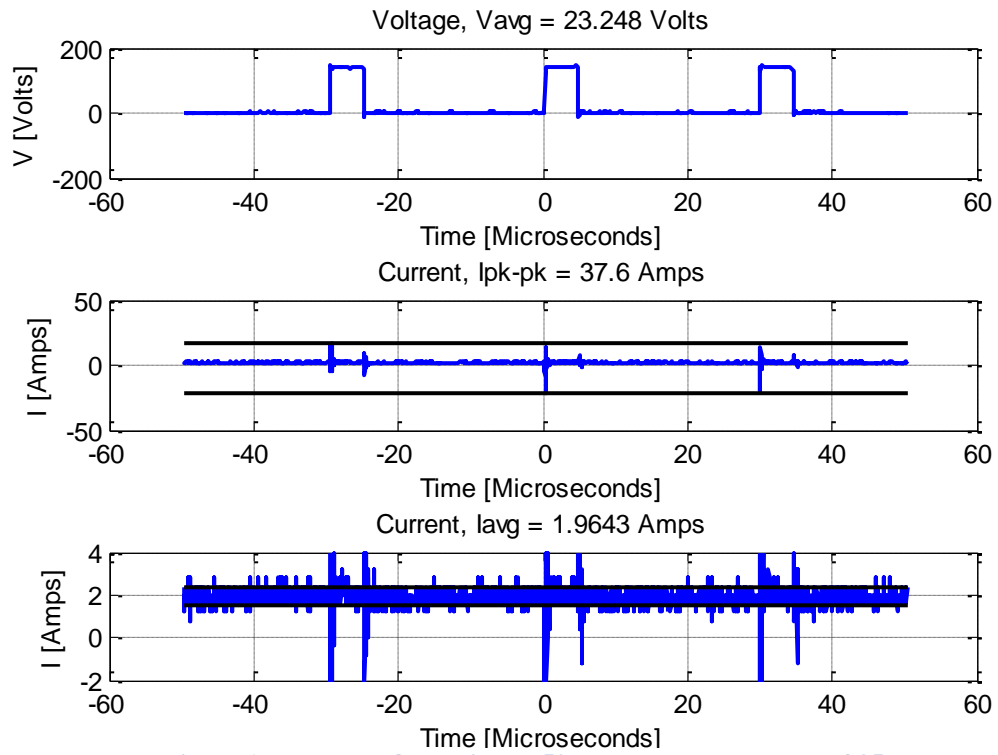
Figure 17 - Normal Operation at 50 RPM and a Res Level of 25
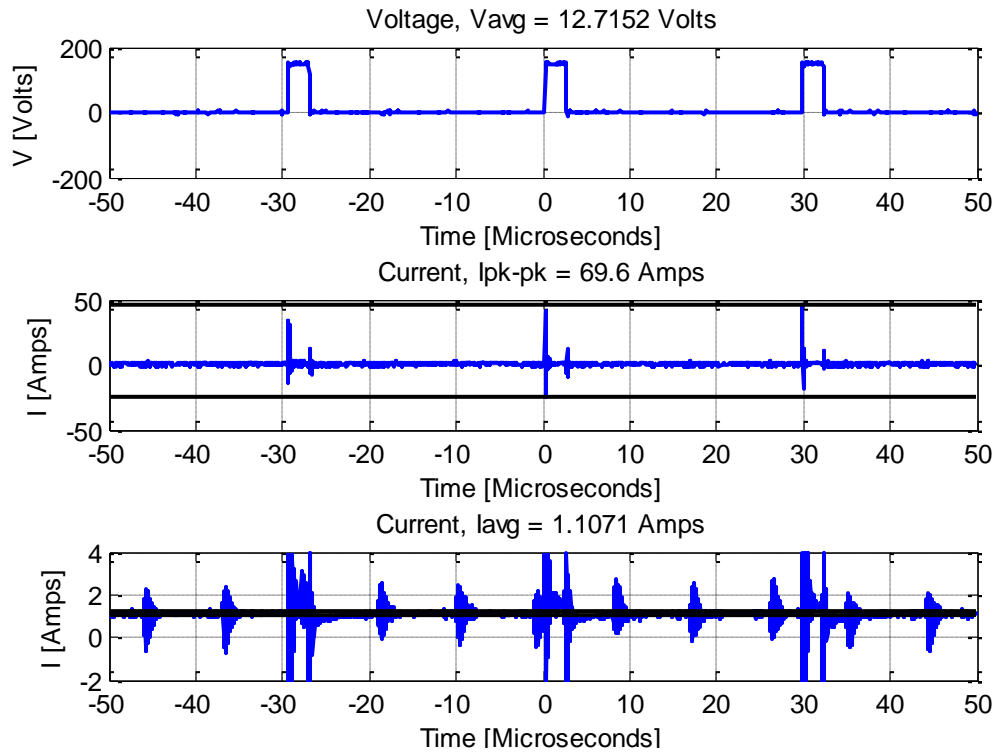
Figure 18 - Normal Operation at 60 RPM and a Res Level of 15
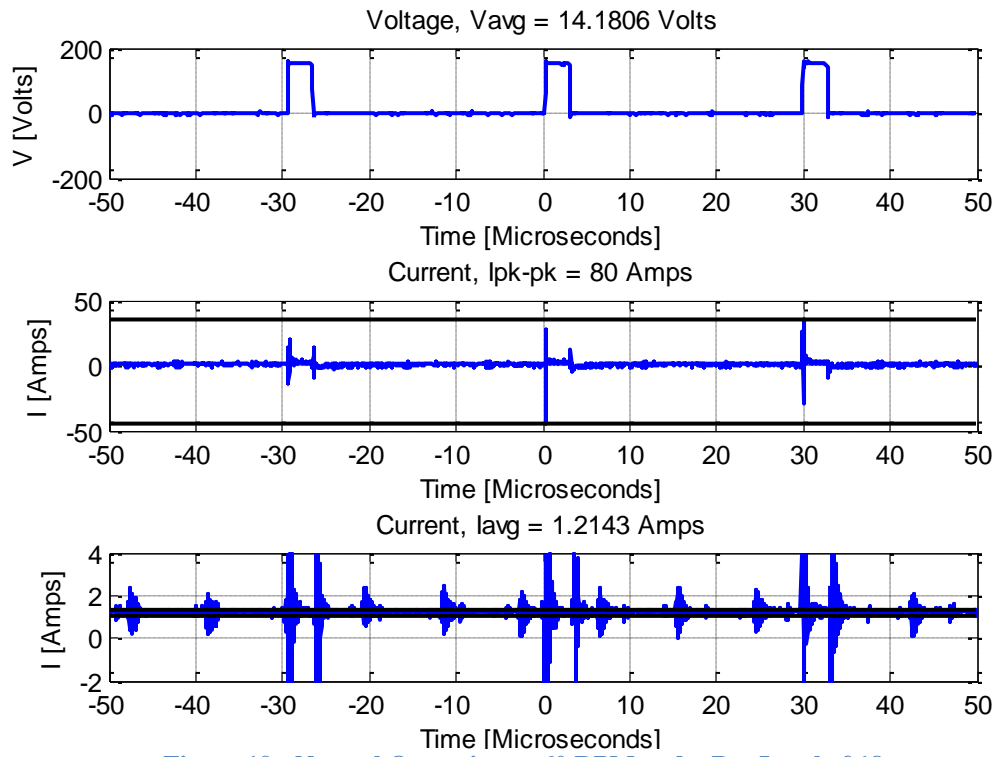
Figure 19 - Normal Operation at 60 RPM and a Res Level of 18
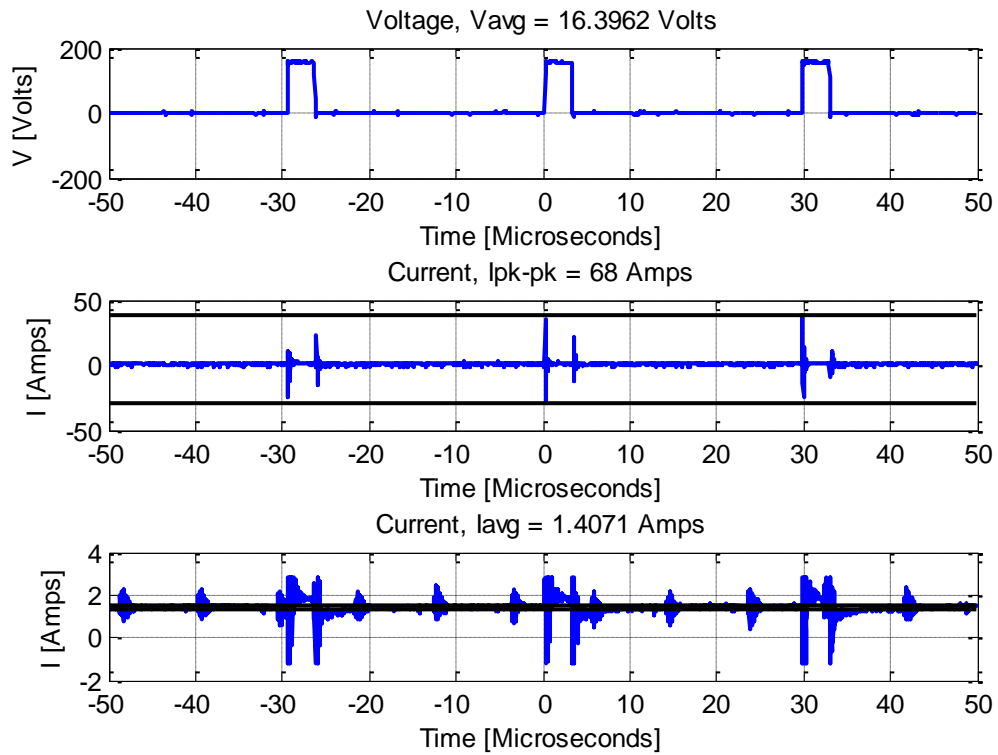
Figure 20 - Normal Operation at 60 RPM and a Res Level of 20

Voltage, Vavg = 18.3482 Volts

Current, Ipk-pk = 100 Amps

Current, Iavg = 1.6429 Amps
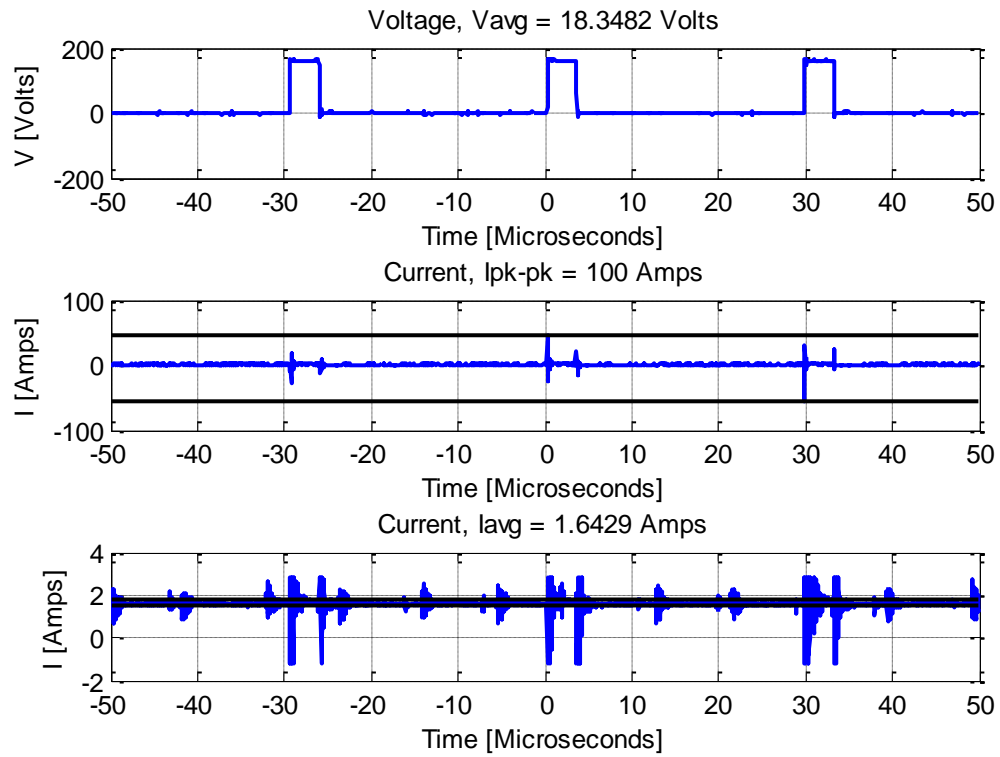
Figure 21 - Normal Operation at 60 RPM and a Res Level of 22

Voltage, Vavg = 21.3954 Volts

Current, Ipk-pk = 76.8 Amps

Current, Iavg = 1.8143 Amps
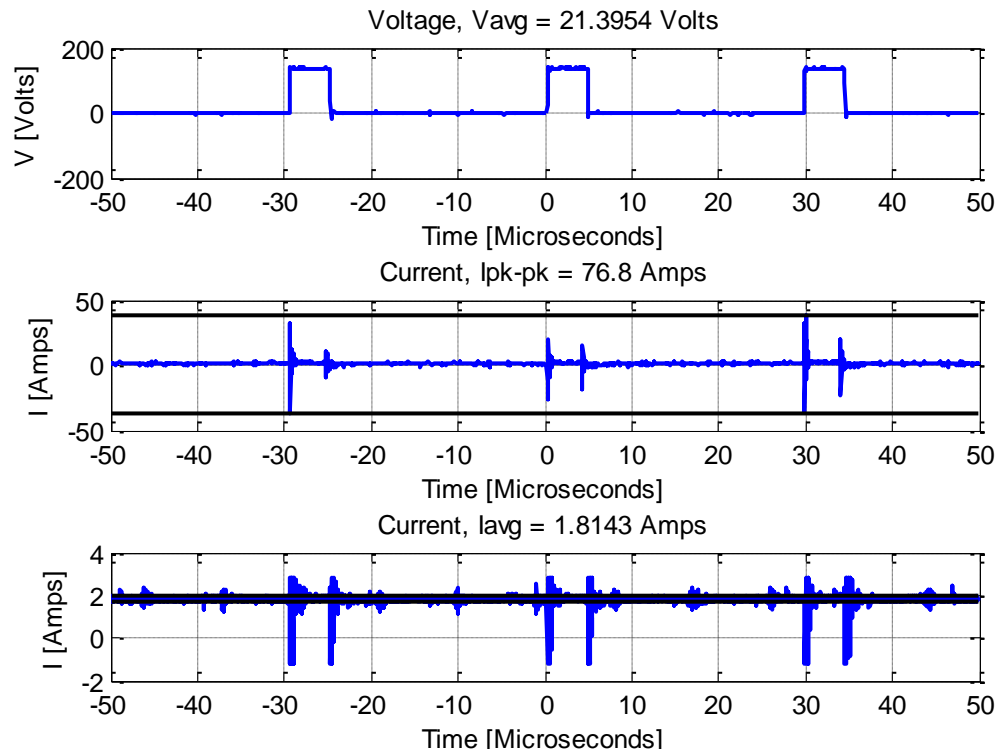
Figure 22 - Normal Operation at 60 RPM and a Res Level of 25

RPM:	50 RPM				60 RPM				70 RPM			
Res Level	Vavg (V)	$I_{pk\text{-}pk}$ (A)	Iavg (A)	Pavg (W)	Vavg (V)	$I_{pk\text{-}pk}$ (A)	Iavg (A)	Pavg (W)	Vavg (V)	$I_{pk\text{-}pk}$ (A)	Iavg (A)	Pavg (W)
1	2.8	2.0	0.0	0.0	n.a.	n.a.	n.a.	n.a.	2.577	2.4	0.0	0.0
2	5.2	53.1	0.4	2.1	n.a.	n.a.	n.a.	n.a.	5.662	41.2	0.4	2.3
5	7.6	53.1	0.6	4.7	n.a.	n.a.	n.a.	n.a.	8.124	22.4	0.6	4.8
10	11.0	49.6	0.8	8.9	n.a.	n.a.	n.a.	n.a.	11.3	41.6	1.0	11.3
15	14.0	61.6	1.2	16.7	12.7	69.6	1.1	14.1	14.71	40.0	1.2	17.2
18	n.a.	n.a.	n.a.	n.a.	14.18	80.0	1.2	17.2	n.a.	n.a.	n.a.	n.a.
20	18.4	56.4	1.6	29.4	16.4	68.0	1.4	23.1	18.22	22.8	1.6	28.8
22	n.a.	n.a.	n.a.	n.a.	18.3	100.0	1.6	30.1	n.a.	n.a.	n.a.	n.a.
25	23.2	37.6	2.0	45.7	21.4	76.8	1.8	38.8	23.22	36.0	2.0	45.6

Table 4 - Normal Operation of Precor Bicycle with Significant Results (n.a. stands for not available)

RPM:	30 RPM					Fast RPM			
Res Level	Vavg (V)	$I_{pk\text{-}pk}$ (A)	Iavg (A)	Pavg (W)	Fast RPM	Vavg (V)	$I_{pk\text{-}pk}$ (A)	Iavg (A)	Pavg (W)
1	2.8	2.0	0.0	0.0	108	2.1	2.0	0.0	0.0
2	4.4	42.8	0.2	0.9	100	6.7	29.2	0.4	2.5
5	6.3	36.8	0.4	2.6	100	8.9	30.8	0.6	5.1
10	9.8	41.6	0.8	7.9	95	12.6	40.8	1.0	12.6
15	13.4	50.0	1.0	13.1	90	16.2	60.0	1.4	22.8
20	15.1	47.6	1.4	21.6	90	19.7	69.6	1.6	32.0
25	20.8	55.2	1.8	36.8	80	24.5	52.4	1.8	43.4

Table 5 - Boundaries of Normal Operation of Precor Bicycle with Significant Results

Information not easily found in the figures or available in the tables above are that the switching frequency of the adjustable DC power supply is 33.78 kHz, found from measuring the period of the voltage waveform to be 29.6 microseconds. The average voltage, Vavg, given in Table 4, Table 5 and the Figures 11-22 was found by taking the average of the data points for a pulse and tail. A threshold voltage of 10 volts was used to find the rise points of the pulses. If the voltage did not exceed the threshold, then the average voltage is the mean of all the points. It was also possible to find the average voltage, Vavg, though the equation below.

$$Vavg = V_{max}D \qquad (5)$$

Where V_{max} max is the maximum voltage of the pulse and D is the duty cycle found by dividing the pulse width by the period of the waveform. It was found that these two

methods resulted in the same results for Vavg. The peak to peak current, Ipk-pk , was found by finding the difference between the upper limit and lower limit as shown in the figures of this section with a solid black line. The average current, Iavg, was found by graphically selecting a lower limit and upper limit, shown with solid black lines, and taking the average of the selected limits. The MATLAB code used to create Figures 11-22 and calculate the data in Tables 4 and 5 can be found in Section A.11.

Figures 11-22 focused on the change in resistance levels for two different speeds. Figure 23 focus on the change in speed for the same resistance level. The average power, Pavg, given in Table 4 and Table 5 were found to be similar for the same resistance levels with changing speeds and is plotted in Figure 24. MATLAB code for creating Figure 23 is found in Section A.12 and Figure 24 in Section A.13.
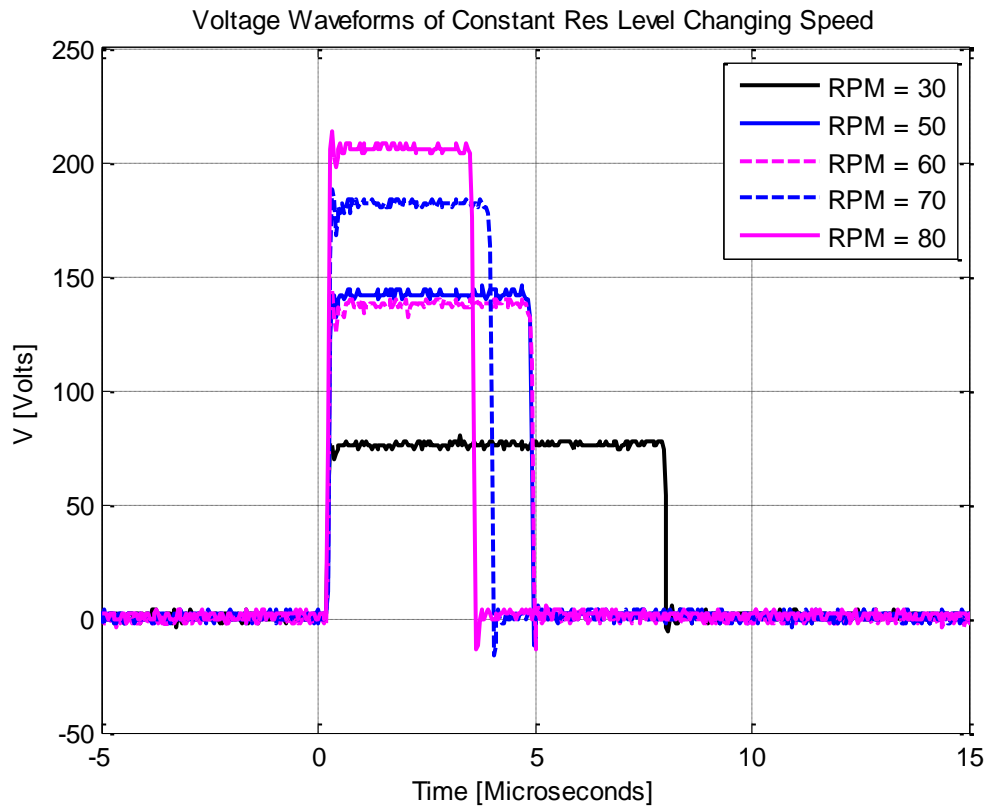
Figure 23 - Voltage Waveform of Normal Op. at Multiple Speeds and a Res Level of 25

28
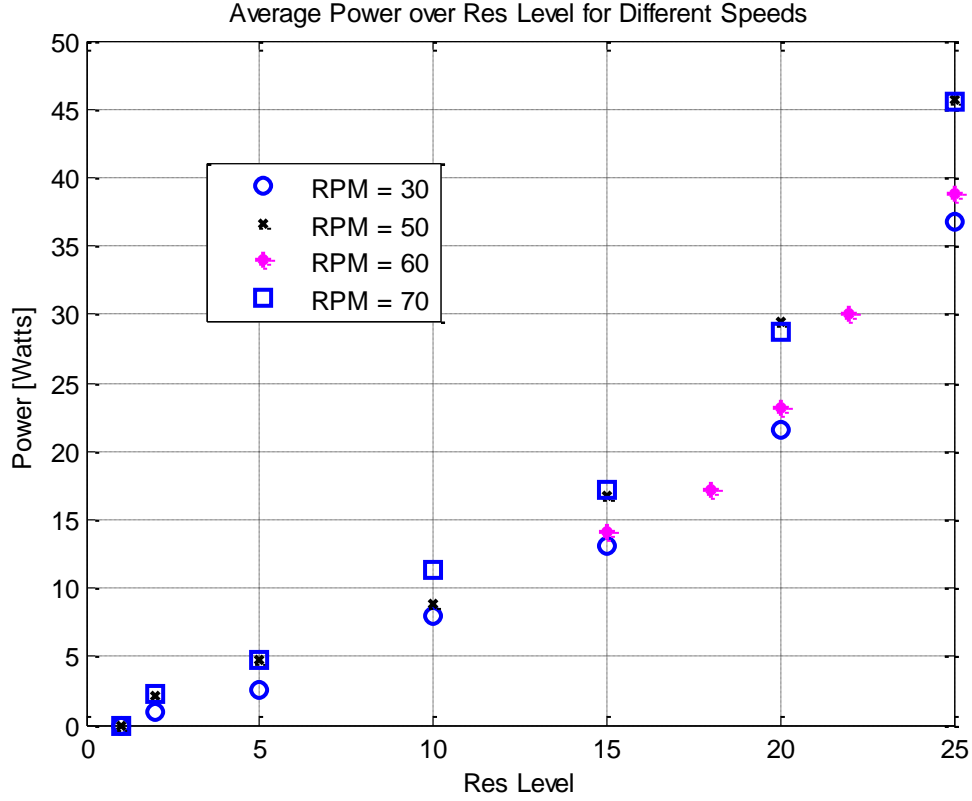
Figure 24 - Power Output During Normal Operation at Multiple Speeds

The data represented in Figure 23 shows how the adjustable DC power supply

changes over different speeds and supports the assumption that the maximum voltage is

related directly to the speed. It is also supported by the theory of PMAC generators and

the partial schematic of the hybrid generator given in Figure 9. The schematic shows a

direct connection between the AC to DC rectifier and the adjustable DC power supply, so

the input voltage to the adjustable DC power supply should be directly related to the

voltage of the 3-phase PMAC generator. The PMAC generator relationship between

voltage and speed can be seen in the equation below

$$\hat{E}_f = k_E \omega_m \qquad \qquad (6) \; [13]$$

Where $\hat{E}_f$ is the induced back-emf, k_E is the voltage constant, and ω_m is the speed of the

motor. The equation above is for a PMAC motor but still shows the relationships for a

PMAC generator. The induced back-emf is directly related to the line voltage. The waveforms in Figure 23 also lead to the assumption that the adjustable DC power supply is trying to create a constant volt-second (being the area under the voltage waveform) for a given resistance level, which allows for a constant power.

The data represented in Figure 24 gives the power output of recorded speeds and resistance levels. An assumption made from this data is that the adjustable DC power supply in the Precor recumbent stationary bicycle tries to create a constant power to the electromagnet for a given resistance level. Although, when data from 60 RPM is compared to 50 or 70 RPM it does not always support this assumption. The possible reason for this is that the data for 30, 50, 70 and fast RPM were taken on a different fitness machine, although the same model and manufacturer, than the data for 60 RPM.

These two assumptions were further examined by recording data outside of normal operation, such as an open voltage test and voltage-current characteristic. For the open voltage test, the electromagnet was removed and the output voltage of the adjustable DC power supply was measured without any load. It was found that the resistance level did not affect the open voltage and as shown in Figure 25 that the pulse stayed at a duty cycle of 100 percent. This data supports the assumption that the speed of the machine is directly related to the voltage input to the adjustable DC power supply and the maximum value of the voltage pulses supplied to the electro-magnet.
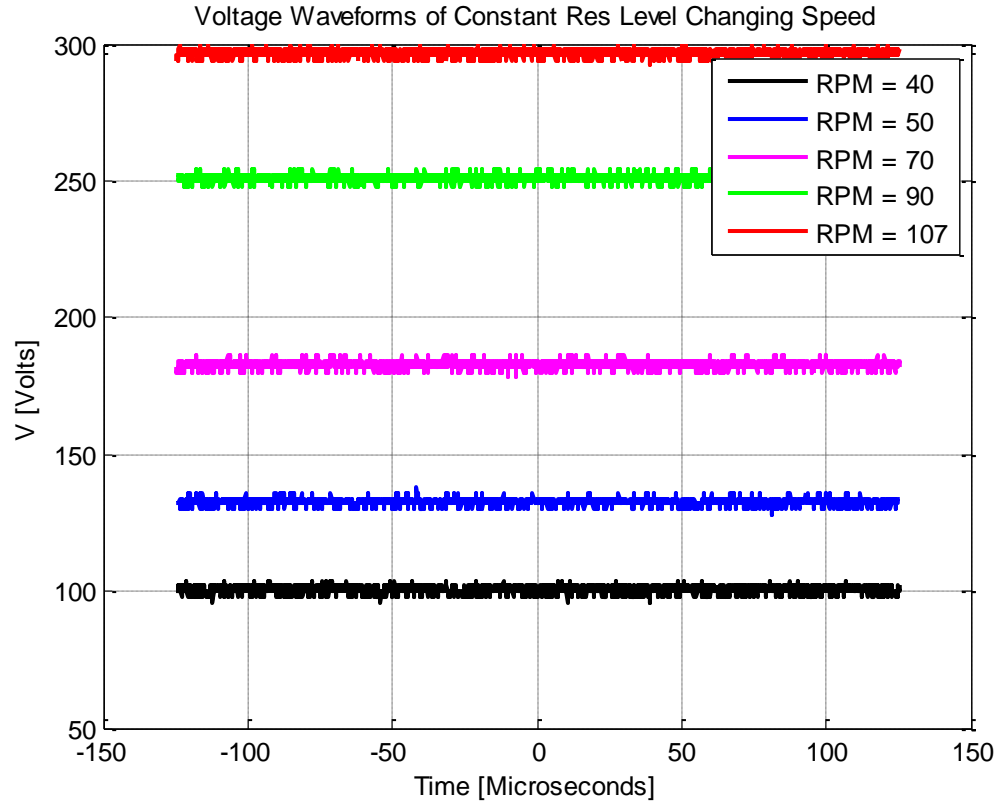
Figure 25 - Open Voltage for Multiple Speeds

To find the voltage-current characteristics of the system, it was necessary to use a low-pass filter to flatten the pulses so that the voltage was steady for the adjustable load resistor. The low-pass filter implemented and how the measurements were done are shown in Figure 26.
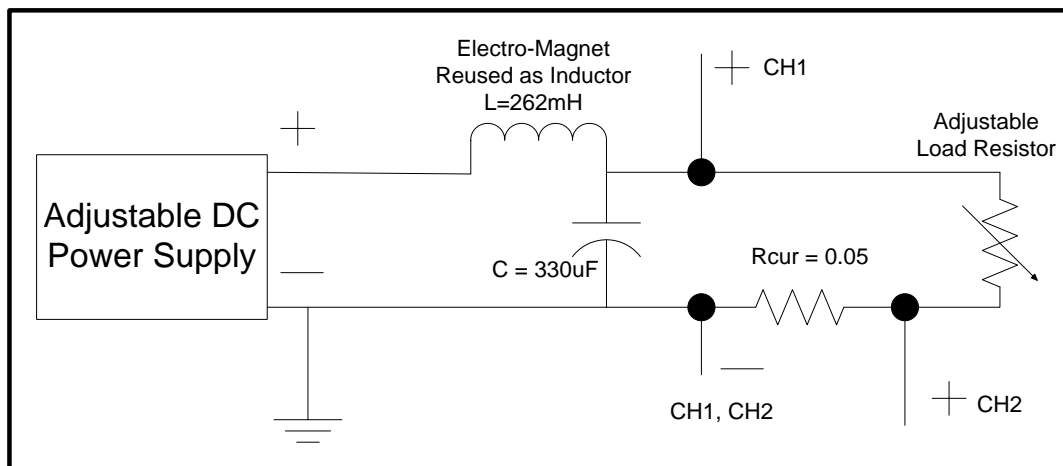
Figure 26 - VI Curve Testing Circuit, Low-Pass Filter and Load Resistor

Measurements were done with the adjustable load resistor at 5, 10, 20, 30, 40, 50 $\pm$ 5% ohms. The data was processed with the MATLAB code found in Section A.16 to find Vavg (channel 1) and Iavg (channel 2). Those measurements are recorded in Table 6 and the expected current is given using ohm's law for comparison with the measured current.

R (ohms)	Resistance Level: 15				Resistance Level: 25			
	V (Volts)	$I_{measured}$ (A)	I=V/R (A)	P (W)	V (Volts)	$I_{measured}$ (A)	I=V/R (A)	P (W)
5.10	6.03	1.06	1.18	6.42	10.61	1.84	2.08	19.49
9.70	10.04	1.04	1.04	10.47	17.06	1.77	1.76	30.21
20.80	16.22	0.79	0.78	12.74	26.96	1.34	1.30	36.20
30.10	18.85	0.61	0.63	11.58	29.92	1.02	0.99	30.56
40.50	21.72	0.59	0.54	12.88	34.64	0.87	0.86	30.18
49.10	23.99	0.51	0.49	12.16	37.16	0.79	0.76	29.20

Table 6 - Voltage-Current Summary of Measured Data
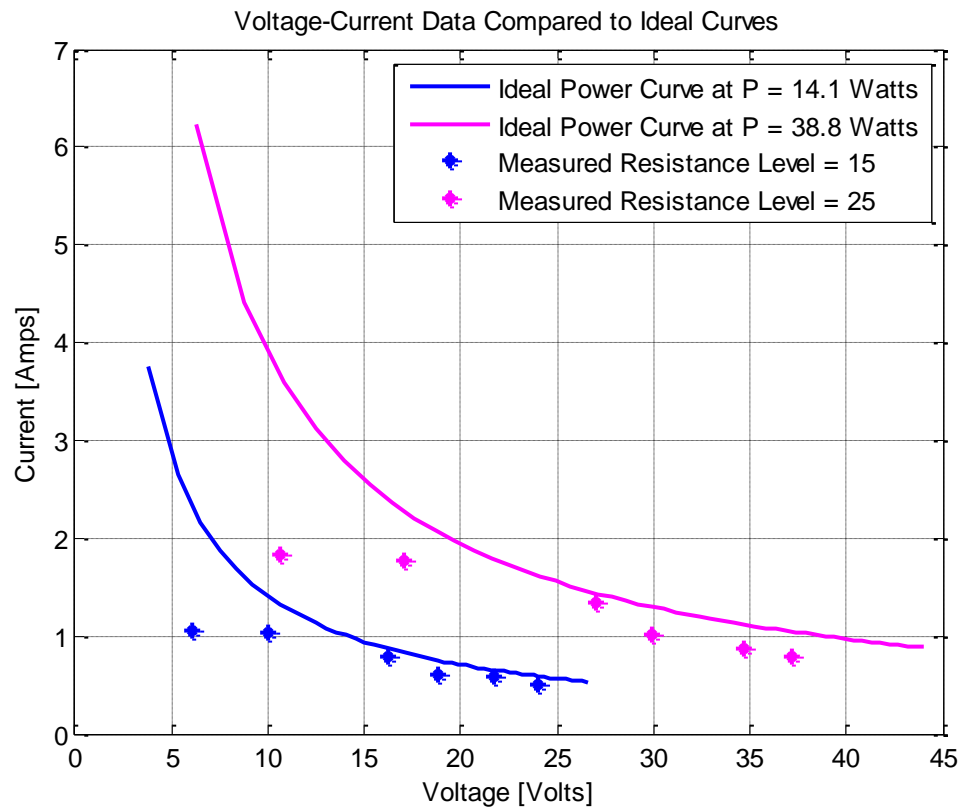
Figure 27 - Voltage-Current Curves at 60 RPM

The voltage-current curve of constant power, to compare to the measured data, was generated by using a range of resistances, equation 4 and equation 7. The constant power curves were generated from the power of 14.1 and 38.8 watts, taken from Table 4 for normal operation with a speed of 60 RPM and a resistance of 15 or 25 respectively.

$$P = I^2 R \tag{7}$$

Where P is power, I is current, and R is resistance.

The data from this test, shown in Figure 27, supports the assumption that the adjustable DC power supply in the Precor recumbent stationary bicycle, C846, is power controlled. The larger current data points were likely skewed away from the model because of a current limiter within the adjustable DC power supply. The current never rose above 2 amps during normal operation, even when at the highest level. The data points were all slightly off the power curves as the low-pass filter would have dissipated some of the power. Figure 27 was created by the MATLAB code provided in Section A.16.

Chapter 3:   Simulation and Design

From additional examination of the fitness machine, it was found that during normal operation, shown in Section 2.2.5, the machine's output worked similarly to a buck converter. It was determined, by testing, the fitness machine had a diode in the same orientation as a buck converter, inserted after the transistor to allow current to continue flowing through the inductor. This allowed for the removal of the two diodes from the buck rectifier to implement a LC low-pass filter, based on the principle that fewer switching components would increase efficiency in power conversion. Although during implementation of the low-pass filter, issues discussed in Section 4.2.1 lead to use of the buck rectifier again.

Issues within the boost converter and discovery of most power being in the resistance level range of 15-25 lead to the removal of the second stage in the three stage circuit to create only a two stage circuit. The three stage circuit is shown in Figure 28 with its circuit combination. The two stage circuit is shown in Figure 29 with its possible circuit combinations.

While testing the National Semiconductor buck regulator, current harmonics were found that followed its switching period and expected duty cycle. An expected reason for these current harmonics was the mismatch of frequencies in the buck regulator, 260 kHz, and fitness machine, 33.78 kHz. These current harmonics lead to the examination of using a lower switching frequency and the design of an Arduino buck converter at 31.25 kHz.
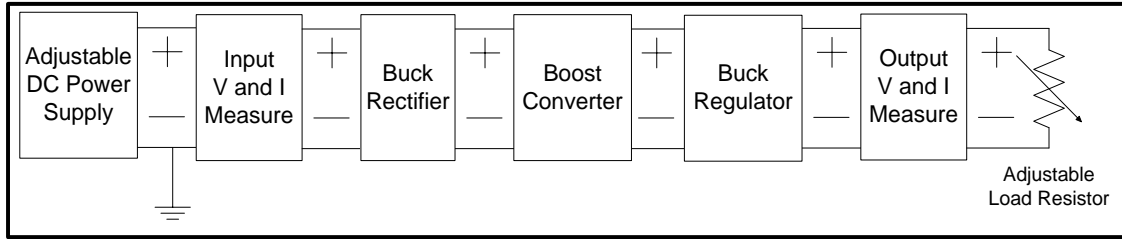
Figure 28 - Three Stage Tested Circuit
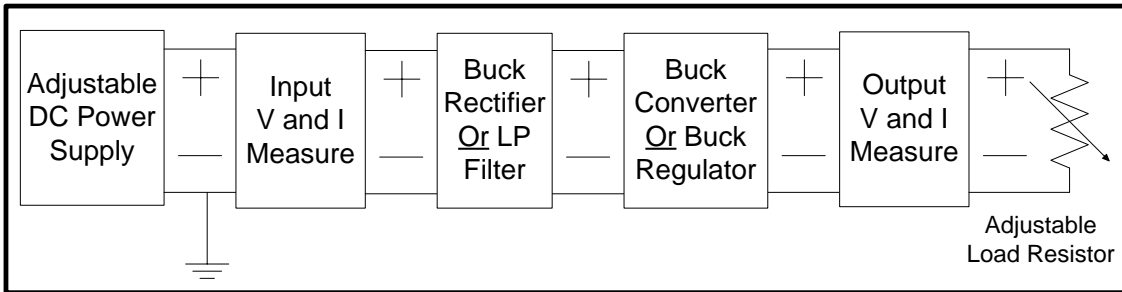
Figure 29 - Two Stage Tested Circuit

3.1 VI Measurement

The voltage and current measurement circuit, shown in Figure 30, was used. When using a resistor to measure current it could not be inserted on the positive voltage line as the oscilloscope shares grounds and would cause a short. The possible issue with placing the current resistor on the ground line is causing ground loops within the system. The use of an isolated current sensor, such as a transformer or Hall sensor, was considered but with the high switching frequency and desire to measure more than an average current this option could not be used.
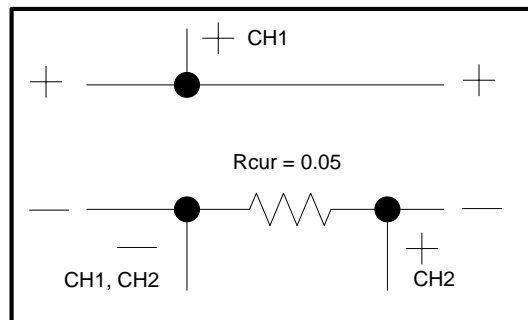
Figure 30 - Voltage and Current Measurement Circuit

3.2   Source Circuit: Adjustable DC Power Supply

The adjustable DC power supply within the fitness machine was modeled as
shown in Figure 31. The DC supply is set at the max voltage from the pulse waveforms.
The MOSFET is controlled by a pulse that has a frequency of 33.78 kHz and duty cycle
corresponding to that measured.
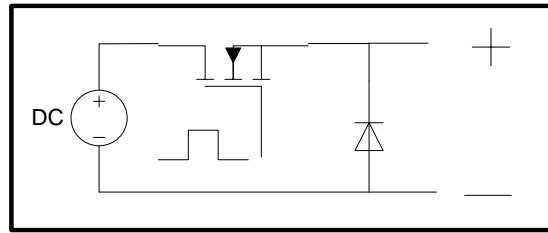
Figure 31 - Adjustable DC Power Supply Model

3.3   Buck Rectifier

The buck rectifier, shown in Figure 32, was originally used with the overall
circuit to protect the fitness machine with the use of diodes. It has no controlled switching
but uses the buck topography to flatten the sharp pulses from the adjustable DC power
supply. The original inductance of the electromagnet, 262mH for the Precor recumbent
stationary bicycle, was over two magnitudes of that were used for this circuit. The reason
for the decrease in inductance was that finding inductors capable of handing the high
currents and inductance would cause large losses in the series resistance of the
component. A 1mH inductor was used as the equations below showed that with a
capacitor of 330uH the circuit would be able to flatten the input voltage and almost avoid
discontinuous modes. As the topography of the circuit is similar to a buck converter the
equations used are for a buck converter. It was assumed that during steady-state the
output voltage of the buck rectifier would be constant and equations using that
assumption were used to size the inductor and capacitor. To estimate the output voltage,

36

the average of the input voltage was assumed to be the output voltage, neglecting the loss in the diodes. The equation below is used to find the required inductance to stay in continuous current mode [14].

$$L = \frac{DT_s}{2I_L}(V_d - V_o) \tag{8}$$

Where L is the inductance, D is the duty cycle, T_s is the switching period, I_L is the average current though the inductor, V_d is the input voltage, and V_o is the output voltage. To design for the right size of inductance, worst case scenarios need to be found for from the data in Section 2.2.5. From Figure 23 the duty cycle can be seen to always be below 30% and the higher the duty cycle the higher the inductance required. The switching period is 29 microseconds and the highest input voltage would be 295 volts, from Figure 25. Designing the circuit for only resistance levels 15 or higher and reviewing Table 4 the lowest current to go through the inductor and the lowest output voltage expected would be 1.1 amps and 12.7 volts respectively. Using these numbers the inductance would need to be 1.1mH or higher. As a design factor of 1.2 would be used, the inductor should be rated for 1.32mH. The last requirement for picking an inductor was to find one with the correct current rating to be sure the ferrite material is not over saturated or overheating occurs. The maximum current in Table 4 was 2 amps and with a design factor of 1.2 the inductor must be rated for 2.4 amps or higher. Finding an inductor with these two ratings was not achievable with the time and funding available and an inductor rated for as 1mH and 2.4 amps was used. The current rating was met, but the inductance was smaller although still in the same magnitude range.

The equation below is used to find required capacitance to keep the voltage ripple within a given range [14].

$$C = \frac{(1-D)T_s^2}{8L(\Delta V_o/V_o)} \qquad (9)$$

Where C is the capacitance of the capacitor, L is the inductance of the inductor, D is the

duty cycle, T_s is the switching period, and $(\Delta V_o/V_o)$ is the output voltage ripple as a

fraction of the average output voltage. The inductance used was 1mH and the same

switching period is used, 29 microseconds. The worst case here for the duty cycle is

minimum instead of maximum, so zero will be used. A voltage ripple of 0.1% is

acceptable in between stages. Using these numbers the capacitance would need to be

105uF or higher and with a design factor of 1.2 the capacitor rating would need to be

126uF. Another requirement of the capacitor is the ability to handle the voltage that it

would withstand. The highest average voltage from Table 4 is 23.22 volts, yet the

capacitor would be charged with as high as 300 volts and with the design factor the

capacitor should be rated for 360 volts. Finding a capacitor with these two ratings was not

achievable with the time and funding available, so a capacitor rated for as 330uH and 315

volts was used. The capacitance is well above that necessary, but the peak voltage was

lacking although still in the same magnitude. The peak voltage is not as much of a

concern as testing would not occur with an input voltage of 300 volts and the actual

voltage across the capacitor when working in steady state would near the average voltage,

much less than 315 volts.

As this was a first stage circuit from the fitness machine the discrete components

would need to be designed for 300 volts, since open circuit voltage testing showed the

maximum output voltage of the fitness machine to be 300 volts. All discrete components

considered within the design can be found in the parts list of Section A.4. The diodes are

rated for a breakdown voltage of 600 volts as a safety factor of 1.2 was used during

design and required a rating of 360 volts or higher.

L = 1mH

C = 330uF
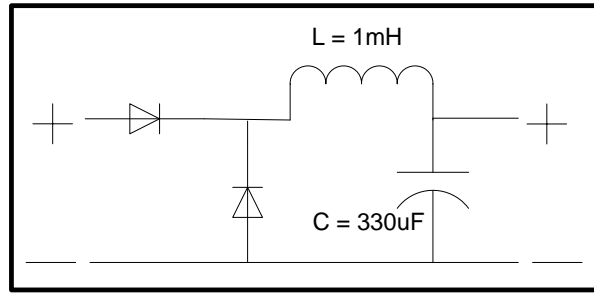
Figure 32 - Buck Rectifier

3.4 LC Low-Pass Filter

The low-pass filter, shown in Figure 33, was designed to replace the buck rectifier

to yield a more efficient circuit. The same components as the buck rectifier were used as

their rated values would need to be able to handle the same current and voltage. The buck

converter equations used in Section 3.3 would come out the same, since the diodes did

not affect the equations. In addition the cut off frequency of this LC low-pass filter can be

calculated using the equation below 0.

$$F_c = {}^1\!/_{\pi\sqrt{LC}} \tag{10}$$

Where F_c is the cut off frequency, L is the inductance, and C is the capacitance. With

1mH and 330uF the cut off frequency is 554 Hz. With a switching frequency 33.78 kHz

for the input voltage the calculated cut off frequency would work well, since it is over a

full order of magnitude under the switching frequency.
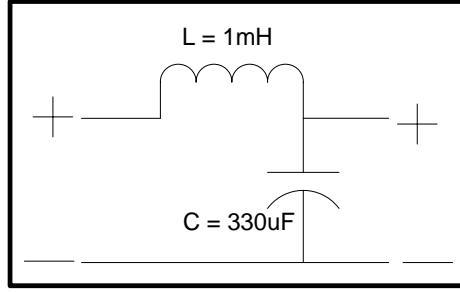
Figure 33 - Low-Pass Filter

3.5   Boost Converter

The boost converter, shown in Figure 34, was implemented as a method to redirect power at lower resistance levels, 2-14, when the average voltage measured was lower than 12 volts. An Arduino Duemilanove was used as the digital controller with the program given in Section A.2. The reason for removing the boost converter is explained in Section 4.2.3.

To reduce the size of the inductor and capacitor a switching frequency of 31.25kHz was used, because higher frequencies reduce the inductance and capacitance needed. The desired output voltage was set as 18 volts because it is the mean of 24V, the most efficient input voltage for the buck regulator, and 12V, the desired output voltage of the buck regulator. The inductance required to keep the boost converter in continuous current mode can be calculated below [14].

$$L = {V_o^2 D (1 - D)^2}\Big/{2 f_s P_o} \tag{11}$$

Where L is the inductance, D is the duty cycle, f_s is the switching frequency, P_o is the output power, and V_o is the output voltage. At steady state, the output voltage and switching frequency should be constant. The duty cycle was programmed with a limit of 80%, but with this non-linear relationship a 33% duty cycle would give the worst case inductance with respect to duty cycle. The lowest output power would give a worst case

40

inductance and from Table 4 the lowest power is 2.1 watts at a resistance level of 2. With these numbers the inductance is calculated to be 366uH and with a design factor of 1.2 the rated inductor value should be 440uH. With the current limited to 2 amps by the machine and since the boost should only increase voltage and not current, another 1mH inductor as used in the buck rectifier that fits the design requirements.

The equation below is used to find required capacitance to keep the voltage ripple within a given ripple [14].

$$C = {DP_o} / {f_s V_o^2 (\Delta V_o / V_o)} \tag{12}$$

Where C is the capacitance, D is the duty cycle, f_s is the switching frequency, P_o is the output power, V_o is the output voltage, and $(\Delta V_o / V_o)$ is the output voltage ripple as a fraction of the average output voltage. The program is limited to 80% duty cycle and for this equation it would give the worst case for selecting a capacitor. The highest power from Table 4 of 45.7 watts gives the worst case scenario, and a voltage ripple of 0.5% is acceptable in between stages. These values calculate a capacitance of 722uH and with a design factor of 1.2 the rated value should be 867uF or higher. The expected maximum voltage on the output of the boost converter would be 50 volts and would require a capacitor rated for 60 volts or higher with the design factor of 1.2. The capacitor used meets both requirements being rated for 1200uH and 65 volts.

Two other discrete components that needed to be sized were the power MOSFET and diode. The selected components can be found in Section A.4. With the a maximum input voltage of 23.22 volts, Table 4, expected and maximum input current of 2 amps the MOSFET needed to be rated for 28.0 volts and 2.4 amps. The MOSFET selected meets these requirements with ratings of 60 volts and 52.4 amps for the drain to source. The

diode would also need to be rated for 2.4 amps and 28.0 volts for if the transistor was not switching on and then the input voltage was quickly grounded, would be the worst case scenario. The diode used fulfills these requirements with ratings of 45 volts for its reverse breakdown voltage and 10 amps.

As described the expected maximum input voltage is 23.22 volts which is more than the desired output of 18 volts. If the input voltage was larger than the output voltage the program should reduce the pulse width until 0% duty cycle was achieved and the voltage just passes though without the transistor being used.

To create the feedback loop for the controller, the output voltage needed to be scaled down between 0-5 volts, because the controller's input can only handle this range. A voltage divider with a scale reduction of 10 is used to divide the expected output voltages of 0 to 50 volts down to 0 to 5. To reduce power loss from the voltage divider a 1K is used as R2 and 10K is used as R1. The resisters were quarter watt and a maximum of 220 milliwatts would be distributed between the two of them, although 50 volts on the output is well above what is expected. These values were calculated using ohms law and Equation 4 for power. As both resistors were a 5% tolerance, they were measured and their measurements were used for the program shown in Section A.2.
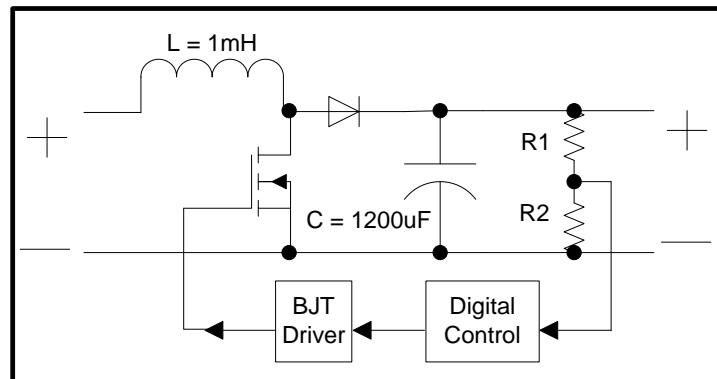
Figure 34 - Boost Converter

42

It was found during piecewise testing, Section 4.1.4, that the digital signal at

31.25kHz was not optimum to drive the MOSFET and a driver circuit was implemented

using NPN BJT transistors, listed in Section A.4. The +5 volt rail was from the Arduino's

5 volt power output. R4 is a 1000 ohm resistor to reduce losses in power and limit the

current through the BJT transistor to below 200mA. R3 is a 100 ohm resistor to allow as

much current to flow to charge the gate of the MOSFET to keep the switching clean at

31.25kHz. This low resistance still only allowed 50mA to flow through the BJT

transistor, 4 times below the rated current. The voltage drops across both resistors were

only 4.3 volts and did not allow their power rating of 250mW to be exceeded.
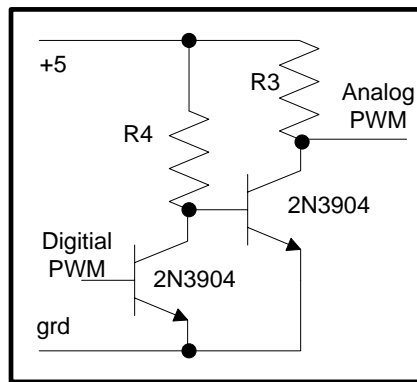
Figure 35 - MOSFET Driver Circuit with BJTs

3.6   NS Buck Regulator

The NS (National Semiconductor) buck regulator circuit, shown in Figure 36,

uses the LM2678T from National Semiconductor to regulate the output voltage at 12

volts. Equations 8 and 9 can be used again to determine the required inductance and

capacitance, respectively. The buck regulator is set at a switching frequency of 260 kHz,

which is a 3.85 microsecond switching period.

When calculating the inductance, using the worst case scenario the maximum

duty cycle is 1, and the lowest current would come from a resistance level of 15. With a

43

constant output voltage of 12 volts and an expected minimum output power of 14.1,

Table 4, the minimum current would be 1.175 A. The expected maximum input voltage is

23.22 volt, Table 4. Using these values the inductance should be 18.4uH and with a

design factor of 1.2 the rated value should be 22.1uH. With a constant output voltage of

12 volts and an expected maximum output power of 45.7, Table 4, the maximum current

would be 3.808 A. The maximum current with a design factor of 1.2 would require the

inductor to be rated for 4.57A. The inductor used, listed in Section A.4, meets both

requirements with an inductance of 120uH and current rating of 5.1A.

When calculating the capacitance the worst case scenario of the duty cycle is 0.

The inductance is 120uH and a voltage ripple of 0.1% is acceptable for the final stage.

These values calculate a capacitance of 15.4uf and with a design factor of 1.2 the rated

value needs to be 18.5uF or higher. The output voltage should stay at 12 volts and with

the design factor the rated voltage of the capacitor should be at least 15. The capacitor

used, listed in Section A.4, fulfills these requirements with the rated values of 330uH and

50 volts.

The LM2678 buck regulator has an internal MOSFET and is rated for 5 amps on

the output with a maximum input voltage of 40 volts. The diode within the buck

regulator, used to allow the continued flow of current when the MOSFET is switched off,

is rated for a voltage of 45 volts and a current of 6A. Both of these component's rated

values fulfill the requirements of the system.

The use of the second diode on the output of the buck regulator is not called for

within the LM2678 application notes. It is implemented for the purpose of not allowing a

flow back of power if there is an energy storage system on the output, such as a battery.

To be sure the output was 12 volts and not subtracted by the forward voltage of the additional diode, the feedback was connected to the cathode of the second diode. The second diode is a simple diode from RadioShack, listed in Section A.4, with a rated break down voltage of 50 volts and continuous current of 6 amps.
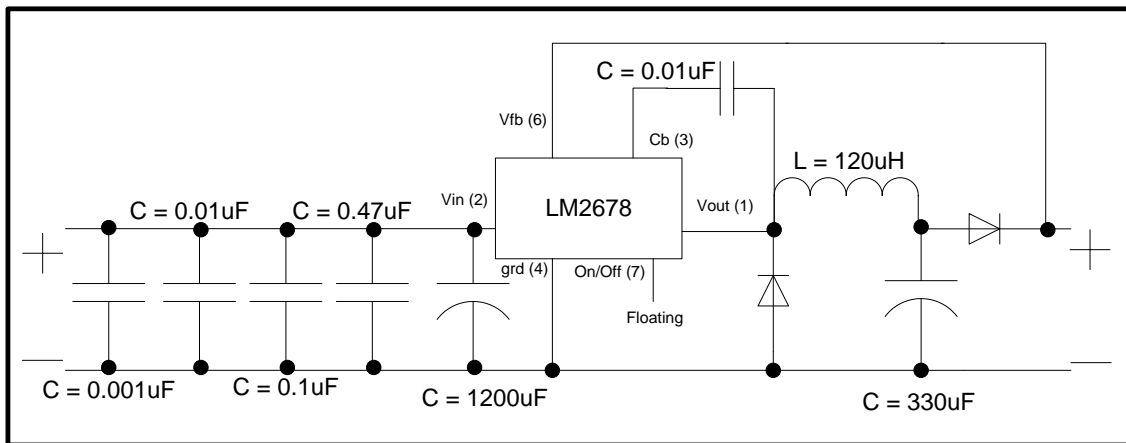
Figure 36 - Buck Regulator, LM2678 [16]

The ceramic capacitors on the input of the buck regulator were placed as a method to reduce current harmonics that were seen when the buck regulator was implemented, as seen in Section 4.1.5. The purpose of ceramic capacitors is to reduce the ESR (equivalent series resistance) of the input capacitors. Electrolytic capacitors have a relatively high ESR value and can result in current harmonics. With capacitance adding and resistance decreasing in parallel, the addition of low ESR capacitors in parallel can help reduce current harmonic issues without reducing the effective capacitance of the input. The reason for multiple capacitors was an attempt to obtain the correct frequency of the ringing within the current. Although no significant change in current harmonics were found during testing the capacitors were kept in place as they would not create a problem. As the attempt with using ceramic capacitors did not work to reduce the harmonics and the level of harmonics recorded were unacceptable to work with an inverter, a buck

converter with a lower switching frequency was implemented as testing showed the harmonics to occur at points of switching.

3.7   Arduino Buck Converter

The Arduino buck converter circuit, shown in Figure 37, uses the same discrete components as the NS buck regulator except for the MOSFET, driver, and controller circuitry. An Arduino Duemilanove was used as the digital controller with the program given in Section A.3. A switching frequency of 31.25 kHz, 32 microsecond switching period, was implemented, which is over 8 times lower than the NS buck regulator switching frequency of 260 kHz. This new switching frequency is also much closer to the fitness machine's switching frequency of 33.78 kHz. Components within this driver limit the input voltage as the driver uses the input voltage to bias the power MOSFET gate. The reason for this circuit to be a converter instead of a regulator is that the output voltage is dynamic to allow an automatic load change with the same resistance. This was implemented as an alternative to energy storage as voltage could rise at the input of the buck converter without a high enough load. It was programmed to regulate the output voltage between 11 to 14 volts.

The dynamics of the output voltage was implemented into the design on the realization that voltage could rise higher than expected on the input of the buck converter. This could occur because the fitness machine's output tries to achieve a constant power output and unless matched by the load, voltage would be built up on the input of the buck converter making it less efficient to match the powers. Without an energy storage system, such as a battery, the output power would be related only to the output voltage, constant load resistor, and heat loss. With a dynamic output voltage the load could be dynamic and

would change depending on the measured input voltage. The output voltage was nominally 12.5 volts, plus or minus 1.5 volts. Knowing the voltage change is a ratio change of 1.12 or 0.78, using Equation 4, and for a fixed resistance the output power could shift by 25% in either direction. It was expected that this would be enough flexibility for the program to avoid a built up of voltage on the input as the driver built had a potential for component failure at input voltages above 30 volts. Although during implementation a resistance too large was used and this 25% flexibility was not enough to avoid component failure during the third test.

The same discrete components were used from the National Semiconductor buck regulator. Equations 8 and 9 can be used again to determine if the change in switching frequency and output voltage would keep the components within requirements.

When calculating the inductance the duty cycle would still be 100%, and lowest current would come from a resistance level of 15. With a maximum output voltage of 14 volts and an expected minimum output power of 14.1, Table 4, the minimum current would be 1A. The expected maximum input voltage is still 23.22 volt. Using these values the inductance should be 196uH and with a design factor of 1.2 the rated value should be 235uH. With a minimum output voltage of 11 volts and an expected maximum output power of 45.7, Table 4, the maximum current would be 4.155 A. The maximum current with a design factor of 1.2 would require the inductor to be rated for 4.986A.

When calculating the capacitance the worst case scenario of the duty cycle is 0. The inductance is 120uH and a voltage ripple of 0.1% is acceptable for the final stage. These values calculate a capacitance of 1.1mF and with a design factor of 1.2 the rated

47

value needs to be 1.3mF or higher. The maximum output voltage being 14 volts and with the design factor the rated voltage of the capacitor should be at least 16.8 volts.

The inductor was only outside of the rated value for inductance by less than a multiple of 2, but in the correct magnitude. The capacitor was outside of the requirement for capacitance by almost 4 times and was not in the correct magnitude. Using the 330uF capacitor it would be expected that the output voltage ripple would be 0.32%. The slight variations in currents and voltages allowed the same diodes to be used and stay within the requirements.

The voltage divider for the input voltage, R1 and R2, uses the same scale and resistors as the boost converter described in Section 3.5. R3 and R4 were found the same way but for a scale reduction of 4 where 0-20 volts are reduced to 0-5 volts. . To reduce power loss from the voltage divider a 5.1 kilohm is used as R4 and 14.7 kilohm is used as R3. The resisters were quarter watt and would expect at max 20 milliwatts distributed between the two of them. As both resistors were 5% tolerance, they were measured and their measurements were used for the program shown in Section A.3.
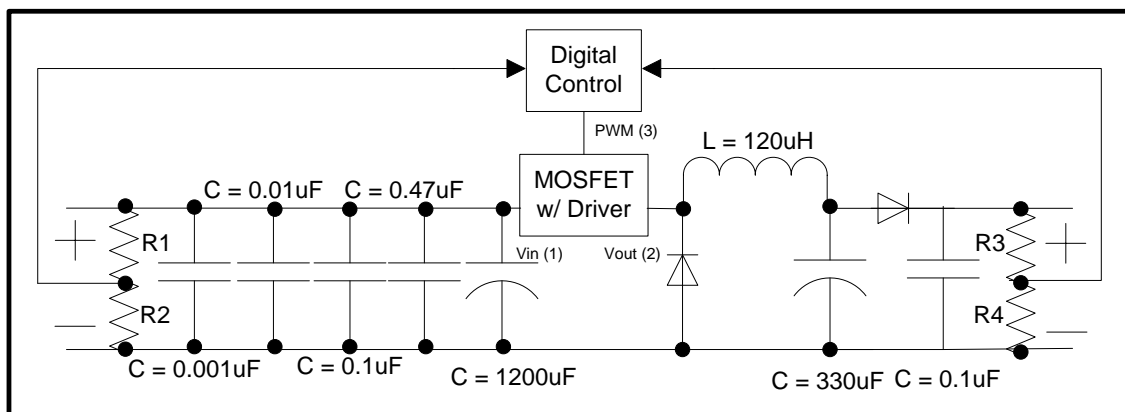
Figure 37 - Buck Converter

The LM2678's internal MOSFET was replaced by the same MOSFET implemented in the boost converter and a driver was designed, shown in Figure 38. The

48

rated drain to source voltage of 60 volts and 52A current still met the requirements. Yet, a

new requirement that was necessary of the MOSFET was the gate to source voltage,

which is rated for $\pm$ 20 volts. With a minimum expected output voltage of 11, the

maximum input voltage could only be 31 volts because of how the driver uses the input

voltage to bias the MOSFET. As described in Section 4.1.4, the digital control from the

Arduino was not ideal at 31.25 kHz, and to solve this issue BJT transistors were used as

buffers and inverters. In the driver, the BJT, controlled by the other BJT, is used to pull

the voltage at the gate down to open the MOSFET. When this BJT transistor is open the

MOSFET gate is pulled up by the bias of the input voltage and closes the MOSFET. R1

was set at 400 ohms to allow fast charging of the MOSFET gate for switching at

31.25kHz, but also to limit current flowing though the BJT pulling the voltage down.

With an input voltage of 40 volts the current that could flow through the BJT transistor

was only 100mA and meet the requirements of the BJT's max current rating of 200mA.

R3 was set at 100 ohms as it would limit the current to the required rating, but still allow

fast switching. R2 was set at 10 ohms to limit the current from the built up gate charge

when discharging.
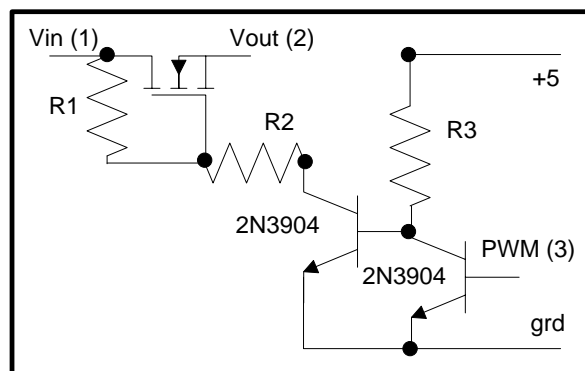
Figure 38 - Buck MOSFET with Driver

3.8   Final Circuit

The final circuit to be implemented, given in Figure 39, uses the voltage and current measurement circuits on the input and output of the circuit for measuring efficiency. The buck rectifier is used as the first stage for flattening the pulses from the fitness machine before being bucked down to controlled voltage of 11 to 14. The circuit was tested with an adjustable load resistor to simulate a variety of loads.
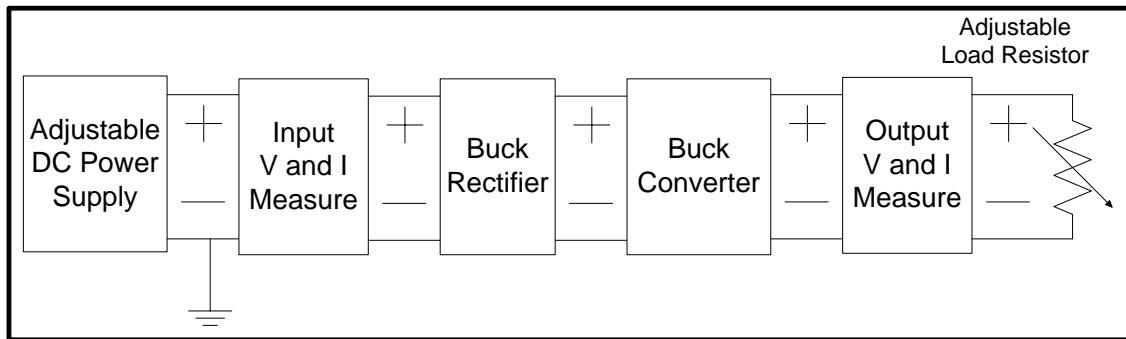
Figure 39 - Tested Circuit Used in Implementation as a Block Diagram

3.9   Heat Sinks

The power dissipated by the switching components was found by either measurement or calculations under a worst case scenario. A heat sink, given in Section A.4, was chosen as it could dissipate 2.5 watts. Finding the heat dissipation required of the diodes was found from the product of forward voltage, expected maximum current, and duty cycle. The diodes used in the buck rectifier have a forward voltage of 1.5 volts, an expected maximum current 2 amps, and a maximum duty cycle of 100%. These values would calculate a loss of 3 watts. The diode used in the buck regulator and converter has a forward voltage of 0.6 volts, an expected maximum current of 5 amps, and a maximum duty cycle of 100%. The buck diode would cause a loss of 3 watts during its worst case scenario. Although these two calculations, found under worst case conditions, gave losses

50

higher than the rated value of the selected heat sink, diode failure from heat was not a concern as the tests would be short in comparison to actual use. The MOSFETS required piecewise testing to determine their losses and heat issues are discussed in their respective sections if there were high losses. Calculations done may call for larger heat sinks when designs are finalized to increase circuit lifetime.

3.10   Simulations

Programs used to help in the design phase for simulating the circuit were MATLAB and Simulink from MathWorks and SPICE.

3.10.1   Simulink

Simulink was used due to availability of the recently developed power systems toolbox and it allowed for more control, because MATLAB could be used alongside with it to improve simulation results. The MATLAB code used to produce the results below and Simulink file screenshot are given in Section A.5 and A.6, respectively. Losses with diodes and MOSFETS were modeled with values from component specification sheets. Series resistances of capacitors and inductors were modeled as zero ohms, ideal conditions. The MOSFET driver was modeled as ideal, because the program did not require the MOSFET's gate-source value to be above 5 volts but only its gate value. The program used in the buck controller follows a similar digital logic order to what was implemented in the Arduino for adjusting the duty cycle to achieve a given desired voltage. It was assumed from piecewise testing that the program was able to change the duty cycle after 1000 cycles of the PWM and this multiplication factor was used in the simulation. In these simulations, the issue of power matching did not arise because it was not possible to replicate the actual controller found in the fitness machine. With the

51

absence for the need of power matching in simulation, the desired output voltage was kept at 12.5 volts. The adjustable DC power supply was modeled as having a voltage source with infinite current and was pulsed with an ideal switch. The diode used for the adjustable DC power supply used the default settings of the power systems toolbox. All significant values can be found within the MATLAB code and would match components described in Sections 3.3 and 3.7. The data used to simulate the input voltage is the duty cycle, period, and peak voltage at 60 RPM for simulations shown here. The load during all simulations was at 10 ohms.
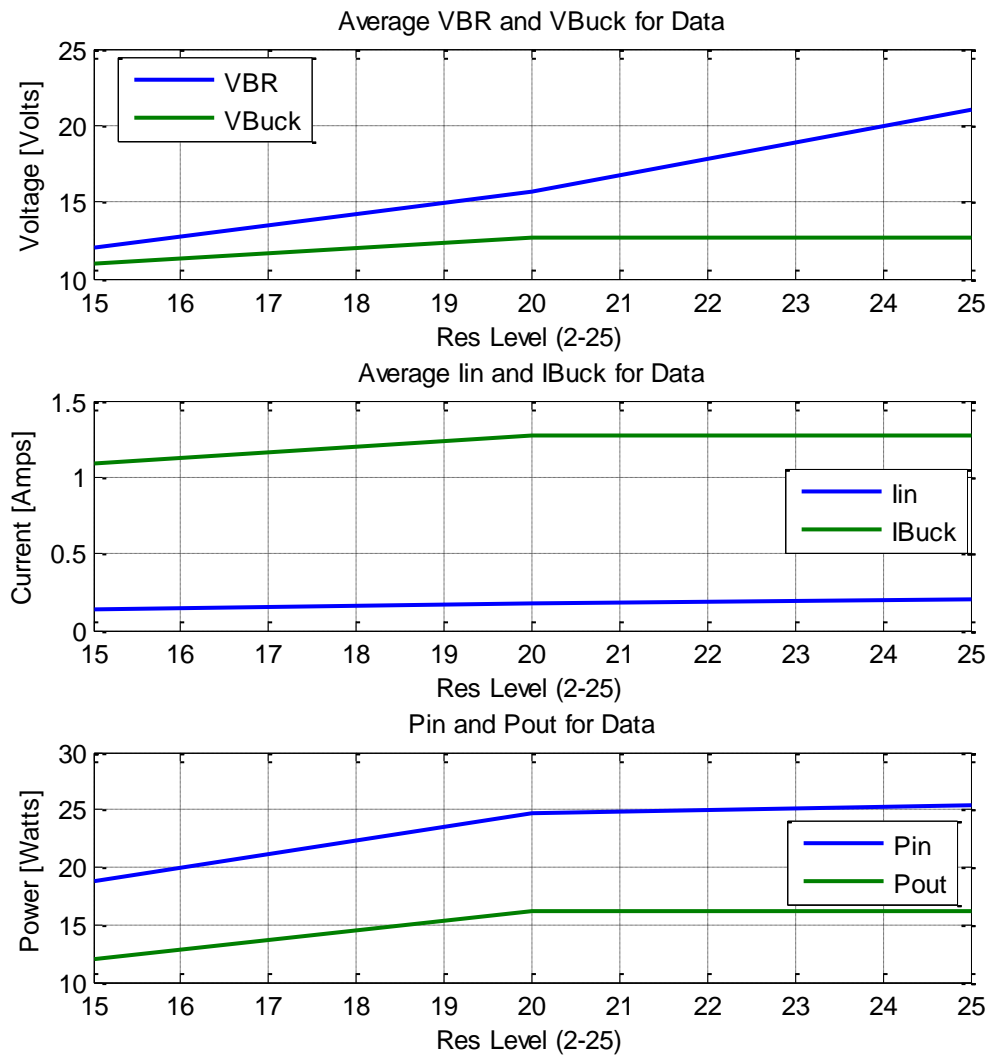
Figure 40 - Average Values for Resistance Levels 15, 20, and 25 at 60 RPM
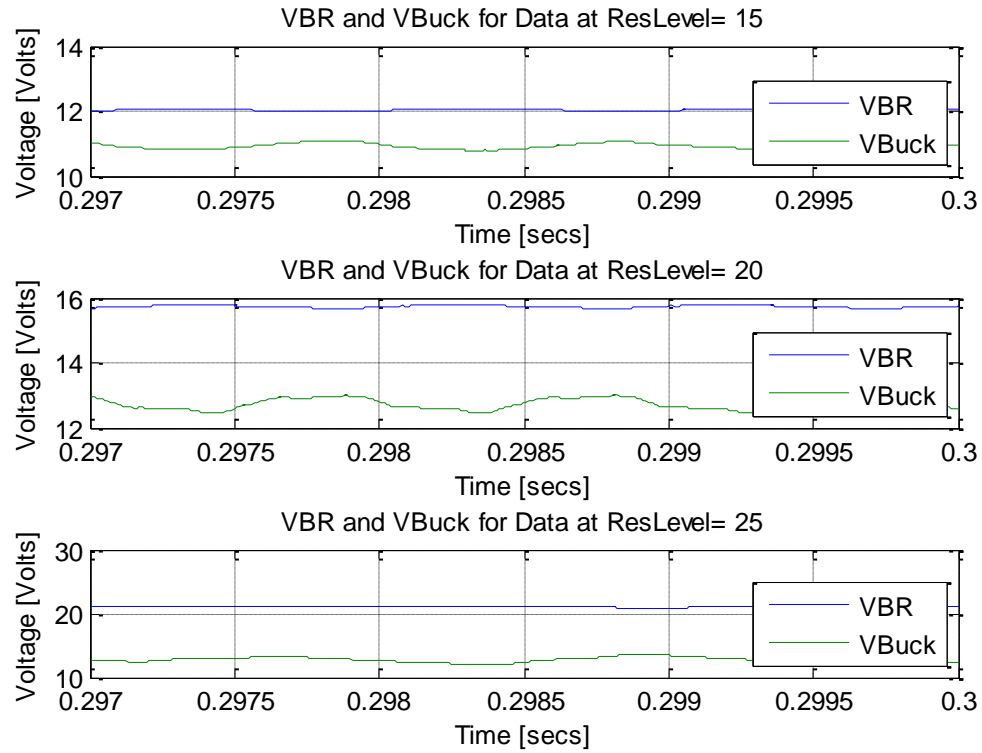
Figure 41 - Simulink Simulation Voltage at Steady State
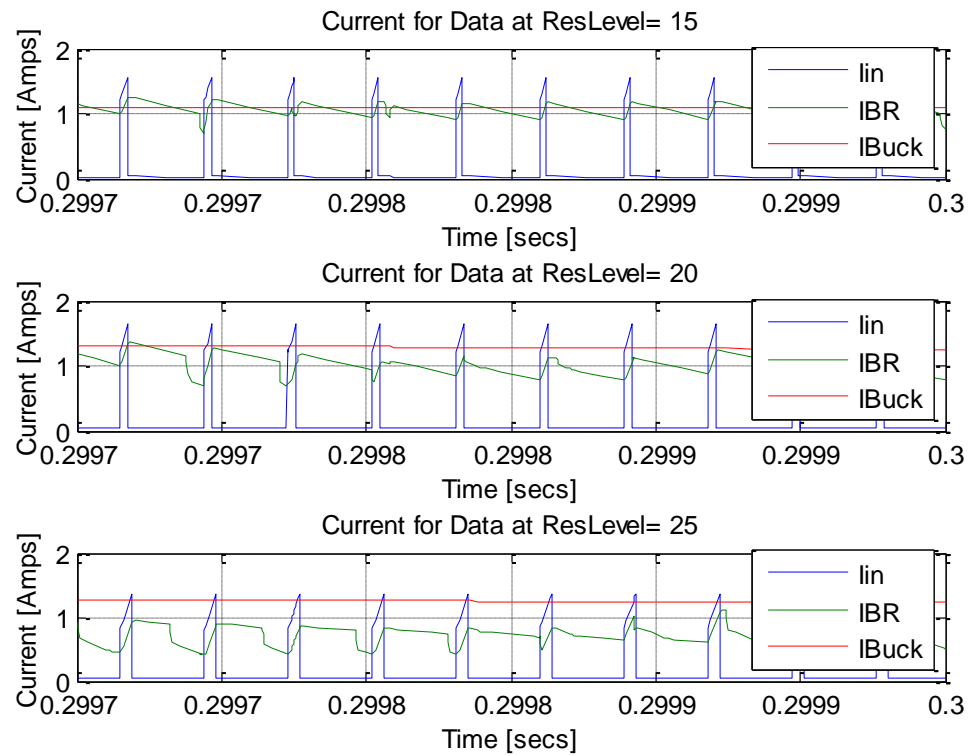
Figure 42 - Simulink Simulation Current at Steady State

Figure 41 and Figure 42 time axis were reduced to the last 1% and 0.1% percent, respectively, to show the simulation waveforms of voltage and current. The runtime of the simulation was set at 0.3 seconds. Only with a resistance level of 20 or 25 was the desired voltage, 12.5 volts, achieved. With a resistance level of 15, the average input voltage was not high enough to achieve 12.5 volts and caused the buck to not be able to achieve 12.5 volts. The power between resistance level 20 and 25 was not much different and showed that the simulated circuit would not pull more power without a new load resistor value and voltage would not buildup on the input of the buck converter. Yet during implementation, it was found that input power was not controlled as much by the load but by the circuit within the fitness machine and did cause the voltage buildup on the input of the buck converter.

During implementation the issue of current spikes and harmonics first arose with the buck regulator, Section 4.1.5. It was also later determined that the harmonics were unacceptable with the data in Section 4.2.4. This problem was not apparent during simulations using Simulink, shown in Figure 42 and called on simulations to be done in a program more specific to circuit analysis.

3.10.2   LTspiceIV

LTspice was chosen because specific circuit models for Pspice were not available and a library of comparable discrete components was available from the developer of LTspice, Linear Technology. With using spice the program would require less ideal assumptions when simulated and using components modeled within the library makes that possible. A screenshot of the schematic file is given in Section A.7 and gives reference to all components used. The case simulated in LTspice was for a resistance level of 25, where the peak voltage is 160, duty cycle is 14%, and period is 29

microseconds. A feedback controller was not added as it was possible to estimate the necessary duty cycle necessary for the Buck to achieve 12.5 volts. The simulation was run for 10 milliseconds and was only recorded from 9.8 milliseconds for steady state waveforms. The simulation for input current, Figure 43, did show the issue of current harmonics with spikes at both the time of the transistor opening and closing for the adjustable DC power supply of the fitness machine. The output current, Figure 44, did have spikes, but were only 0.8% of the average current. During implementation, the harmonics were much larger for both the input and output current but the relationship of input to output spikes was the same, input being larger than output. The figures below were created using MATLAB, but the data was exported from LTspice after running the simulation in Section A.7.
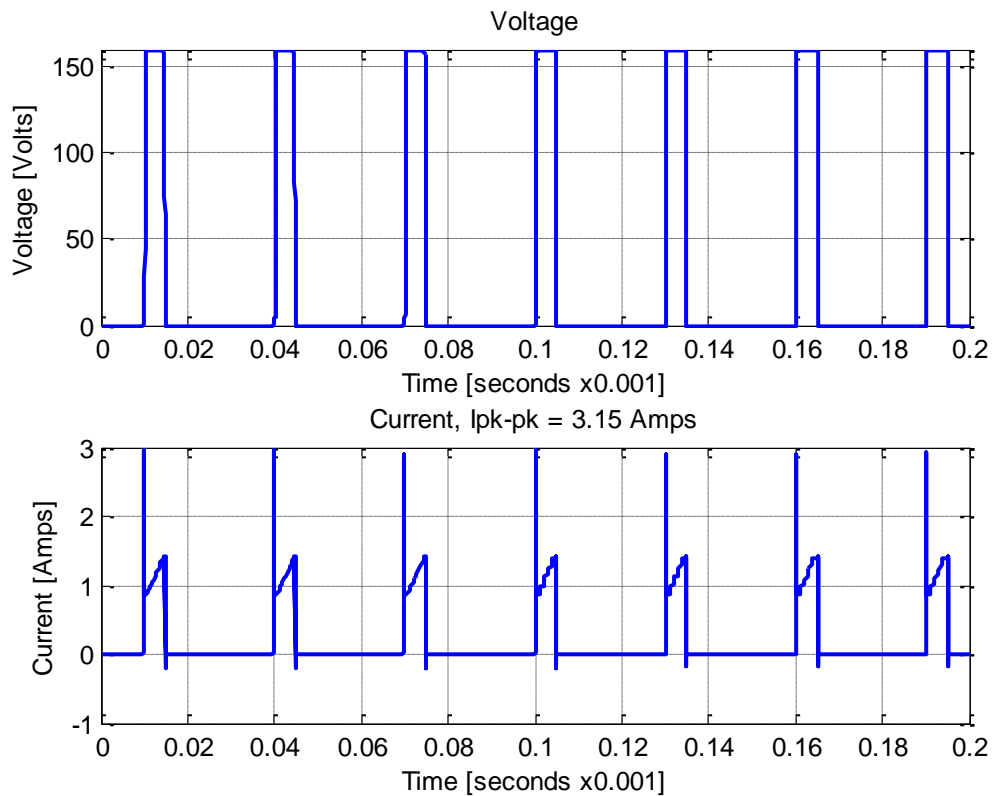
Figure 43 - Spice Simulation Input Voltage and Current
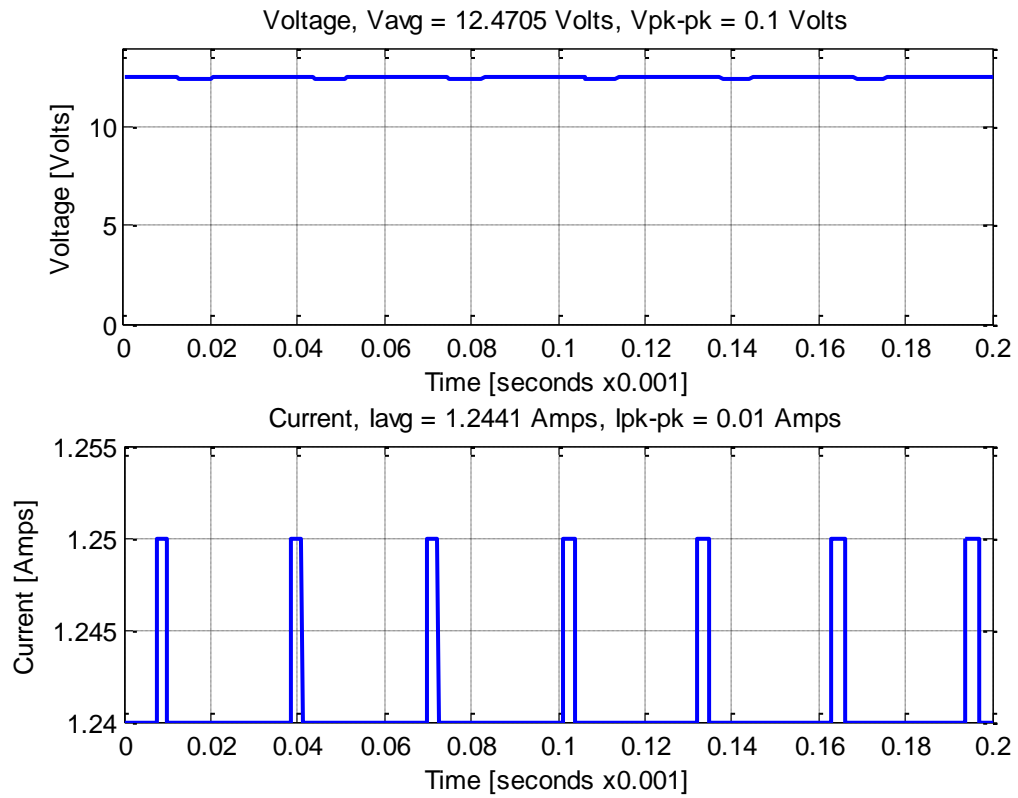
Figure 44 - Spice Simulation Output Voltage and Current

56

Chapter 4:   Implementation

Multiple rounds of testing the circuit were done both in a controlled lab for piecewise (individual stages) testing and at SUNY Cortland with the Precor recumbent stationary bicycle, C846. Piecewise testing was done on each individual stage of the circuit, including the LC low-pass filter, buck rectifier, boost converter, buck regulator, and buck converter. Testing at SUNY Cortland was done cumulatively with the first stage of a circuit tested before adding another stage. The oscilloscope used in testing is the Tektronix TDS2002B and is capable of recording measured data though its USB slot.

4.1   Piecewise Testing

Before testing the overall circuit at SUNY Cortland, piecewise testing with controlled input voltages and currents was done. The lab available did not have a pulse generator meant for high voltage or high power so the DC power source, Instek GPS-3303, was used. Without a power pulse generator the buck rectifier and low-pass filter could not be tested for their primary purpose of flattening the pulse coming from the fitness machine, but only for power rating and possible manufacturing issues.

Other stages that expected a DC voltage input were given a controlled voltage while being loaded by a resistor set to pull an expected current value. This allowed for testing the circuit for component failure and performance before traveling on-site to Cortland University.

4.1.1 VI Measurement Circuit

The voltage and current measurement circuit was first tested using a 10.1 ohm load, the DC power source display, and the oscilloscope. The circuit can be seen in Figure 30. The power source display gave 12.0 V and 1.18A. The oscilloscope measured with the voltage and current measurement circuit 12.1V and 1.25A, as shown in Figure 45. The circuit had an error of 6% in current and 1% in voltage. This can be attributed to knowing only the current resistor value to one significant digit. To keep losses low and avoid current harmonics the current sensing resistor was kept at 0.05 ohms. Figure 45 was created using MATLAB code from Section A.17.
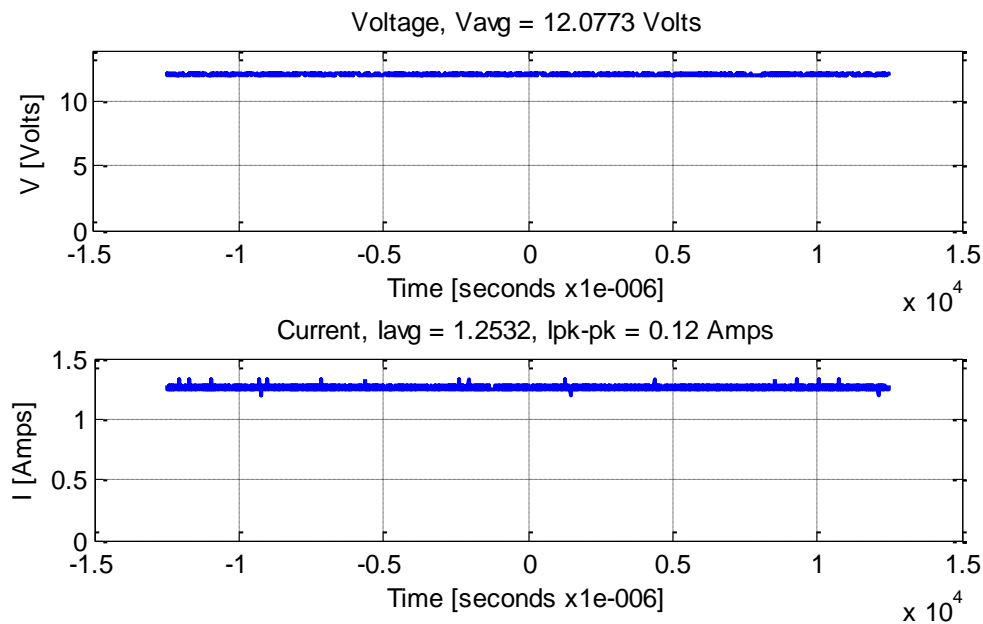
Figure 45 – Piecewise Test VI Measurement Circuit Piecewise Test

4.1.2 LC Low-Pass Filter

The low-pass filter, described in Section 3.4, was tested to replace the buck rectifier to achieve a higher efficiency. Although, during implementation discussed in Section 4.2.1, issues lead to use of the buck rectifier again. The low-pass filter was tested with a load of 20 ohms and the lab DC power supply set at 18.1V and 0.88A. The input

data, shown in Figure 46, gave an input power of 16.3 watts. The output data, shown in

Figure 47, showed an output power of 16.2 watts. This gives an efficiency of 99.4%. This

high efficiency makes sense as all the components in the circuit were passive.
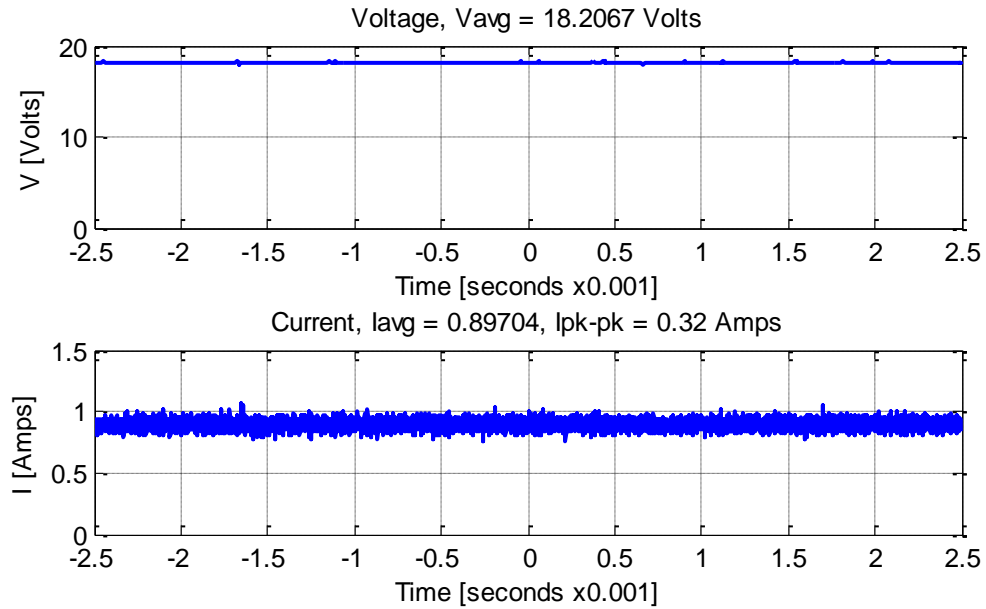
Figure 46 - Piecewise Test Input Data for Low-Pass Filter
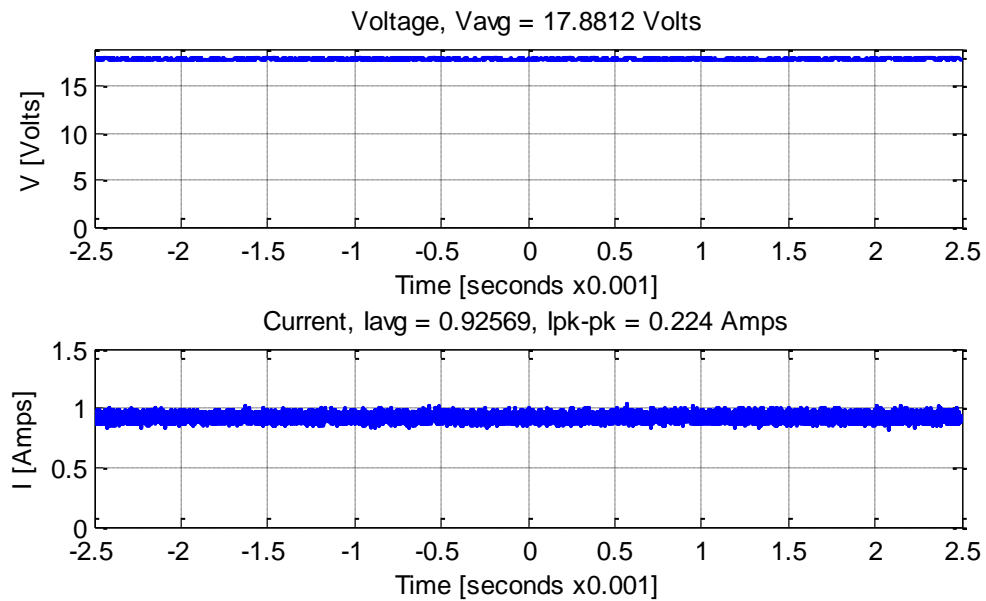
Figure 47 - Piecewise Test Output Data for Low-Pass Filter

4.1.3 Buck Rectifier

The buck rectifier, as described in Section 3.3, was used early on to protect the fitness machine and flatten the pulse created by the adjustable DC power supply, and during implementation was found to be the best option. The buck rectifier was tested with a load of 20 ohms and the lab DC power supply set at 10.0V and 0.42A. The input data, shown in Figure 48, gave an input power of 4.8 watts. The output data, shown in Figure 49, gave an output power of 4.4 watts. This gives an efficiency of 91.7%. The lower efficiency compared to the low-pass filter results from the use of the active components and diodes.
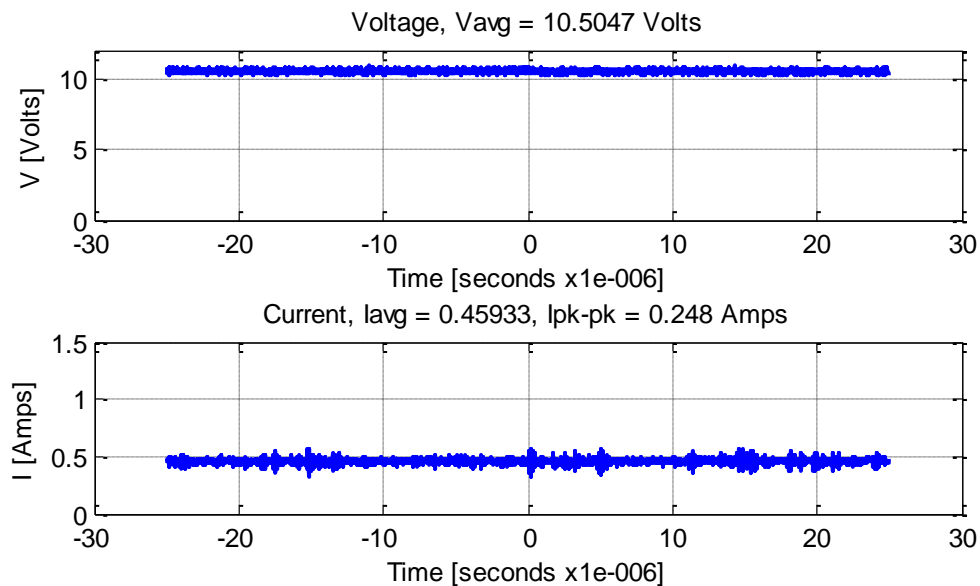
Figure 48 - Piecewise Test Input Data for Buck Rectifier
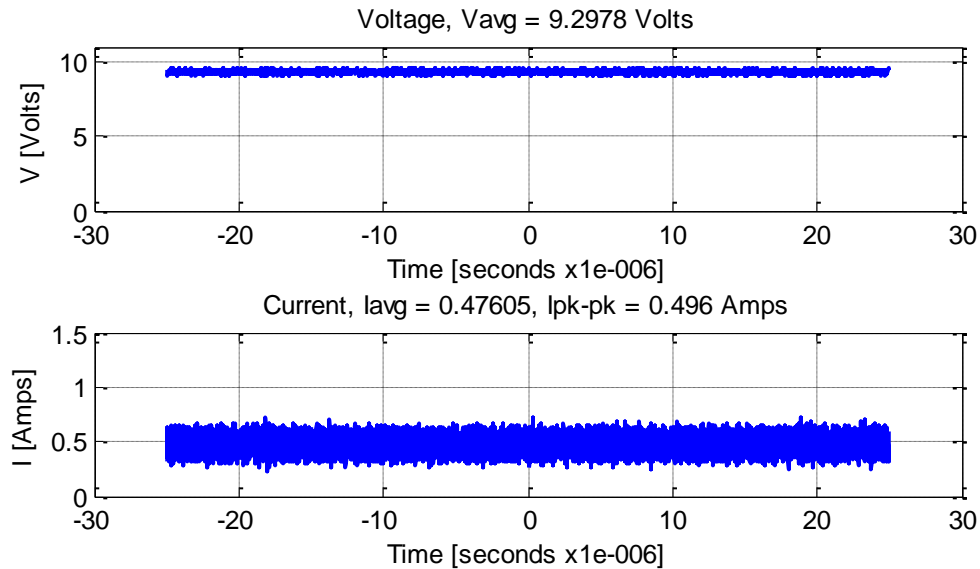
Figure 49 - Piecewise Test Output Data for Buck Rectifier

4.1.4 Boost Converter

The boost converter, described in Section 3.5, was to be used to boost lower

resistance level voltages to a higher voltage so that they could be used in the 12 volt line

between machines. The boost converter was tested with a load of 20 ohms and the lab DC

power supply set at 12.2V and 1.44A. The input data, shown in Figure 51 gave an input

power of 18.8 watts. The output data, shown in Figure 52, gave an output power of 16.7

watts. This gives an efficiency of 89.0%. This test trial was done while the boost

converter was trying to achieve an 18 volt output with the program settling on a duty

cycle of 30.25%. This was achievable by using BJT transistors, 2N3904, as a power

MOSFET driver. The comparison of driving pulse width modulation with and without the

use of BJT transistors is given in Figure 50. These two test trials are while running the

boost converter with the same input voltage, desired output voltage and resistive load. It

was found that with just using a digital signal the pulses had spikes above 5 volts and

below 0 volts. Using the BJT transistors it became smoother and more efficient. The

increased efficiency was quickly seen in the input current being higher by 0.24A without the driver circuit and with both having an input voltage of 12.2 volts the power loss was reduced by 2.9 watts. Figure 50 was created using the MATLAB code in Section A.18.
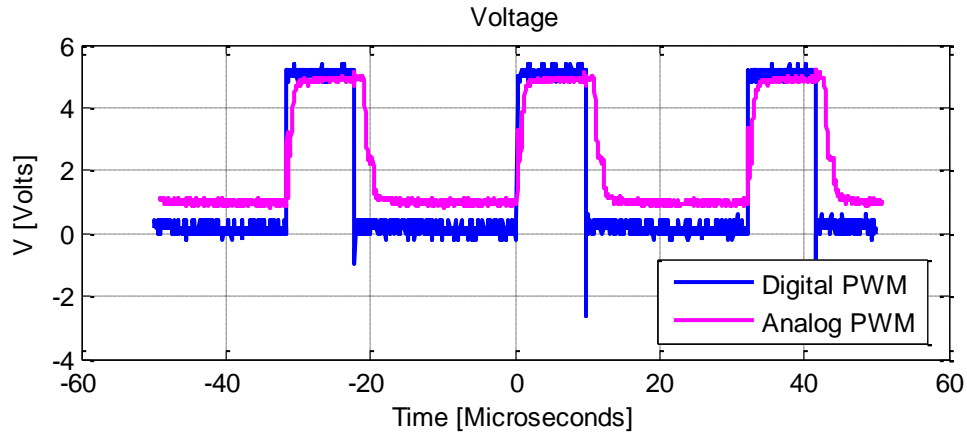
Figure 50 - Piecewise Test Pulse Wave Modulation, Digital vs. Analog
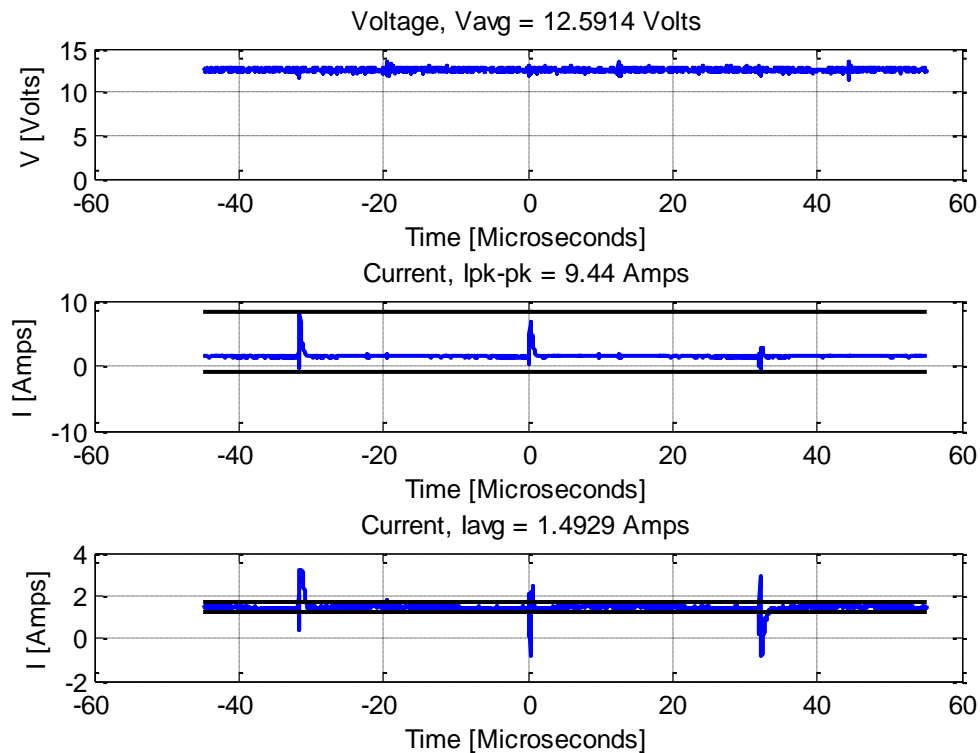
Figure 51 - Piecewise Test Input Data for Boost Converter
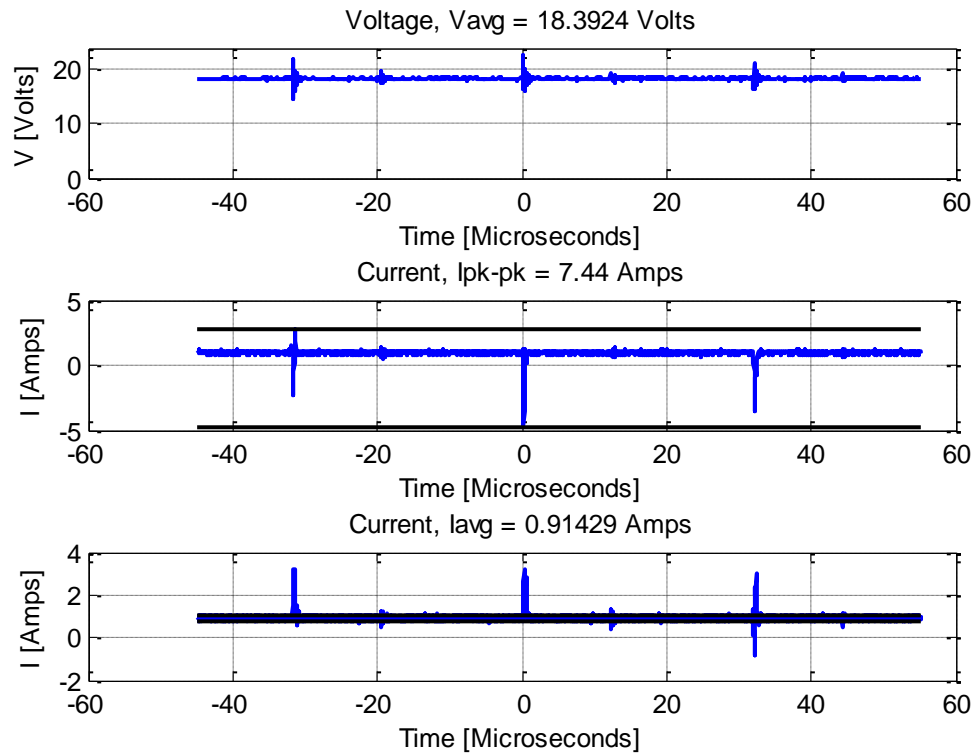
Figure 52 - Piecewise Test Output Data for Boost Converter

4.1.5 NS Buck Regulator

The NS (National Semiconductor) buck converter, described in Section 3.6, is

used to step the voltage down to a regulated value of 12 volt for a common voltage

between machines used. The buck regulator was tested with a load of 20 ohms and the

lab DC power supply set at 18.1V and 0.43A. The input data, shown in Figure 53, gave

an input power of 7.8 watts. The output data, shown in Figure 54, gave an output power

of 7.4 watts. This gives an efficiency of 95.4%. The current spikes that were recorded

while testing the boost converter were short and could be considered as noise but the

current for the buck regulator has a significant ringing affect. With further investigation

the ringing was occurring during the change of the pulse width modulation (PWM)

within the controller, either rising or falling. This can be seen with the switching period is

3.84 microseconds, from knowing the switching period to be 260 kHz. It can be

63

estimated from Figure 53 that the start of the smaller ringing relative to the start of the

larger rings is 2.7 microseconds away and would infer a duty cycle of 70%. Knowing the

input and output voltage the duty cycle of the buck converter PWM was calculated to be

68% with the equation below.

$$V_o = DV_{in}$$ (13) [17]

Where V_o is the output voltage, V_{in} is the input voltage and D is the duty cycle. The duty

cycle being off by only 3% is neglect able and supports the assumption that the ringing is

related to the time when the MOSFET is changed from opened to closed or vice versa.
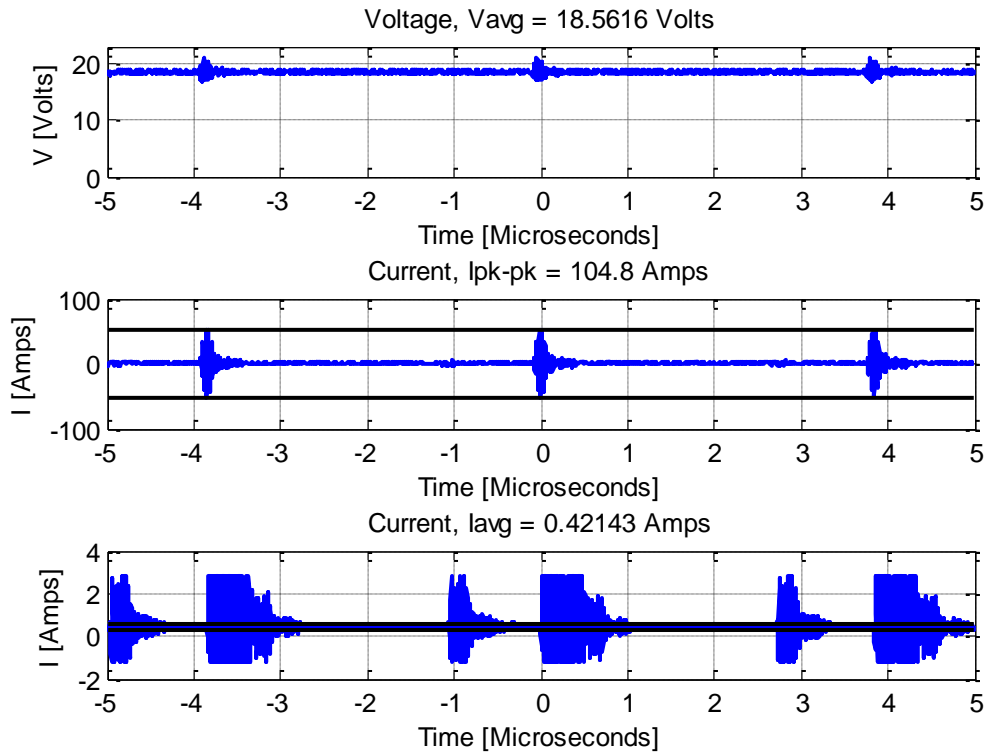
Figure 53 - Piecewise Test Input Data for Buck Regulator
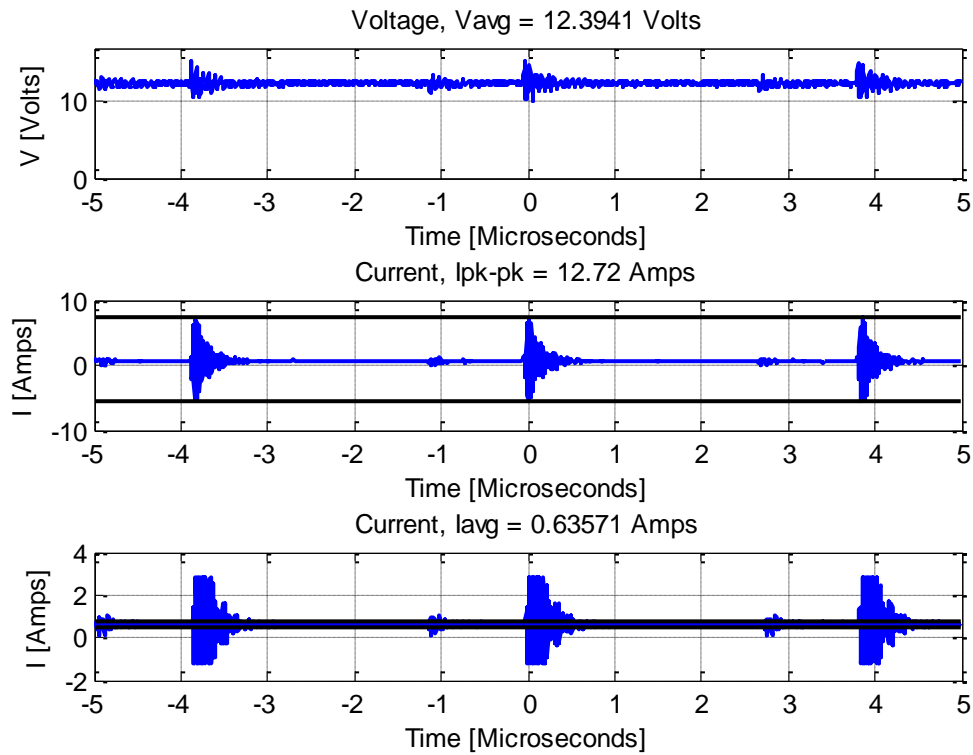
Figure 54 – Piecewise Test Output Data for Buck Regulator

4.1.6 Arduino Buck Converter

The buck converter, described in Section 3.7, was to be used to replace the

National Semiconductor buck regulator to control more attributes and reduce current

harmonics. The buck converter was tested with a load of 20 ohms and the lab DC power

supply set at 18.5V and pulled 0.50A. The input data, shown in Figure 56 gave an input

power of 9.70 watts. The output data, shown in Figure 57, calculated an output power of

7.86 watts. This gives an efficiency of 81.7%. This low efficiency does raise concern

about heat buildup with tests at higher power. This test trial was done while the boost

converter was trying to achieve a 12.5 volt output with the program settling on a duty

cycle of 80.5%. The driving pulse width modulation with the digital pulse width

modulation from the Arduino is given in Figure 55, created using the MATLAB code in

Section A.18, and shows how the driver achieves the necessary bias on the power

MOSFET.
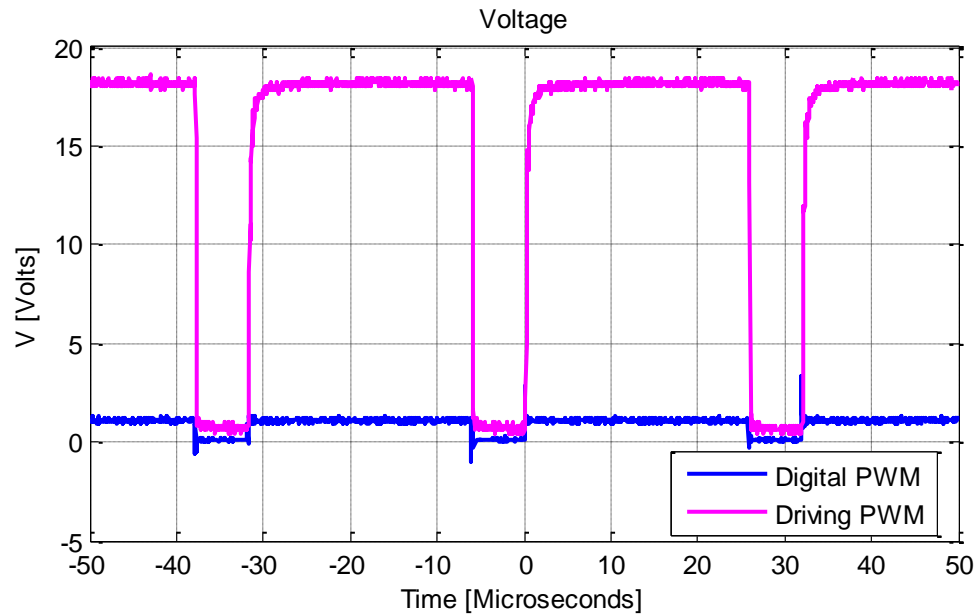
Figure 55 - Piecewise Test of Arduino Buck Driver Circuit
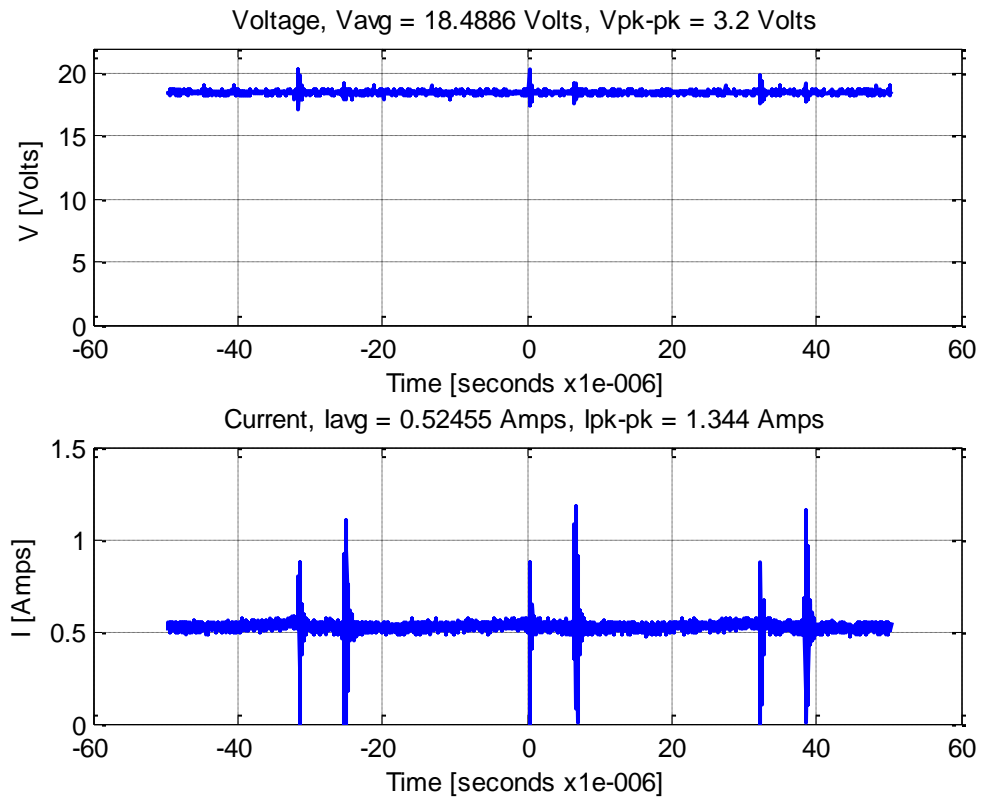
Figure 56 - Piecewise Test Input Data for Arduino Buck Converter
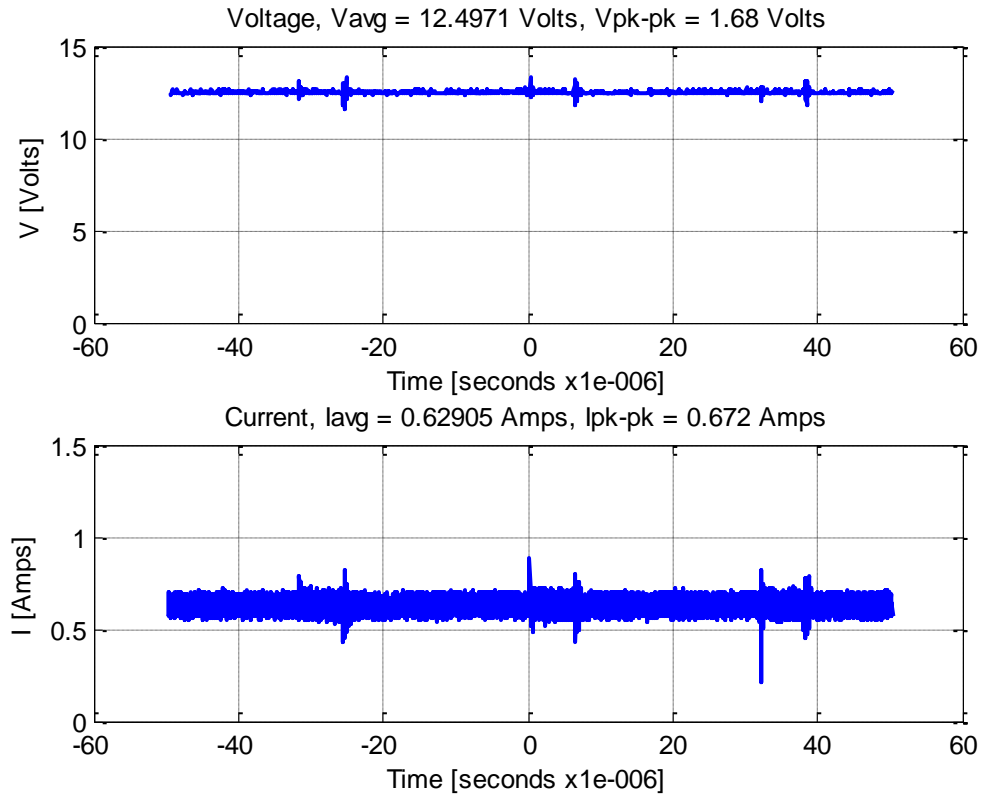
Figure 57- Piecewise Test Output Data for Arduino Buck Converter

4.2   Cumulative Testing with Precor C846i

During on site implementation, the circuit was tested cumulatively as an earlier

stage in the circuit was required for the next stage to work properly and reduce the

possibility of component failure. The fitness machine used for all implementations was

the Precor recumbent stationary bicycle, C846. This process was modified when lower

resistance levels were eliminated from the requirements of the circuit for functionality

and allowed the booster converter stage of the circuit to be removed. After investigation

of the source circuit, both the buck rectifier and low-pass filter were tested, but for all

multistage tests the buck rectifier is used and not the low-pass filter. Before

implementation on the fitness machine, measurements of normal operation under the

same user inputs, resistance level and speed, were recorded and can be seen in Figure 18, Figure 20, and Figure 22 with data in Table 4.

As expected, during these tests the physical resistance the user felt was significantly reduced and only when increasing the load on the tested circuit was the user experiencing a notable physical resistance. The resistance level would contribute to what physical resistance the user felt, as the power going through the tested circuit was still being limited by the adjustable DC power supply.

The figures of input data and figures of output data in Section 4.2 were created using MATLAB code from Section A.11 and A.15, respectively.

4.2.1   LC Low-Pass filter

The low-pass filter (LPF) was tested at a resistance level of 25, at 60 RPM, and with a 20 Ohm load. Figure 58 is a block diagram of the cumulative testing done in this section. The input data, shown in Figure 59, gave an input power of 18.2 watts. The output data, shown in Figure 60, calculated an output power of 54.8 watts. These two measurements lead to the issue energy conservation as output power was greater than input power. It was intended for the low-pass filter to improve efficiency, but not to this degree. The issue is believed to arise from measuring input power and the use of the diode in the fitness machine.
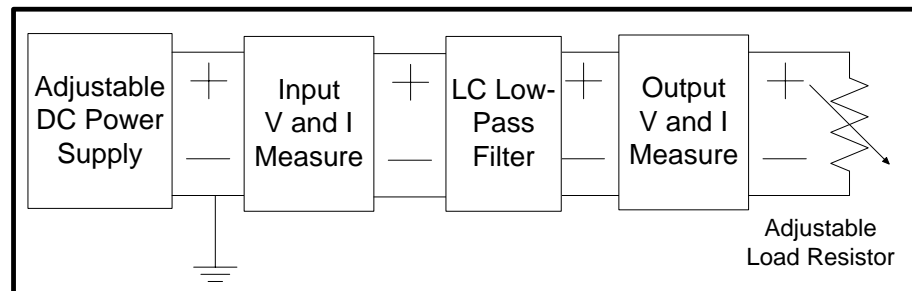
Figure 58 - Block Diagram of Cumulative LC Low-Pass Filter Implementation
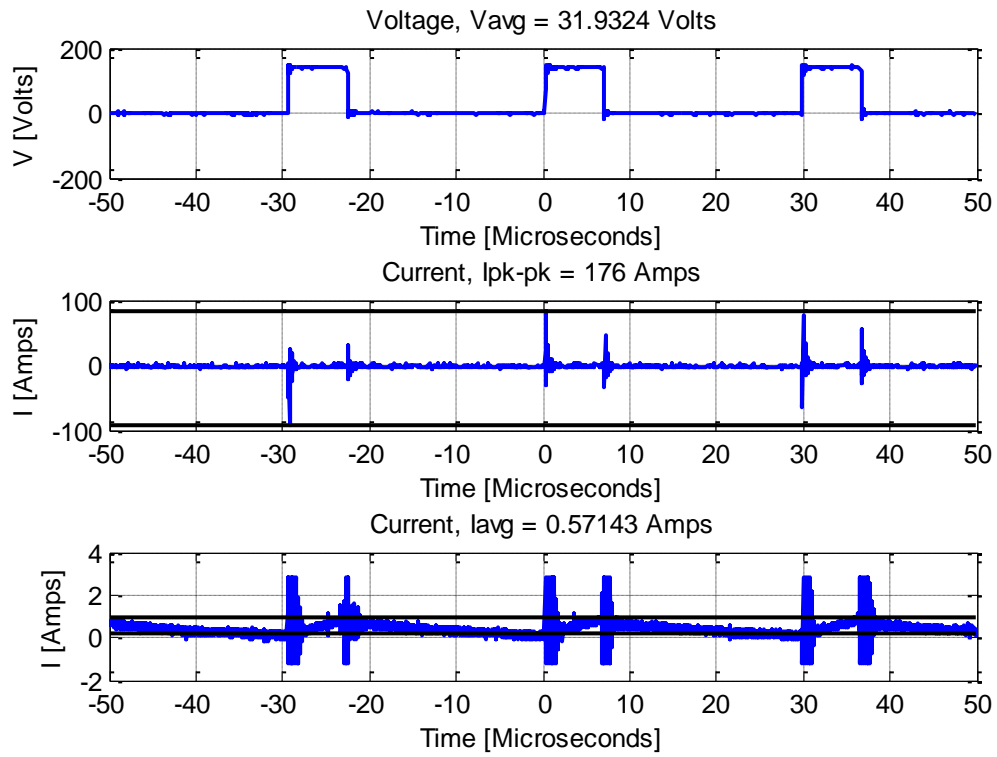
Figure 59 - Implementation Input Data for Low-Pass Filter at Res Level 25
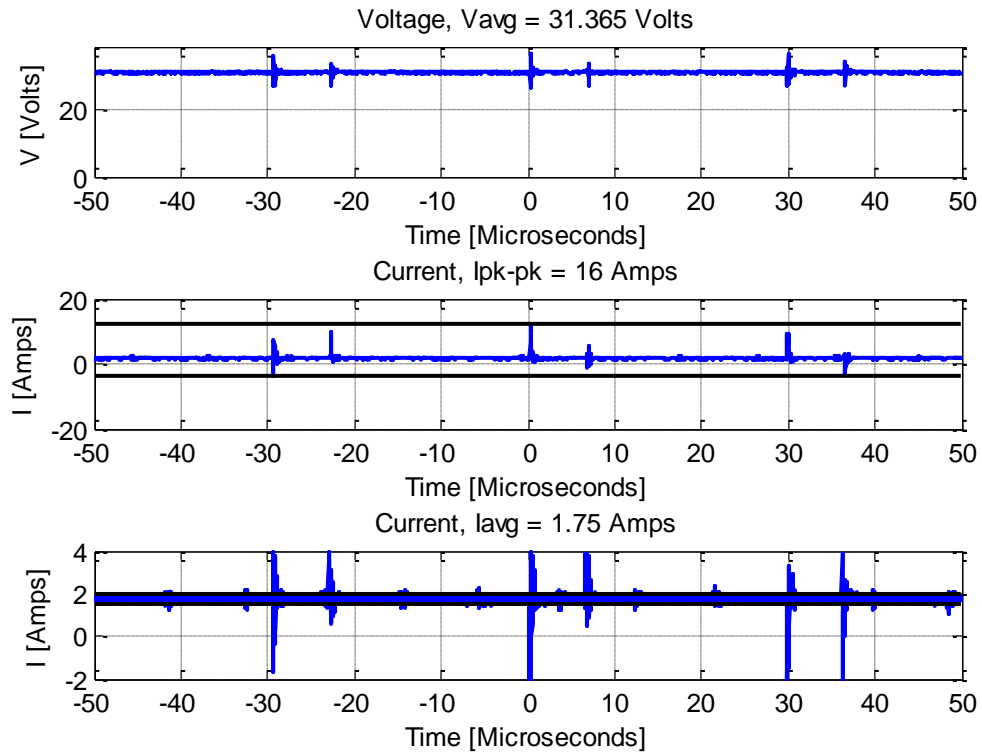
Figure 60- Implementation Output Data for Low-Pass Filter at Res Level 25

4.2.2 Buck Rectifier

The buck rectifier was implemented with a load of 20 ohms and the fitness machine was run at 60 RPM. The buck rectifier would replace the low-pass filter, so only the current circuit is used as the first stage in the concluding tests, as shown in Figure 61. The input data, shown in Figure 62, gave an input power of 14.27 watts. The output data, shown in Figure 63, gave an output power of 14.20 watts and gives an efficiency of 99.5%
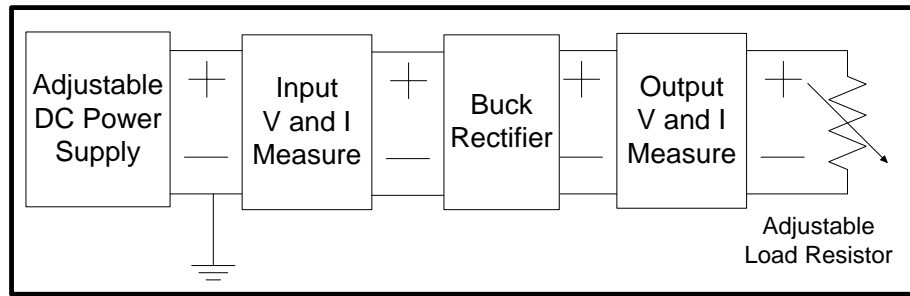
Figure 61 - Block Diagram of Cumulative Buck Rectifier Implementation
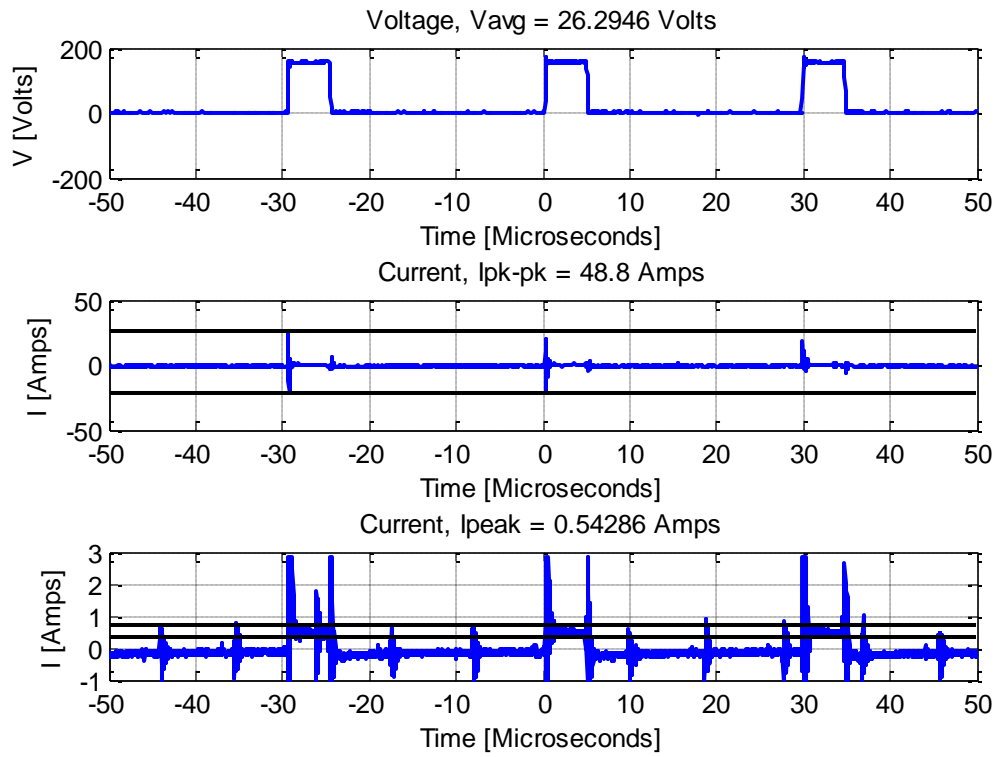
Figure 62 - Implementation Input Data for Buck Rectifier at Res Level 15
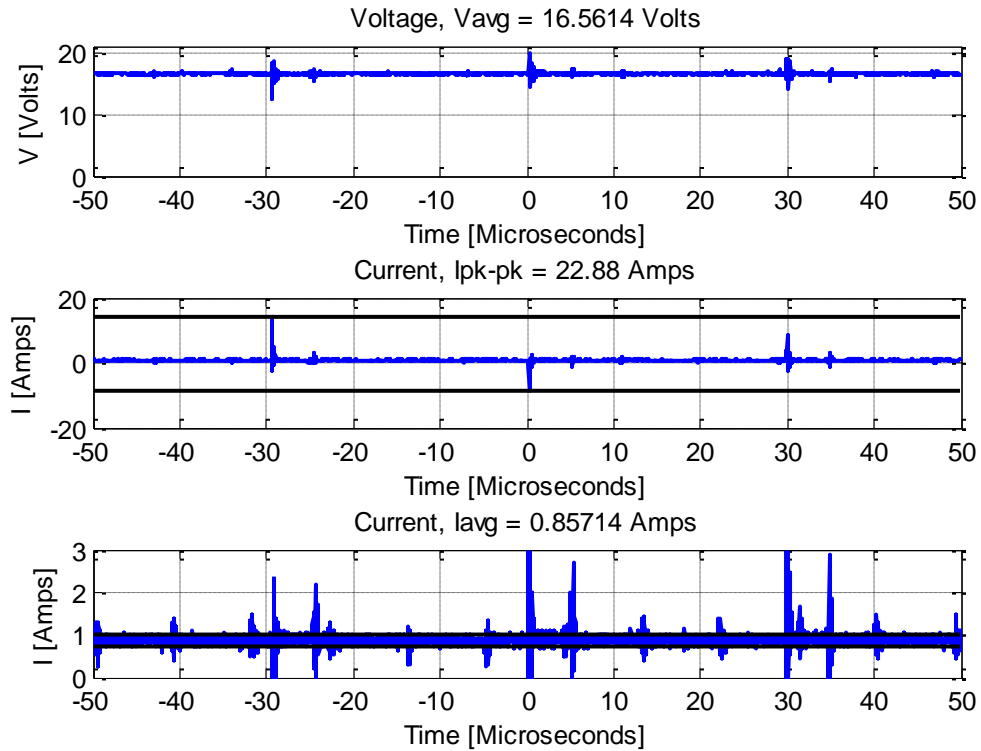
Figure 63 - Implementation Output Data for Buck Rectifier at Res Level 15

4.2.3 Boost Converter

The boost converter was tested at a resistance level of 20, a speed of 60 RPM, and a 20 Ohm load. A buck rectifier was used as the first stage and the boost converter as the 2nd and final stage, shown in Figure 64. During these tests it was found that with a feedback voltage the boost converter would increase the duty cycle to the maximum set in the program and cause the output voltage to decrease instead of increases, which is unexpected. Table 7 correlates the duty cycle to the achieved voltage output, where the maximum duty cycle was the duty cycle used during steady state as the desired voltage was never achieved unless the duty cycle was 0 percent.
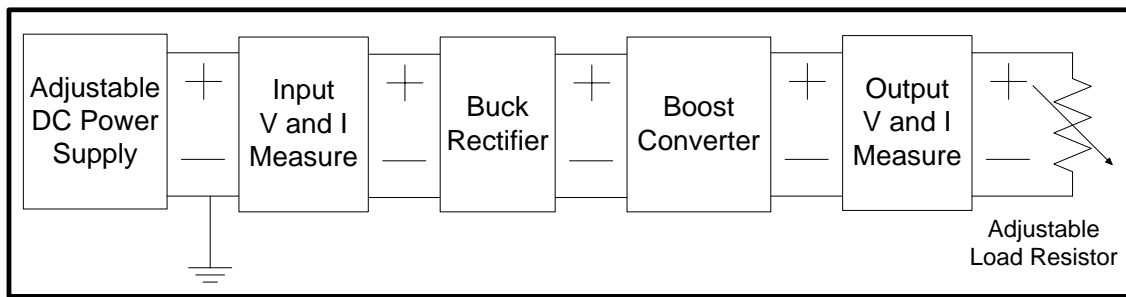
Figure 64 - Block Diagram of Cumulative Boost Converter Implementation

DC Max (%)	Vdesired (V)	Vout (V)
45.0	24.0	12.0
35.0	18.0	15.7
25.0	24.0	16.8
15.0	24.0	18.0
0.0	18.0	19.0

Table 7 - Implementation Data for Boost Converter with Varying Maximum DC

The data in Figure 66 and Figure 67 reflect a constant 35% duty cycle. The input data, shown in Figure 66, gave an input power of 21.1 watts. The output data, shown in Figure 67, gave an output power of 13.6 watts. This gives an efficiency of 64.7% and in this case the boost converter was stepping 9.4 up to 15.7 volts.

In Figure 65, the voltage spikes in the MOSFET driver are related to the current

spikes from the fitness machine. This is shown by noting the period between the larger

spikes of approximately 30 microseconds apart, which is the same as the period of the

input voltage given in Figure 66. Also the period between the smaller spikes and larger

spike before it are approximately 5 microseconds, which is the same as the pulse widths

of the input voltage given in Figure 66. Figure 65 was created with the MATLAB code

given in Section A.19.
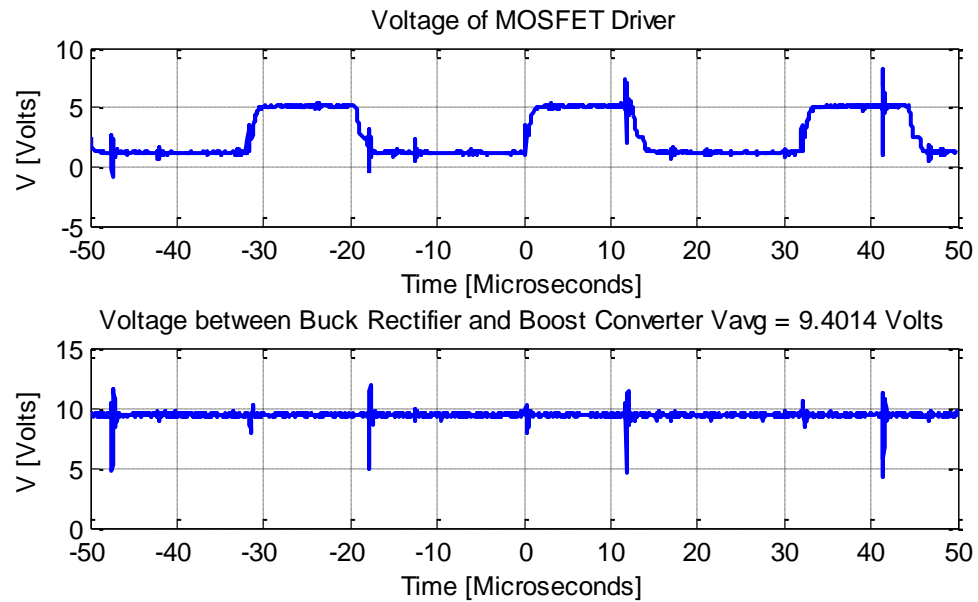
Figure 65 - Implementation Data for Boost Converter
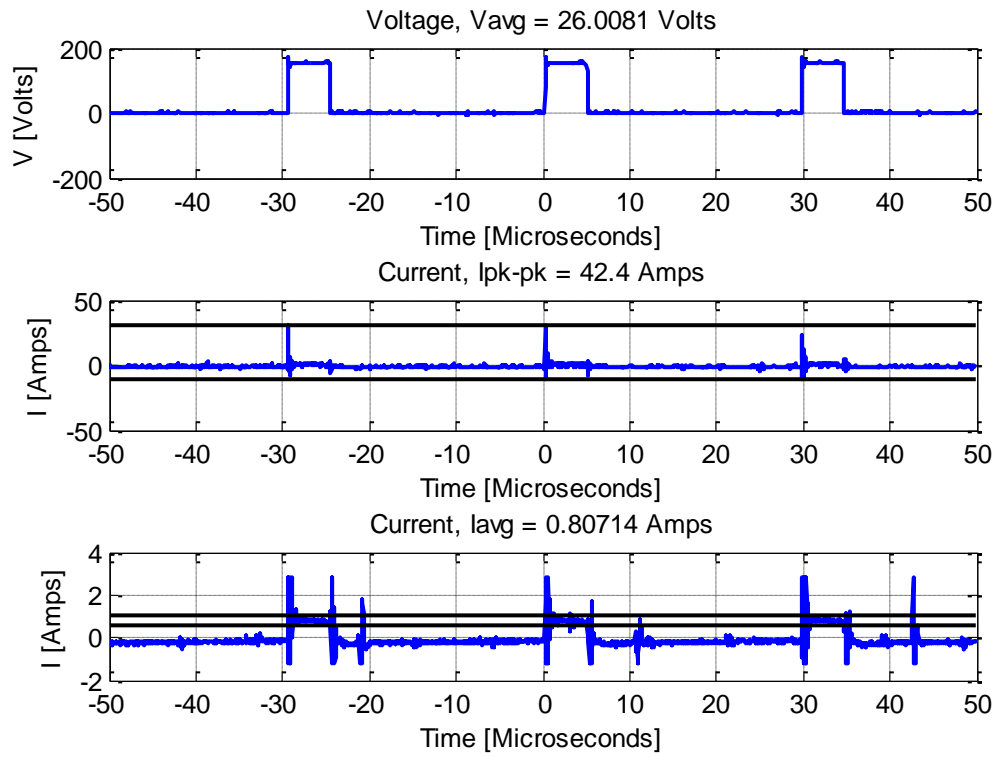
Figure 66 - Implementation Input Data for Boost Converter
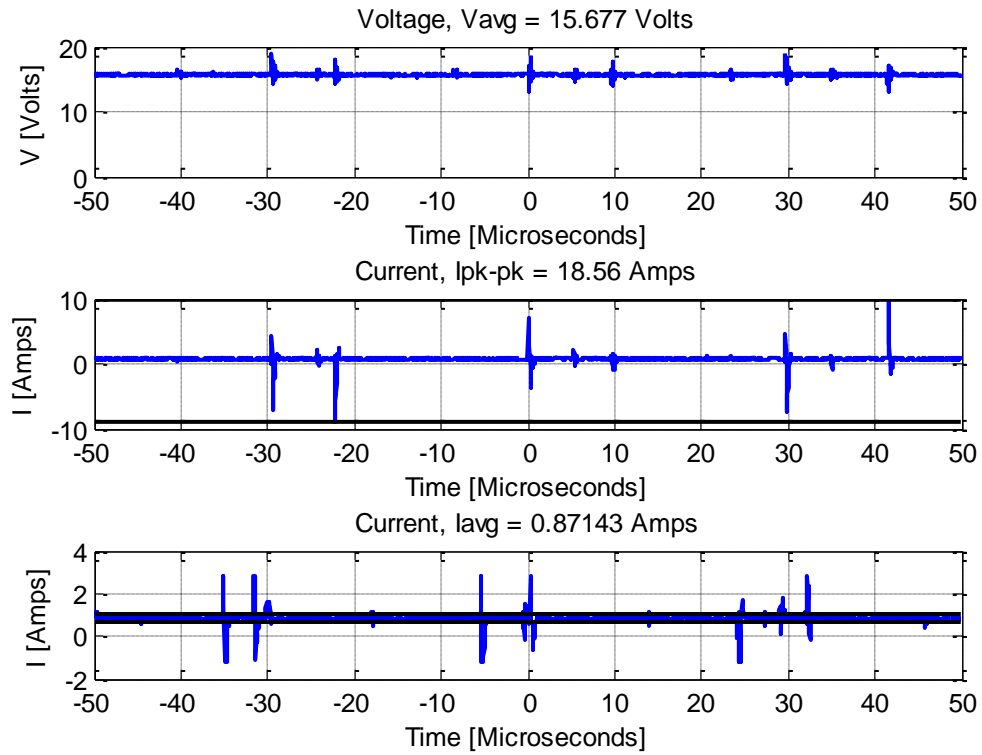
Figure 67- Implementation Output Data for Boost Converter

74

4.2.4 NS Buck Regulator

The National Semiconductor buck regulator was tested with a speed of 60 RPM, varying load, and resistance level of 15 or 25. A buck rectifier was used as the first stage and the buck regulator as the 2nd and final stage, shown in Figure 68. Figure 69, Figure 70 and Figure 71 give a specific case of the data graphically where the system is working ideally. Significant information all cases are given in Table 8 and Table 9.

The tables give quick insight into what occurred for the different conditions. If the output voltage was below 12.4, then the system was bogged down by the load and the NS buck regulator was unable to achieve the desired voltage with the given power. If the input voltage to the buck regulator, also known as the output voltage of the buck rectifier (Vbr), was higher than the average voltage coming from the fitness machine, then power was building up due to insufficient power dissipation by the load. The case of a resistance level of 25 and a load with the resistance of 10 ohms gave an efficiency of 120% which is not feasible. As this is the only case where this happened for the circuit, the data may have been measured when the system was not in steady state as expected.
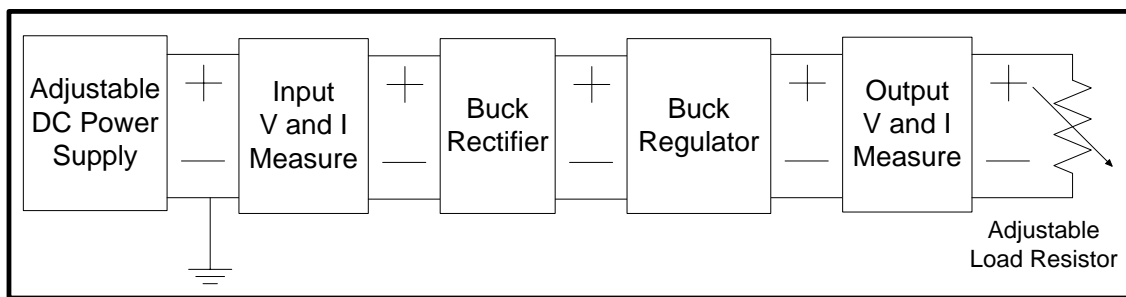
Figure 68 - Block Diagram of Cumulative Buck Regulator Implementation
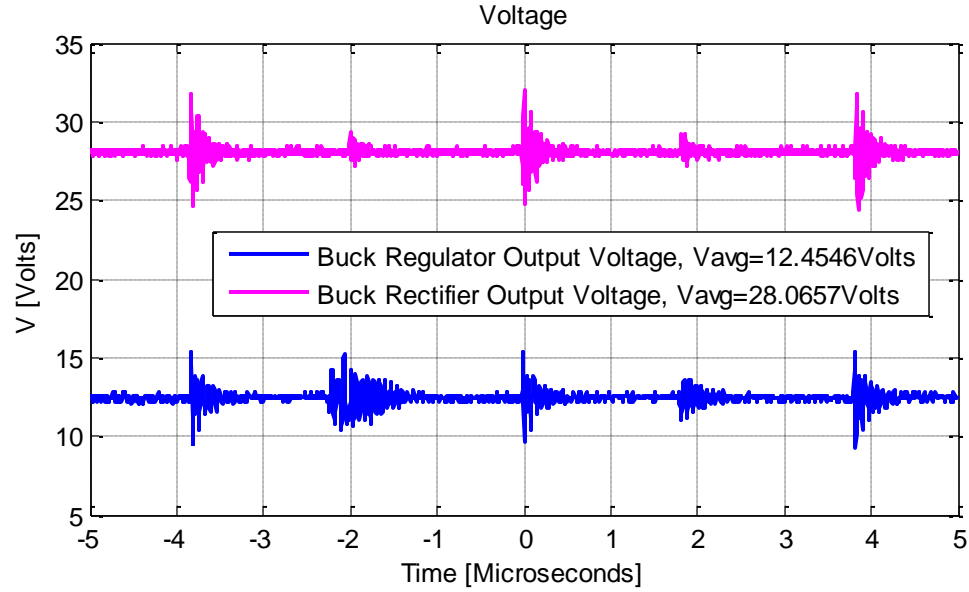
Figure 69 - Implementation Data for Buck Rectifier at a Res. Level of 15 with a 20Ω Load

R (ohms)	Input Vavg (V)	Ipeak (A)	P (W)	Between Vbr (V)	Output Vavg (V)	Iavg (A)	P (W)	Eff
5.00	19.66	0.63	12.36	7.52	5.87	1.17	6.85	0.55
10.00	23.80	0.60	14.20	12.20	10.38	1.09	11.34	0.80
20.00	33.47	0.27	9.09	28.07	12.45	0.65	8.14	0.90

Table 8 - Implementation Data of NS Buck Regulator at Resistance Level 15

R (ohms)	Input Vavg (V)	Ipeak (A)	P (W)	Between Vbr (V)	Output Vavg (V)	Iavg (A)	P (W)	Eff
5.00	32.97	0.93	30.61	11.50	10.03	2.01	20.20	0.66
10.00	50.54	0.26	13.36	46.40	12.43	1.29	15.98	1.20

Table 9 - Implementation Data of NS Buck Regulator at Resistance Level 25
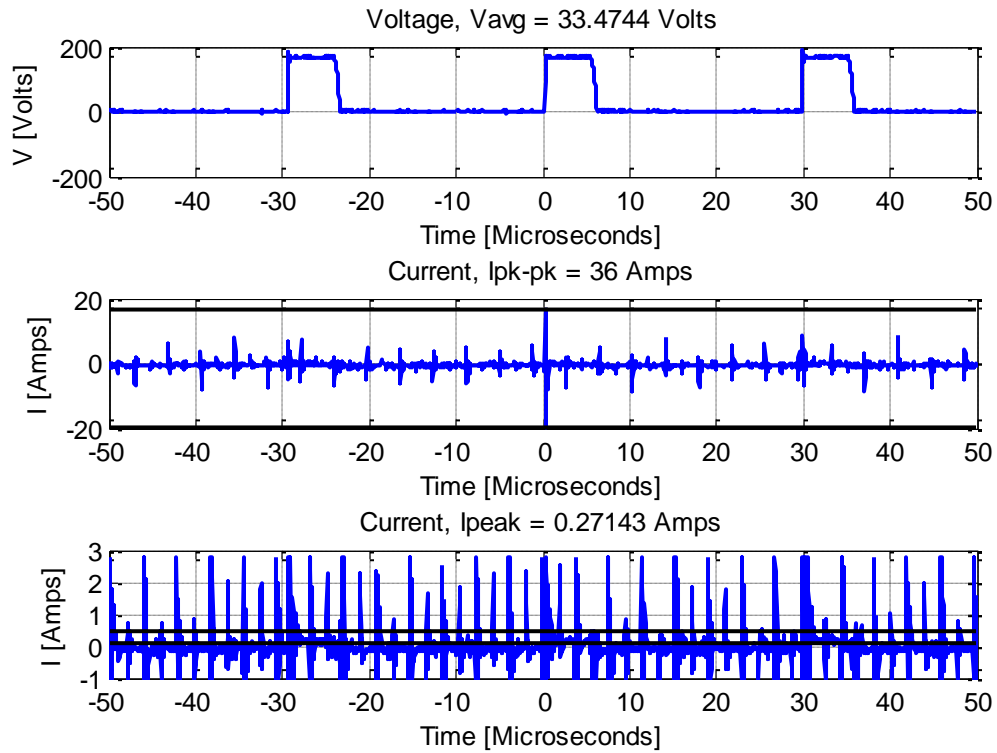
Figure 70- Implementation Input Data for Buck Regulator at a Res. Level of 15 and 20Ω Load
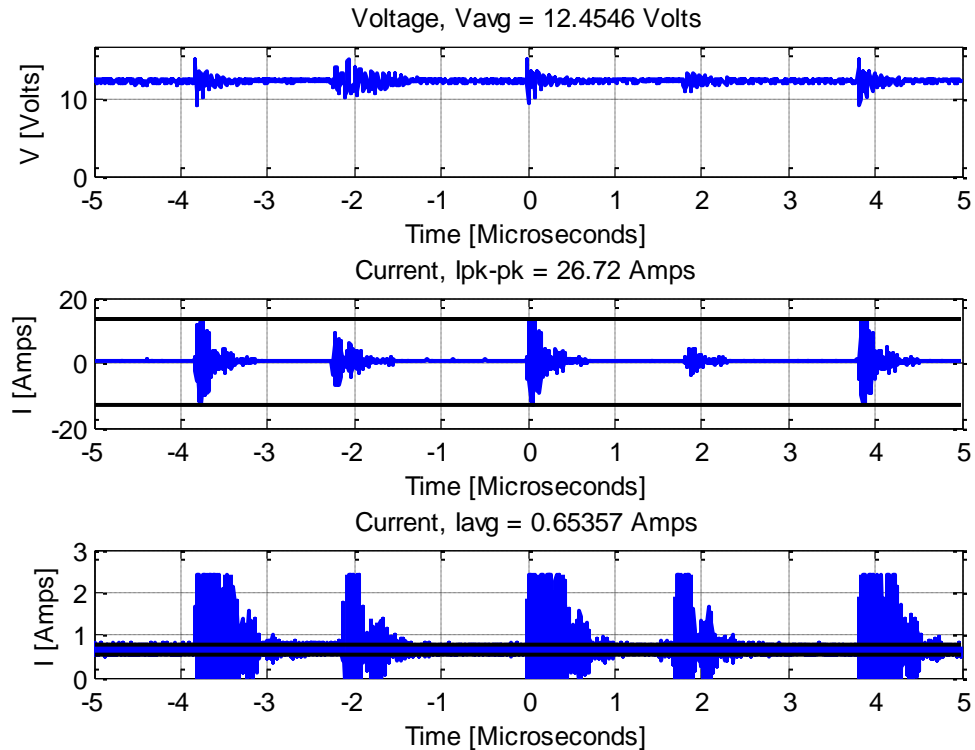
Figure 71- Implementation Output Data for Buck Regulator at Res. Level of 15 and 20Ω Load

The efficiency of the circuit was also evaluated in terms of how it helped meet the goals of the project. The tested circuit would be most efficient when the power going the electromagnet is redirected to the grid. To find the efficiency of the circuit in redirecting the power, the power coming from the buck regulator should be compared to the measurements done in Section 2.2.5 for the same user inputs. Data from Table 8, Table 9 and Table 4 are combined for comparison in Table 10. The ratio is referring to the ratio of power output by the buck regulator compared to the power to the electromagnet during normal operation. A ratio over 1 would mean that the fitness machine is over worked during operation and could potentially short or over heat components within the original print circuit board and reduce lifetime of the machine. A ratio close to 1 but not over would be the most effective in redirecting power from the electromagnet under normal operation to instead the grid.

Resistance Level:	15		25	
Condition	Power (W)	Ratio	Power (W)	Ratio
Normal Operation	14.1	1.00	38.8	1.00
Buck (R=20)	8.14	0.58	n/a	n/a
Buck (R=10)	11.34	0.80	15.98	0.41
Buck (R=5)	6.85	0.49	20.20	0.52

Table 10 - Effectiveness of Power Redirected

When looking over the output current and voltage in Figure 71, it became apparent that this circuit may not be able to be used along with an inverter as the waveforms were not clean and the current contained harmonics that were too large. Another issue that could be easily seen with the input current in Figure 70 is the different switching frequencies. To help in reducing the number of frequencies and the size of the current harmonics, a buck converter controlled by an Arduino was implemented to be much closer to the switching frequency of the fitness machine. Also with the use of a

programmable controller, the buck converter could change the output power and help in reducing issues from not having power matching.

4.2.5   Arduino Buck Converter

The buck converter was tested at a variable load that was adjusted to be sure that system was working within the set parameters described in Section 3.7. The buck converter replaced the buck regulator and is in the second stage, as shown in Figure 72. A speed of 60 RPM was used for two resistance levels. For a user input of a resistance level of 15 and 60 RPM, the input data, shown in Figure 75, show an input power of 17.07 watts. The output data, shown in Figure 76, calculate an output power of 15.17 watts. This gives an efficiency of 88.9% and in this case the buck converter was stepping 27.4 down to 12.9 volts. During normal operation at these user inputs, the power to the electromagnet is 14.1 watts, from Table 4, so the tested circuit outputs a ratio of 1.07 of that power.

During a user input of a resistance level of 20 and 60 RPM, the input data, shown in Figure 77, show an input power of 26.53 watts. The output data, shown in Figure 78, calculate an output power of 25.90 watts. This gives an efficiency of 97.6% and in this case the buck regulator was stepping 32.4 down to 14.5 volts. During normal operation at these user inputs, the power to the electromagnet is 23.1 watts, from Table 4, and the tested circuit outputs a ratio of 1.12 of that power.

The buck converter was not tested at a resistance level of 25 because of a component failing within the driver circuit. As described in Section 3.7, the program was set up to keep input voltages lower than 30 volts. Although with a maximum output voltage of 14 volts and load resistance set at 10 ohms at the time, only 19.6 watts could

be dissipated, which lead to the input voltage rising to a point of component failure. Even

with this mistake, the tests done do give much insight into the circuit improvement

compared to the National Semiconductor buck regulator.
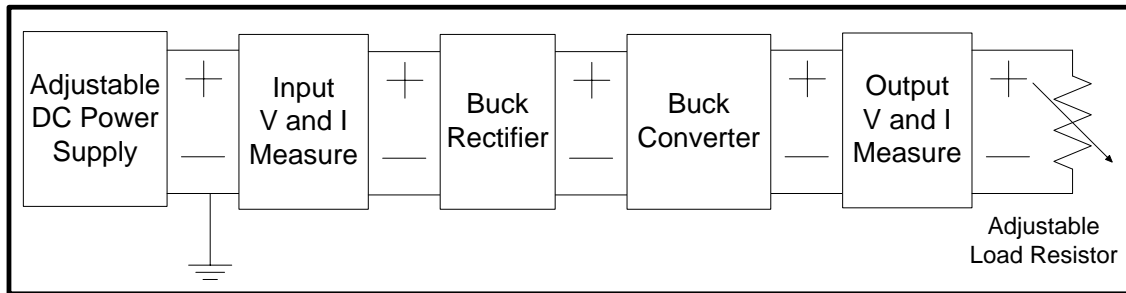
Figure 72 - Block Diagram of Cumulative Buck Converter Implementation
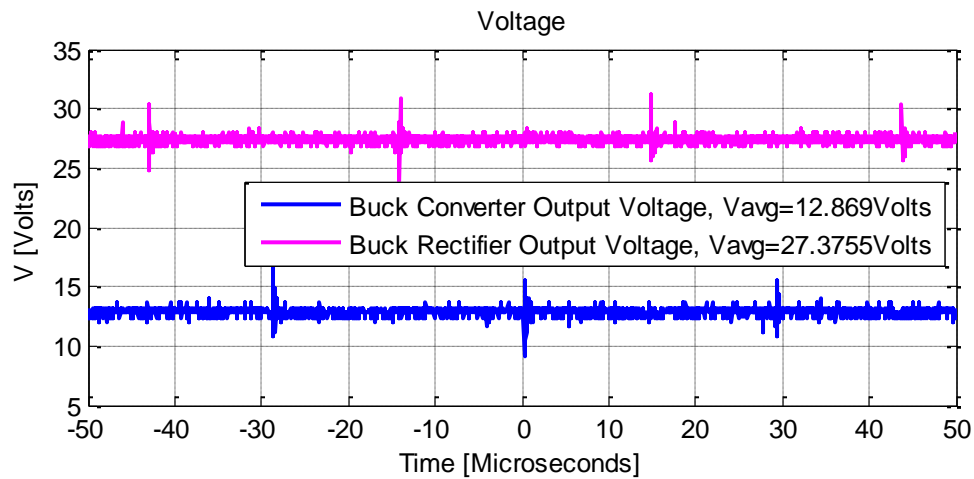
Figure 73 - Implementation Data for Arduino Buck Converter at Res Level 15
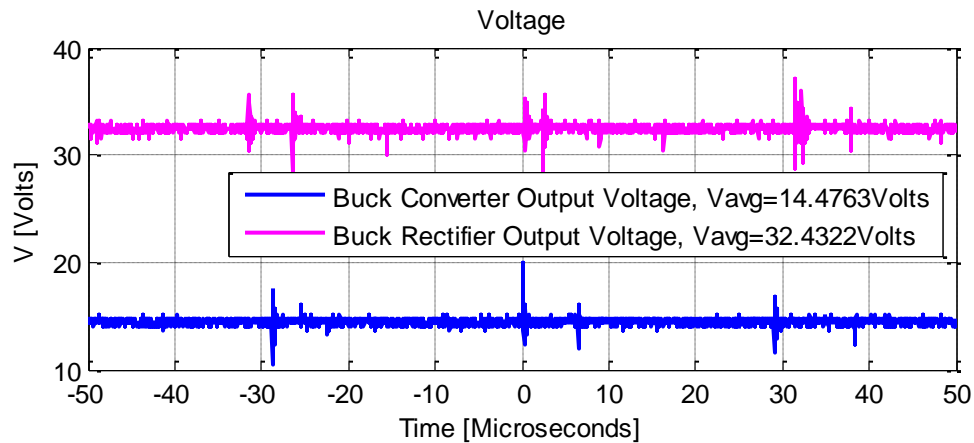
Figure 74 - Implementation Data for Arduino Buck Converter at Res Level 20
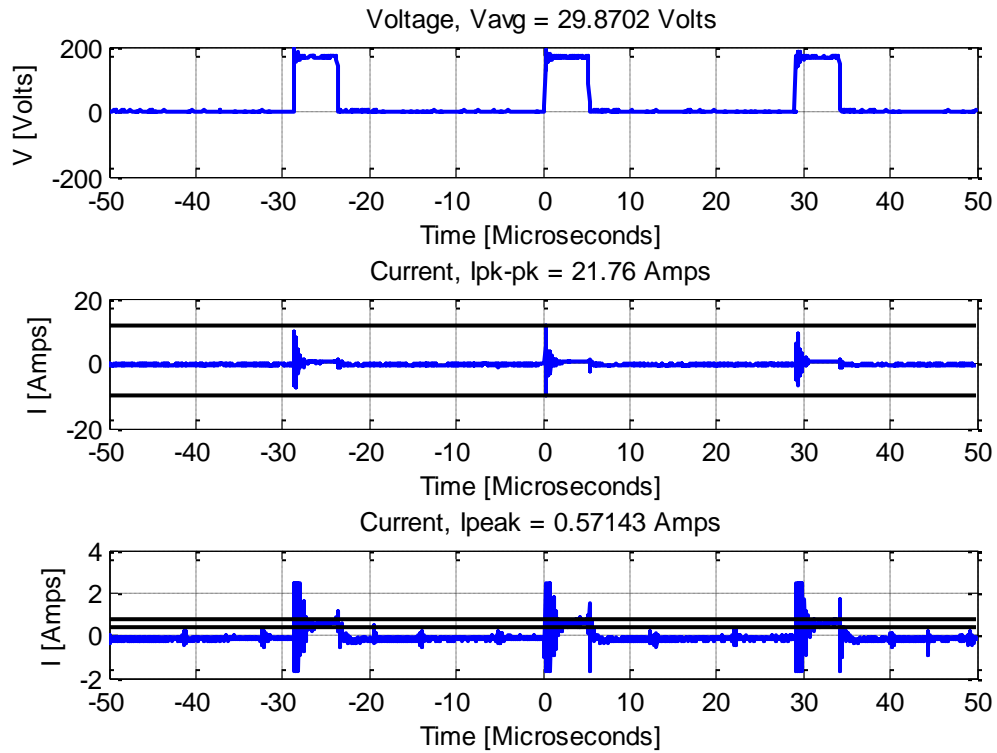
Figure 75 - Implementation Input Data for Arduino Buck Converter at Res Level 15
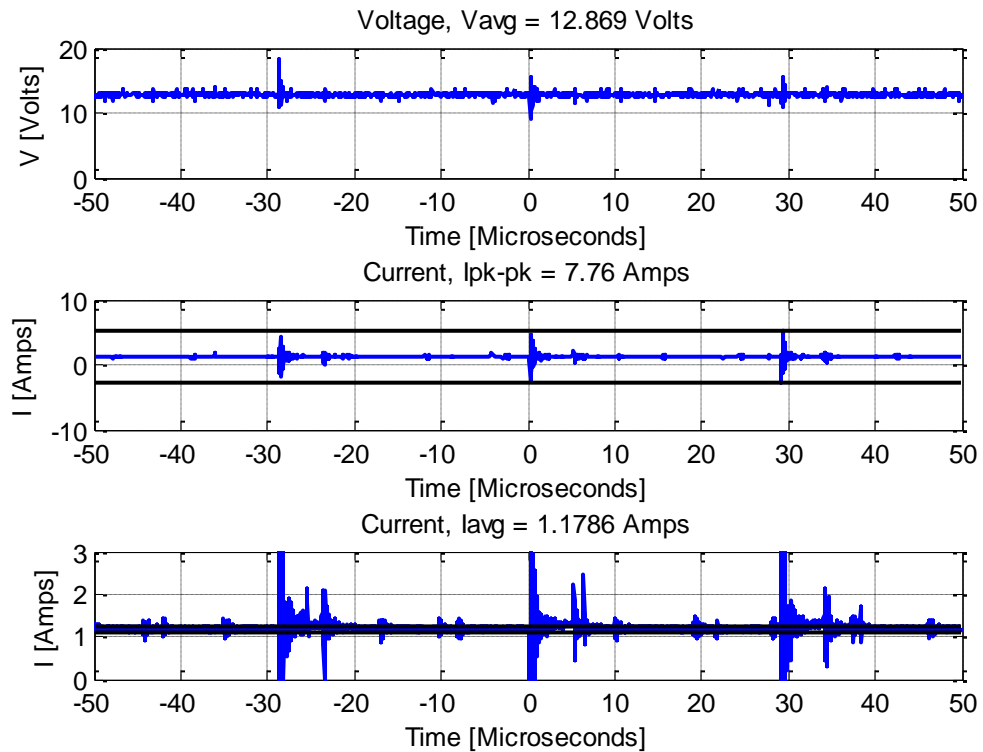
Figure 76 - Implementation Output Data for Arduino Buck Converter at Res Level 15
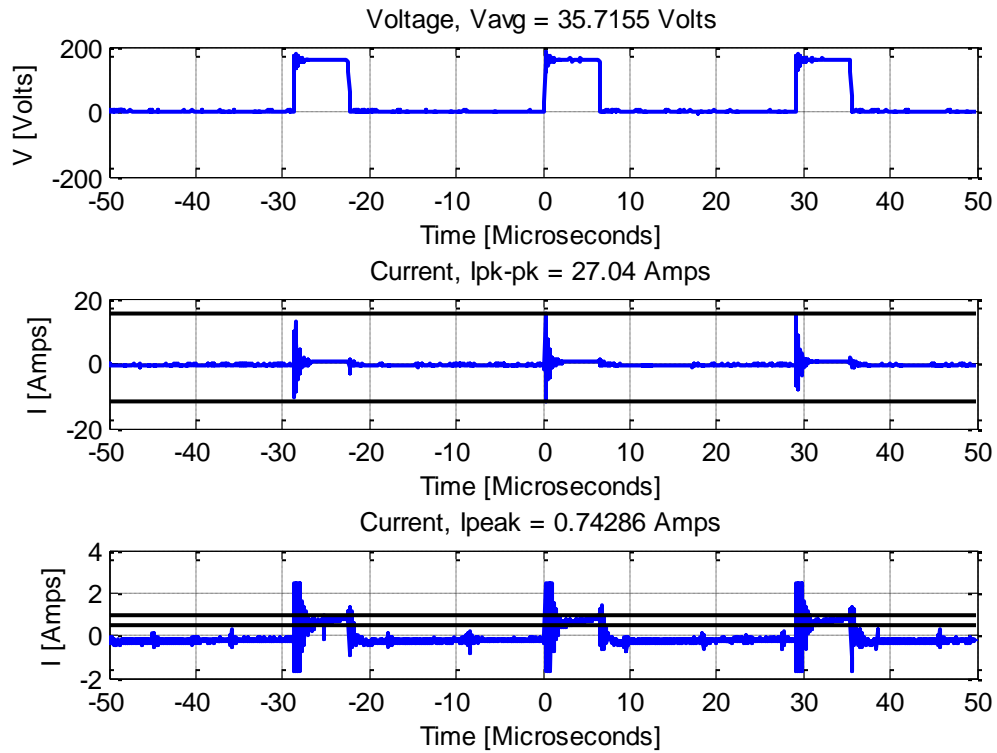
Figure 77 - Implementation Input Data for Arduino Buck Converter at Res Level 20
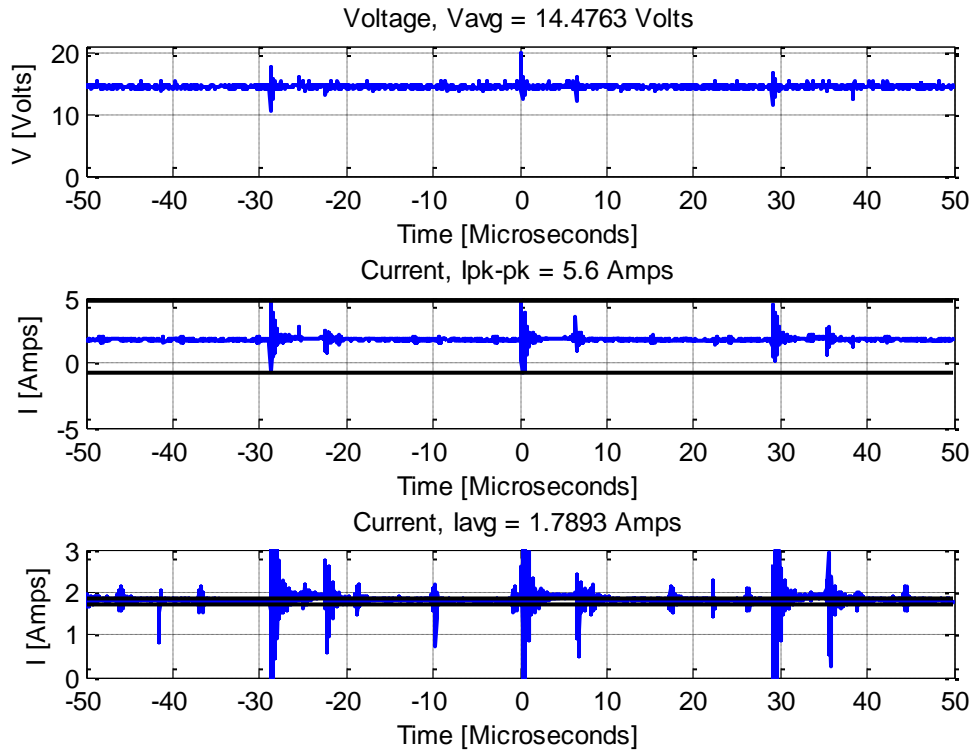
Figure 78- Implementation Output Data for Arduino Buck Converter at Res Level 20

Chapter 5:   Conclusion and further research

Final designs are discussed using the results as motivation for using a buck rectifier in place of a LC low-pass filter, removing the boost converter, and utilizing an Arduino for the buck converter. Further design suggestions and improvements are given as a possible approach to a commercial product that can be connected to the grid. A projection of cost is found from the components used in the final design and design suggestions. This alteration in the hybrid generator circuit creates changes in the normal function and information displayed of the fitness machine, and considerations of these changes are discussed. The primary objective of retrofitting fitness machines utilizing hybrid generators to produce a dc voltage was successful, but issues of current harmonics need further research for conversion into grid power. The secondary objective to minimize alterations for a reduction in cost per watt was also successful.

5.1   Buck Rectifier vs. LC Low-Pass Filter

The data that leads to the conclusion for eliminating the low-pass filter can be found in Section 4.2.1. The issue found was an apparent output power greater than input power. It is believed that this arises because of the method used to measure input power and the use of the diode in the fitness machine. When utilizing the diode inside the fitness machine, the voltage and current measurements for power calculations occur in a mid-stage circuitry and not a natural point between the fitness machine and tested circuit. To avoid this issue, the buck rectifier was used in the final design as the diode in the buck rectifier circuit would be utilized instead the diode inside the fitness machine. The buck

83

rectifier creates a single break point between the fitness machine and tested circuit as the diode inside of the fitness machine is not used. This allowed for a more accurate input power measurement during testing and implementation.

5.2 Removing the Boost Converter

The data that led to the conclusion for removing the boost converter can be found in Section 4.2.3. It was found during implementation at SUNY Cortland, that the output voltage when the boost was at a duty cycle of 0% was higher than output voltage of the boost whenever it was higher than 0%. This contradicted the piecewise testing in the lab and resulted in a reassessment of the need of for boost converter.

The boost converter was designed for resistance levels where the average voltage was less than 14 volts, resistance levels 1-14, and to boost to 14 volts so that the buck regulator could output 12 volts. When reviewing the normal operation data in Table 4, the power during these resistance levels were less than 12 watts and would not produce much power. After consideration, the desired range of operation for this retrofit was changed from a resistance level of 2-25 to 15-25. During normal operation these higher levels produce a high physical resistance, but with the electromagnet removed the physical resistance is significantly reduced, as expected. The change in desired range of operation allowed for the removal of the boost converter in the tested circuit for the Precor recumbent stationary bicycle, C846

The boost converter might be necessary for other fitness machines that use the hybrid generator as the hybrid generator is essentially the same for some machines, but the printed circuit control board that contains the adjustable DC power supply may differ. The adjustable DC power supply in other fitness machines could produce lower voltages

84

but higher currents to achieve the same power of physical resistance. This would require additional research to be done on the other fitness machines, given in Table 1, as was done here with the Precor recumbent stationary bicycle, C846.

5.3 Circuit Performance

The performance of the circuit was evaluated by the common method of power in/out efficiency and its ability to redirect energy from the electromagnet by comparing the output power to the power going to the electromagnet during normal operation with the same speed and resistance level. The data used to determine these evaluations are given in Section 4.2.5. The circuit was tested with a user speed of 60 RPMs at a resistance level of 15 and 20, and the efficiency was 88.9% and 97.6 %, respectively. The value that determined the ability to redirect energy was the power ratio, which is a ratio of the tested circuit's output power over the normal operation power. The power ratios for the same speed and at a resistance level of 15 and 20 were 1.07 and 1.12, respectively. The ideal power factor would be 1, because under 1 the power would not be producing enough energy and over 1 could be reducing the lifetime of the generator by passing more current through the windings than its designed rating.

5.4 Design Suggestions and Improvements for Further Research

5.3.1 DC Link and Micro inverter

To achieve the conversion of energy to the grid, a grid tie inverter is required. Utilizing a commercial inverter would greatly reduce design and qualification testing needed to connect to the grid. The inverter selected should have the necessary UL or equivalent certifications. A rapidly growing technology is micro-inverters as an

alternative to central inverters. A reason for using micro-inverters over central inverters, are the lower input voltage and scalability.

One shortcoming of the ReRev system is that the single inverter for 25 fitness machines is not a scalable option, as gyms may have only half the number of machines or just over 25 machines. The use of micro-inverters would help this issue by allowing the scale of the system to be 2-3 machines per inverter.
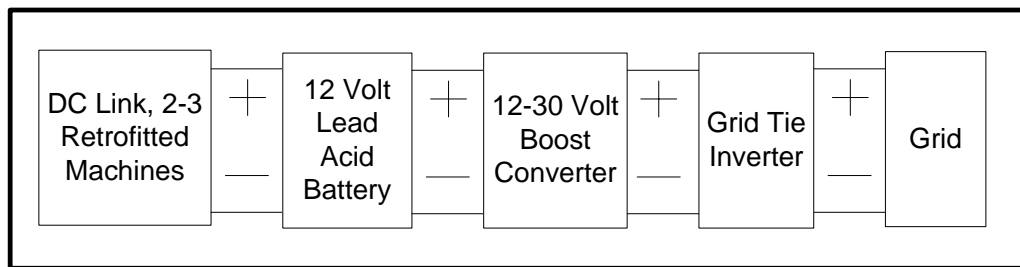
Figure 79 - Suggested System for Connecting to the Grid

The suggested system for connecting the tested circuit for retrofitting to the grid is shown in Figure 79. The DC link comes from the tested circuit described in Section 3.8 with two to three machines connected in parallel.

A battery is used to reduce the issues arising from voltage and power fluctuations from the machines. A sealed lead acid battery could be used for its large capacity and stability. The battery is designed to handle a maximum of 5.1 Amps when charging. This would handle the expected maximum current of one machine running as the inverter starts and becomes the load reducing the charging current of the battery.

The limited availability of commercial available grid-tie inverters requires a circuit to boost the dc link from 12 volts to 30 volts. It would be feasible to place multiple batteries in series to achieve this but a battery management system would need to be customized for this application to remove the issue of imbalanced battery voltages. A better method is to use a boost converter similar to what is described in Section 3.5, with

the appropriate components for expected higher currents and voltages. The digital controller of the boost converter could run off of the 12 volt battery and monitor the DC link for when the inverter and boost converter should be utilized.

As there are many inverters that work off of 12 volts, such as the car inverters, they are not designed to be tied into the grid. The micro-inverter suggested to be used is M190 from Enphase, datasheet in Section A.8. The inverter is compliant with UL1741 and IEEE1547 which can reduce approval time with power companies. The rated maximum current is 10 amps which is acceptable when the input voltage to the inverter is at least 24 volts, making the power rating over 210 watts. This is within the necessary parameters of a design factor of 1.2 and an expected maximum power input of 135 watts, 3 machines at a power output of 45 watts each. This inverter would require a 240 volt split phase connection at the site and is available for $120 [18]. It may also be possible for the micro inverter to be replaced with the ReRev system to utilize a validated central inverter for this application and should be researched further.

5.3.2   Component Limits that Need Improvements

As described in Section 4.2.5, there was a component failure in the MOSFET driver circuit where the BJT that is used to pull down the MOSFET gate voltage failed. Due to excessive heating it would suggest that either the voltage across the emitter and collector rose above 40 volts or too much current was flowing through the BJT. A different BJT could be used with a higher voltage rating. Although, the MOSFET would have likely failed before this because of the gate to source voltage of the MOSFET would have been past its rated value before the BJT, so it is more likely that the current passing through the BJT caused the failure. This issue could be solved by a BJT with a higher

current rating or increasing the value of resistor 1 in Figure 38, described in Section 3.7 as controlling the current flow.

Two improvements that could be done for the Arduino Buck Converter would include using a power MOSFET with a larger gate to source voltage rating and creating a failsafe system to protect the circuit from overvoltage. Increasing this value from ± 20 volts to ± 30 volts would improve the allowable input voltage from 31 volts to 40 volts. The input voltage was only increased to 40 volts because of the BJT's rated voltage across emitter to drain. The suggested MOSFET for this improvement is listed in the additional parts list in Section A.9.

5.3.3   Current Harmonics

The issue of current harmonics was first seen in piecewise testing of the NS buck regulator, Section 4.1.5, and was addressed by replacing it with the Arduino buck converter, section 4.1.6. During piecewise testing, this caused a reduction of output current ripple caused by current harmonics from 2000%, Figure 54, to 107%, Figure 57, under similar working conditions. During implementation, this caused a reduction of output current ripple caused by current harmonics from 4088%, Figure 71, to 658%, Figure 76, under similar working conditions. Although the current harmonics was significantly reduced, the current waveforms from the final tests, Section 4.2.5, may not be adequate for the grid-tie inverter and a commercial project. This issue found should be considered for further research.

5.3.4   Recording Power Data for User Records

A current sensor is required on the output of the tested circuit for the purpose of recording power production by the user. The Hall effect sensor suggested is listed in the

additional parts list in Section A.9. The current range of $\pm$ 5A is acceptable for the

expected output current of 4.155 amps, Section 3.7, and peak current, Section 4.2.5, with

a design factor of 1.2 as the expected output current and peak current are under 5 amps.

The sensor has a sensitivity of 180mV/A, which allows for the Arduino to be accurate to

0.1 Amps. This should be acceptable for recording output power and energy for users.

5.3.5   Possible Partnership with Companies

A partnership with companies such as Precor, Octane, and Cybex would be

beneficial for the exchange of ideas and redesign of the adjustable dc power supply in

fitness machine to be more efficient with the project and tested circuit. This could be

highly effective in redirecting energy as there is a possible larger issue as the fitness

machine was not manufactured for this.

5.5   Cost Estimates

The tested circuit's cost to retrofit an individual machine is $67.03, Section A.4,

and the cost of converting the 12 volts to grid electricity is estimated to be $209.82,

Section A.9, for optimally three machines. The estimated cost per machine would be

$92.29. Comparing this to the estimated output power of 25.9 watts, Section 4.2.5 for a

median resistance level of 20, the cost per watt is 3.57 dollars per watt. The ReRev

system had an estimated price $680 per individual machine for 100 watt produced for an

average user, Section 1.3.1, to achieve a comparable 6.80 dollars per watt. The tested

circuit is more cost effective but not significantly so.

The median resistance and the average user are two different characteristics and

may not be correct for comparison. The average user may not perform at the median

resistance of the retrofitted machine and would not be the average user's power

production potentially allowing for the power output to increase significantly. More specifically, the value of 90% of 45.6, Table 4 at 70 RPMs and a Res Level of 25, corresponds to 41 watts. A 58% increase in power and potentially achieving 2.25 dollars per watt. This is half the cost per watt of the ReRev system and could be a significant improvement. Yet, comparing this estimated cost to a commercial cost may not be sufficient without applying a factor of cost for manufacturing and further research for overall system integration.

5.6   Machine Considerations for Retrofit

The removal of the eddy current braking resistance would make information displayed on the user console incorrect. The calorie production would need to be calculated from the generator to be accurate. As one of the goals of the project is to record energy produced by the user, this could be displayed instead of calories. To edit information outputted to the user console, it would only require an interrupt in the connection between the console to the control PCB to read and rewrite what was necessary. This would also allow for additional information to make the tested circuit more accurate with the use of lookup tables. Instead of the buck converter control system from the tested circuit only seeing the input voltage and output voltage to adjust the duty cycle, it could use information such as the user resistance level and speed to increase response time by anticipating voltages.

Another consideration is the fitness machines were designed with a generator to remove the need of power cables placed across gym floors. The retrofitting of any machine to divert energy to the grid would require the need of these cables to be wired to a central location and returns the possibility of creating a tripping hazard for users.

5.7   Overall

The tested circuit is the first of its type to redirect energy from a stand-alone fitness machine incorporating a hybrid generator with eddy current braking. The goal of minimal alterations while redirecting a significant amount of energy was achieved. The goal of reducing costs to retrofit these machines in comparison to the leader, ReRev, was successful, but cost to achieve a commercial product that can be connected to the grid was only estimated and not tested. Further research is necessary for completion of the Human Power Plant project and would allow a significant increase for power output and should be explored.

Appendix

A.1 - US60784325

United States Patent [19]

Hsu

[11] **Patent Number:** **6,084,325**

[45] **Date of Patent:** **Jul. 4, 2000**

[54] **BRAKE DEVICE WITH A COMBINATION OF POWER-GENERATING AND EDDY-CURRENT MAGNETIC RESISTANCE**

[76] Inventor: **Cheng-Chien Hsu**, 9th - 1 Fl., 117, Sung Te Road, Taipei City, Taiwan

[21] Appl. No.: **09/237,928**

[22] Filed: **Jan. 27, 1999**

[51] **Int. Cl.**^{7} **A63B 21/00**
[52] **U.S. Cl.** **310/74**; 310/93; 318/161; 318/375; 188/161; 242/288; 482/2; 482/63
[58] **Field of Search** 310/74, 77, 93; 318/375, 376, 377, 378, 379, 380, 381, 150, 161; 188/158, 159, 160, 161, 162, 164; 242/288; 482/2, 63, 64

[56] **References Cited**

U.S. PATENT DOCUMENTS

4,612,494	9/1986	Kawamura	310/74
4,775,145	10/1988	Tsuyama	272/73
5,072,930	12/1991	Sun	272/73
5,234,083	8/1993	Lee	188/267
5,236,069	8/1993	Peng	188/267
5,254,061	10/1993	Leask	482/63
5,586,624	12/1996	Ko et al.	188/164
5,659,231	8/1997	Svarovsky et al.	318/368
5,711,404	1/1998	Lee	188/164
5,879,273	3/1999	Wei et al.	482/63

Primary Examiner—Nicholas Ponomarenko
Assistant Examiner—B. Mullins
Attorney, Agent, or Firm—Rosenberg, Klein & Lee

[57] **ABSTRACT**

The present invention relates to a brake device with a combination of power-generating and eddy-current magnetic resistance having an outer]-shaped fly wheel fastened on a central axle of a frame and fitted with a permanent magnet on the inner circular edge to form a rotor type, and the fly wheel is connected with a stator core fastened on the frame; moreover, one end of the central axle is stretching out of the frame and fitted with a belt wheel; the front end of the frame is fitted with a brake core adjacent to the outer edge of the fly wheel to supply a planned eddy current magnetic resistance to the fly wheel; in accordance with such design, the device generates power by means of the exercise force of users to drive the fly wheel to rotate, after passing through a DC power supply, it provides display & controlling gage with power source so that the power-generating and the eddy current magnetic resistance are integrated to reach the effect of reducing the volume and the producing cost.

9 Claims, 7 Drawing Sheets

FIG. 1

FIG. 2

FIG. 3

F I G. 4

F I G. 5

9

7	DC power supply

6	commutating & wave-filtering circuit

8	adjustable DC power supply

32

A

2

44   4

55

5

1
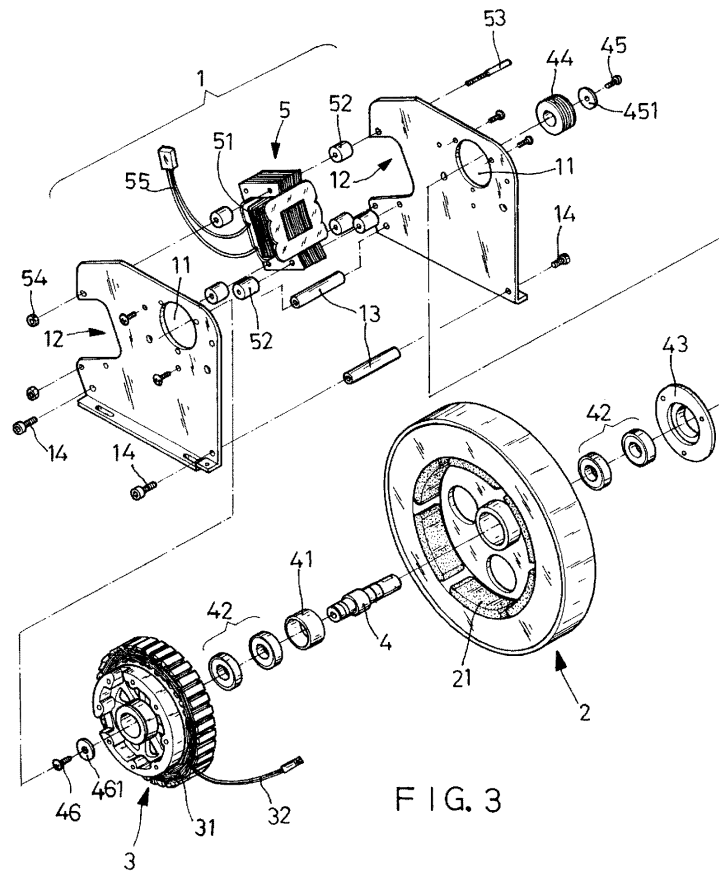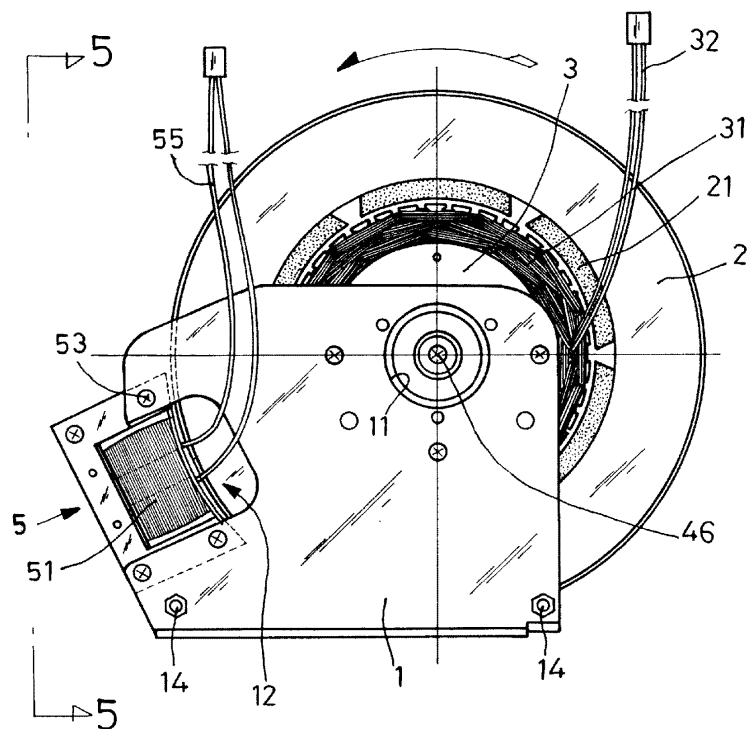
F I G.6
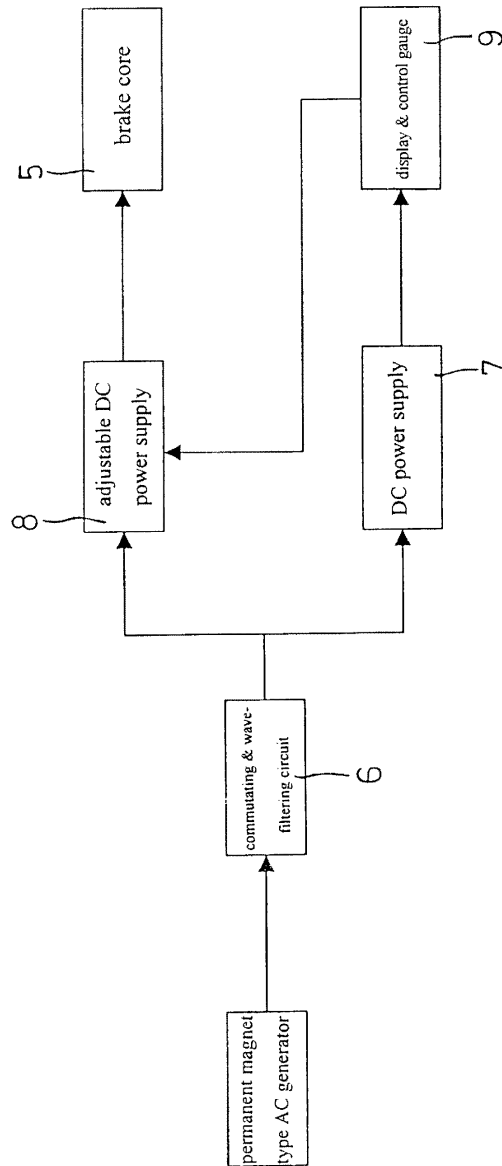
F I G. 7
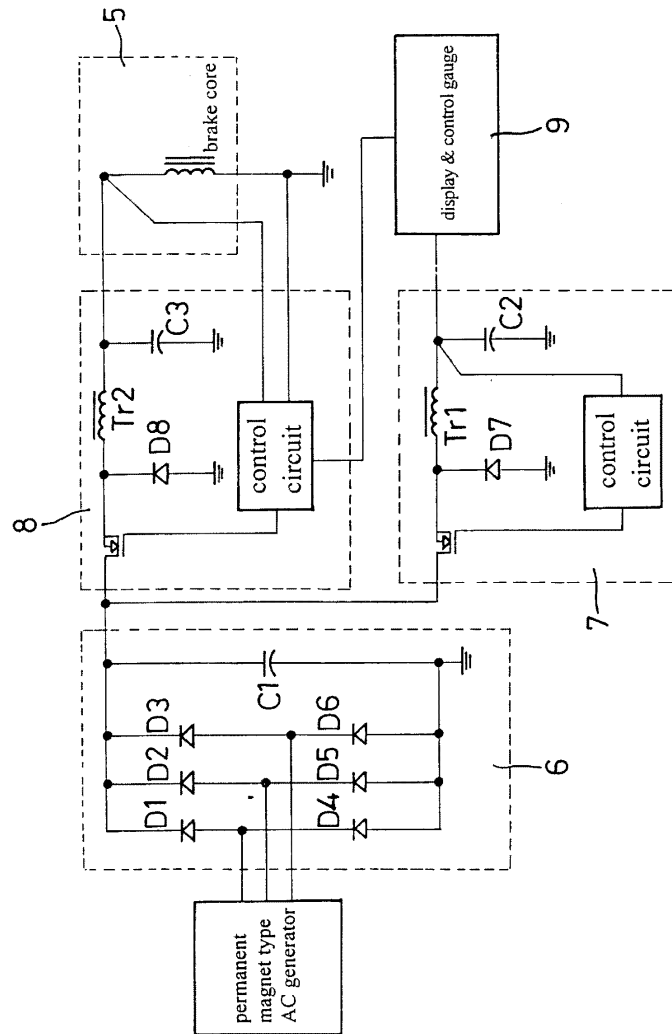
F I G. 8

1

BRAKE DEVICE WITH A COMBINATION OF POWER-GENERATING AND EDDY-CURRENT MAGNETIC RESISTANCE

BACKGROUND OF THE INVENTION

1. Field of the Invention

The present invention relates to a brake device mounted on the gymnastic equipment to control the motion loading of, and more particularly to a two-in-one magnetic control device which makes use of the externally rotary fly wheel to generate power and to control the loading condition.

2. Description of the Prior Art

The brake (loading) device for conventional indoor exercise equipment makes use of no other than friction type, oil pressure type, fan type, etc. The friction type brake device has inconvenience of oil leakage, noise-making and reduction of braking effect at a high temperature while the fan type has drawbacks with huge volume, poor appearance, narrow loading range and difficult adjustment.

Accordingly, the eddy current type resistance formed by the change of the magnetic field is made used recently. Since it belongs a non-contact form of magnetic control, it was highly appreciated on the market. Such device was disclosed in the application (No. 79206996) in Taiwan R.O.C. which is called "permanent magnet type adjustable brake device" (U.S. Pat. No. 5,096,024); one amendment thereto was applied as No. 79206996 and U.S. Pat. No. 5,437,353. In addition, it was also disclosed in the R.O.C. Patent No. 80211672 "Eddy combined magnetic field resistance brake device" (U.S. Pat. No. 5,234,083), R.O.C. Patent No. 82218230 "Magnetic loading system of magnetic control for gymnastic car", R.O.C. Patent No. 82215087 "Loading adjustment device with magnetic control for gymnastic car", R.O.C. Patent No. 85207333 "Magnetic control braking device with lateral movement type for gymnastic car", R.O.C. Patent No. 86213735 "Magnetic control wheel for gymnastic car", and the following U.S. Pat. Nos.:
1. 5,072,930;
2. 5,236,069;
3. 5,586,624; and
4. 4,775,145.

In the above-mentioned applications of magnetic control device with eddy current type, their basic principle is that conductor is placed in the variable magnetic flux so that a reverse electromotive force is generated on the locally closed circuit inside of the conductor so that the so-called eddy current is produced. The flow direction of this eddy current building the magnetic effect must be contrary to the variable direction of the original magnetic flux creating this current. Moreover, the Max-well's Equation tells that this magnetic force is proportional to the square of the density of the magnetic flux. It is just required by the brake (loading) of the gymnastic equipment.

Although the magnetic control device with eddy current type has its advantages and features, it is difficult for the loading part, when the permanent magnet is used to be the magnetic field source, to be connected to the external digital signal to reach the goal of computerization and digitalization, unless a motor and a motor controller are extra installed to change the relative position of the magnet and the conductor, or electromagnetic coil and extra added power are used to overcome this difficulty which bring much inconvenience in usage and the practicalness is therefore reduced, so that it can only be applied to the gymnastic equipment with lower price. Nevertheless, the accuracy and the real effect are taken more and more seriously to the gymnastic equipment, and it can only be reached by means of the computerization and digitalization. In addition, the gymnastic equipment with digitalized functions should be

2

equipped with gauges and controllers which also require power. When the power is supplied from outside, it brings a lot of troubles and restrictions.

Accordingly, the inventor has developed a permanent magnetic three-phase AC brake device by the way of generator to be the loading for the gymnastic and rehabilitative equipment. A conventional permanent magnetic three-phase AC generator makes use of the magnetic field created by the current value on the stator coil which is a "reverse filed" resulting in a reverse torque to form a "loading", so that the current value of the stator coil must be very great, otherwise an appropriate resistance is not able to be produced. Thus, it results in disadvantages of a huge volume and an expensive production price. Furthermore, the permanent magnetic AC generator has resonance point, so that the loading control is very unstable. Consequently, it is not a completely practical brake device.

Besides, the outer edge of a circular copper strip is coaxially cut into a central gap an electromagnet to form the braking resistance. However, the copper strip is thin and large, and the flatness processing and installation are very difficult, so that the gap between the copper strip and the electromagnet is not able to be fix when the copper strip rotates. Therefore, the loading is very unstable, the whole structure is complex and it is not proper to be installed in the gymnastic equipment.

SUMMARY OF THE INVENTION

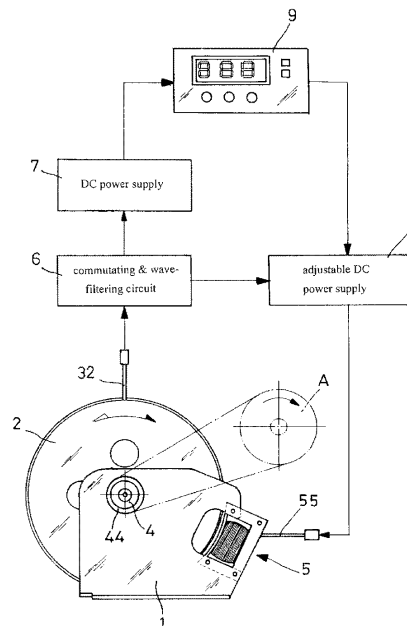It is a main object of the present invention to provide a brake device with a combination of power-generating and eddy-current magnetic resistance whose whole structure is complete, whose volume is small and which is suitable for all kinds of gymnastic equipment.

It is another object of the present invention to provide a brake device to have both power-generating effect and loading control effect, and the power can be supplied to parts concerned without an external connection to the power supply in order to reach the goal of convenient use.

It is a further object of the present invention to provide a brake device with stable loading and with high accuracy to control the motion speed.

In order to reach the above objects, the present invention includes a fly wheel having an outwardly flanged peripheral, rim, portion fastened on a central axle of a frame and fitted with a permanent magnet on the inner circular edge to form a rotor type, and the fly wheel is connected with a stator core fastened on the frame; moreover, one end of the central axle is stretching out of the frame and fitted with a belt wheel; the front end of the frame is fitted with a brake core adjacent to the outer edge of the fly wheel to supply a planned eddy current magnetic resistance to the fly wheel; in accordance with such design, the device generates power by means of the exercise force of users to drive the fly wheel to rotate, after passing through a DC power supply, it provides display & controlling gage with power source so that the power-generating and the eddy current magnetic resistance are integrated to reach the effect of reducing the volume and the producing cost.
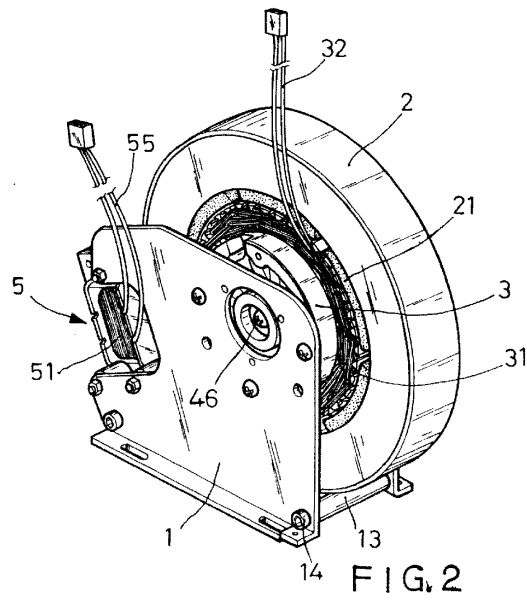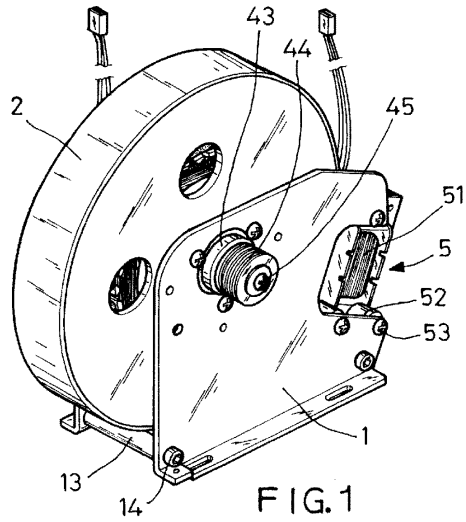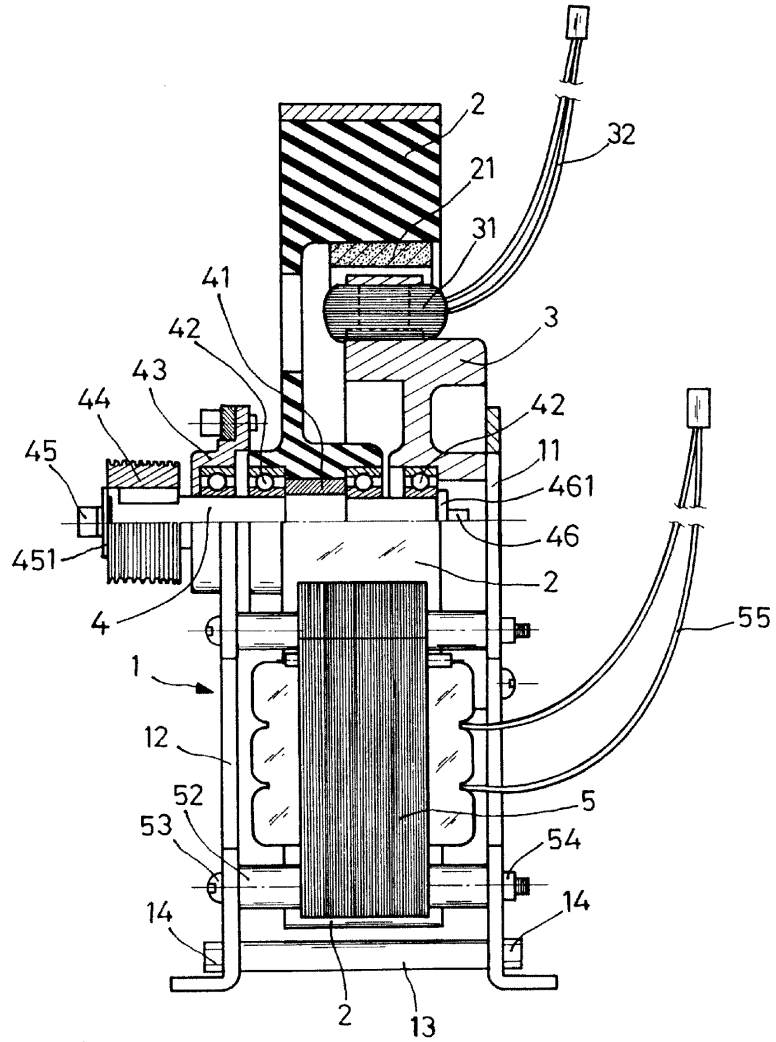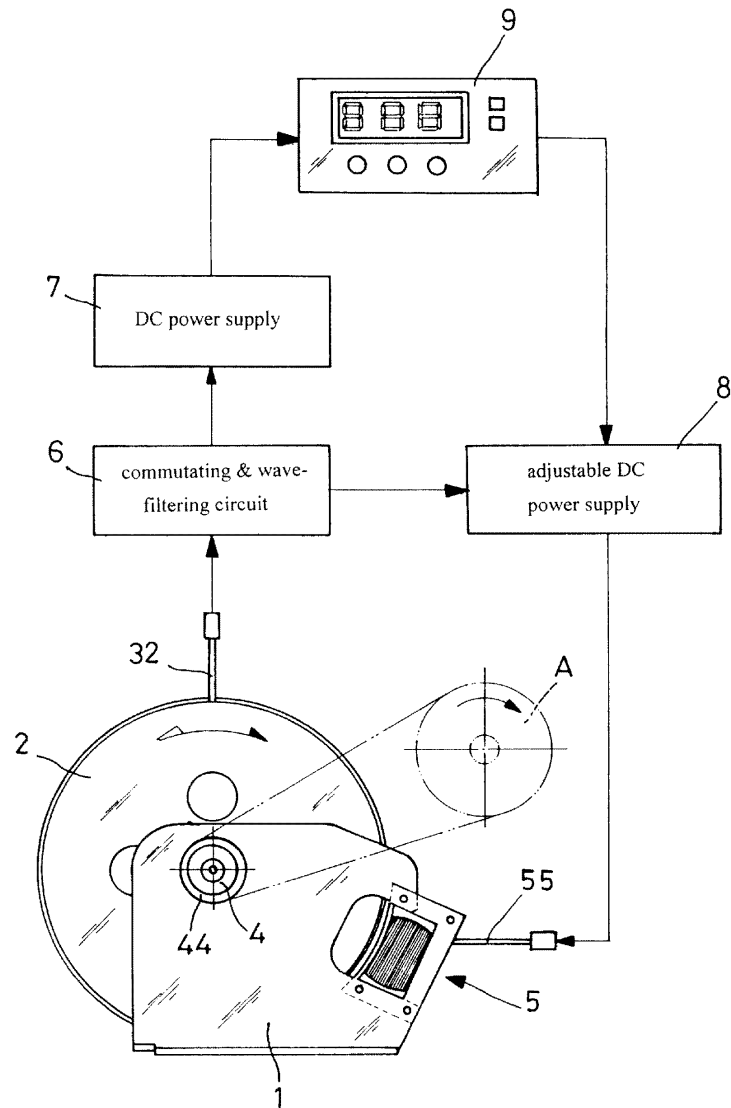
BRIEF DESCRIPTION OF THE DRAWINGS

The drawings disclose illustrative an embodiment of the present invention which serves to exemplify the various advantages and objects hereof, and are as follows:

FIG. 1 is a perspective view of a preferred embodiment of the present invention;

FIG. 2 is another perspective view of the preferred embodiment of the present invention from the other side;

FIG. 3 is a perspective exploded view of the preferred embodiment of the present invention;

FIG. **4** is a side elevation view of the preferred embodiment of the present invention;

FIG. **5** is a half sectional view in accordance with FIG. **4** along the line **5—5**;

FIG. **6** is an installation drawing for the overall control of the present invention;

FIG. **7** is a block diagram for the overall control of the present invention; and

FIG. **8** is a circuit diagram for the overall control of the present invention.

DETAILED DESCRIPTION OF THE PREFERRED EMBODIMENT

First of all, referring to FIGS. **1** through **3**, a preferred embodiment of the brake device with a combination of power-generating and eddy-current magnetic resistance in accordance with the present invention includes:

a frame **1** consisting of two symmetric plates on which a borehole **11** is fitted and which has an indentation **12** on the front edge thereof respectively;

a fly wheel **2** with a body having a flanged peripheral portion which is fitted with a permanent magnet **21** on the inner circular edge to form a rotor type, and the fly wheel **2** is connected with a stator core **3** fastened on the frame **1**, and the fly wheel **2** is also fastened between two plates of the frame **1** by means of a central axle **4** to pass through the required ring **41** and a number of bearings **42** and one end of the central axle **4** passes through a bearing collar **43** mounted on the borehole **11** of the corresponding plate, and a belt wheel **44** is fitted for the purpose of drive use;

a brake core **5** comprised of E-shaped silicon steel plates overlapped together around which a coil **51** circles, and the two sides of the brake core **5** are fastened by plugs **52**, bolts **53** and nuts **54** on the indentations **12** of the frame **1**, and the brake core **5** is placed adjacent to the outer circular edge to receive a planned eddy current magnetic resistance for the fly wheel **2**.

Furthermore, the outer side of the belt wheel **44** is fastened by a washer **451** and a bolt, and the other side of the central axle **4** corresponding to the belt wheel is fixed by a washer **461** and bolts **46**.

Afterwards, referring to FIGS. **4** and **5**, the structure of the present invention is complete and small after assembly, and the stator core **3** and the brake core are respectively connected to the cables **32** and **55** so that it is easy to be mounted on the gymnastic or rehabilitative equipment. At the same time, referring to FIG. **6**, when the wheel of the gymnastic equipment (not shown) rotates, the fly wheel **2** on the frame **1** is driven to rotate by means of the belt wheel **14**, and the permanent magnet **21** at the inner edge of the fly wheel **2** and the stator core **3** form a magnetic circuit to make the coil **31** to generate voltage. This is the principle for the permanent magnet type AC generator. The present invention makes use of this principle to take the fly wheel **2** as the power source to generate the alternating current while it is also used to control the loading at the same time. Consequently, when the fly wheel **2** rotates, not only the stator core **3** is able to produce the voltage, but also the magnetic field caused by the current value on the coil **31** of the stator core **3** is a reverse magnetic field corresponding to the fly wheel **2** so that a reverse torque (reverse electromotive force) is formed. Accordingly, the stator core **3** itself is also a loading for the fly wheel **2**; however, this reverse torque is not great. In order to produce a braking resistance to the fly wheel **2**, the electromotive force must be immense. To reach it, the producing cost and the volume will be therefore increased. In the prior art, it is not a practical design to make use of the reverse field of the stator core **3** to control the loading. It is

not considered to have an application value for the industry after applied in the market. Therefore, the present invention is developed to improve the prior art. The voltage produced by the stator core **3** passes through a commutating & wave-filtering circuit **6** in order to obtain a stable circuit, and then passes through a DC power supply **7** and an adjustable DC power supply **8**. The DC power supply **7** supplies the DC power required by the display & control gauge **9** on the gymnastic equipment so that the whole gymnastic equipment is able to be computerized without connecting to the external power source. The adjustable DC power supply **8** converts the AC voltage produced by the permanent magnetic type AC generator to the DC voltage to supply the current required by brake core **5** on the side of the fly wheel **2**. So, the current produced by the brake core **5** and the magnetic field produced by the stator core **3** is different since a real eddy current formed by the brake core will cause a magnetic resistance effect on the fly wheel **2**. After testing, only this "eddy magnetic resistance" is able to provide an enough braking resistance without a resonance point. Moreover, the magnetic resistance value of the brake core **5** is able to be directly adjusted by the digital signal of the display & control gauge **9**, so that the motion speed can be controlled, the loading can be stabilized and the accuracy can be increased.

In accordance with the above-mentioned technique and means, the power generating and the eddy current magnetic resistance are ingeniously integrated in the present invention. When the fly wheel **2** is driven to rotate, the power-generating effect is produced at once, and the inner stator core **3** exerts an effect of slighter reverse field resistance on the inner circle of the fly wheel **2**. By means of the alternating current produced which passes through the adjustable DC power supply **8** to provide the DC power required by the brake core **5**, a greater "eddy current magnetic resistance" is formed. Accordingly, in the application of the present invention, a small part of the braking resistance can be formed by the stator core **3** and effected on the fly wheel **2** while the most part of the braking resistance is provided by the brake core **5**. The greatest characteristic of the brake device with a combination of power-generating and eddy-current magnetic resistance—such two-in-one brake device—lies in that the stator core **3** is only loaded with a very slight braking resistance, so that the power is little consumed and the volume and the producing cost are therefore able to be reduced. To make use of the brake core **5** to produce most of the braking resistance, it can not only reduce the volume and the producing cost of the generator, but also the power produced by itself can supply the brake core **5** to perform an effective motion loading.

FIG. **7** illustrates a block diagram of the above-mentioned embodiment of the present invention while FIG. **8** shows a circuit diagram of the preferred embodiment. Through this controlling circuit, the above-mentioned two-in-one brake device can reach its effect. After a practical test, it really has the application value to the industry.

Many changes and modifications in the above-described embodiment of the invention can, of course, be carried out without departing from the scope thereof. Accordingly, to promote the progress in science and the useful arts, the invention is disclosed and is intended to be limited only by the scope of the appended claims.

What is claimed is:

1. An electromagnetic induction braking system comprising:

    (a) a frame including a pair of support plates disposed in spaced manner one from the other, each said support plate having a front edge portion defining an indentation, each said support plate having formed therein a borehole;

5

(b) a fly wheel rotatably supported between said support plates of said frame, said fly wheel having a central opening and a flanged peripheral portion radially offset therefrom, said fly wheel including at least one permanent magnet secured to said peripheral portion;

(c) a stator core coupled to said frame, said stator core having a plurality of electrically conductive windings, said stator core being electromagnetically coupled to said fly wheel for generation of an induced electric signal responsive to the rotation thereof;

(d) a brake core securely received in said indentations of said frame support plates and disposed adjacent said peripheral portion of said fly wheel for electromagnetic coupling therewith, said brake core including a plurality of electrically conductive windings formed about a plurality of plates of predetermined shape and material composition; and,

(e) a feedback assembly coupled to said stator and brake cores, said feedback assembly including at least one power supply for electrically energizing said brake core responsive to said induced electric signal generated by said stator core;

whereby said brake core is adapted to electromagnetically impart to said fly wheel a braking force for opposing the rotation thereof.

2. The electromagnetic induction braking system as recited in claim **1** wherein said power supply of said feedback assembly is an adjustable DC power supply.

3. The electromagnetic induction braking system as recited in claim **2** wherein said feedback assembly further includes control means coupled to said adjustable DC power supply for controlling said electrical energization of said brake core responsive to said induced electric signal generated by said stator core.

4. The electromagnetic induction braking system as recited in claim **3** wherein said control means of said feedback assembly includes means for gauging and displaying a system parameter.

5. The electromagnetic induction braking system as recited in claim **3** wherein said feedback assembly further includes:

(a) a conditioning circuit coupled to said stator core for commutating and wave-filtering said induced electric signal generated thereby; and,

(b) a supplemental power supply coupled to said conditioning circuit for energizing said control means responsive to said induced electric signal.

6. The electromagnetic induction braking system as recited in claim **5** further comprising coupling means for rotatably coupling said fly wheel to said frame, said coupling means including:

(a) a central axle passing through said central opening of said fly wheel and said respective boreholes of said frame support plates;

(b) a plurality of annular bearings coaxially coupled to said central axle; and,

(c) at least one bearing collar coaxially coupled to said central axle and secured to one said frame support plate.

7. The electromagnetic induction braking system as recited in claim **6** wherein said predetermined shape of said plates of said brake core is substantially an E-shape.

6

8. The electromagnetic induction braking system as recited in claim **7** wherein said predetermined material composition of said plates of said brake core includes a silicon steel material.

9. An electromagnetic induction braking system comprising:

(a) a frame including a pair of support plates disposed in spaced manner one from the other, each said support plate having a front edge portion defining an indentation, each said support plate having formed therein a borehole;

(b) a fly wheel having a central opening and a flanged peripheral portion radially offset therefrom, said fly wheel including at least one permanent magnet secured to said peripheral portion;

(c) coupling means for rotatably supporting said fly wheel between said frame support plates, said coupling means including:

(1) a central axle passing through said central opening of said fly wheel and said respective boreholes of said frame support plates;

(2) a plurality of annular bearings coaxially coupled to said central axle; and,

(3) at least one bearing collar coaxially coupled to said central axle and secured to one said frame support plate;

(d) a stator core coupled to said frame, said stator core having a plurality of electrically conductive windings, said stator core being electromagnetically coupled to said fly wheel for generation of an induced AC electric signal responsive to the rotation thereof;

(e) a brake core securely received in said indentations of said frame support plates and disposed adjacent said peripheral portion of said fly wheel for electromagnetic coupling therewith, said brake core including a plurality of electrically conductive windings formed about a plurality of substantially E-shaped plates formed of a silicon steel composition; and,

(f) a feedback assembly coupled to said stator and brake cores, said feedback assembly including at least one adjustable DC power supply for electrically energizing said brake core responsive to said induced electric signal generated by said stator core, said feedback assembly further including:

(1) means coupled to said adjustable DC power supply for controlling said electrical energization of said brake core responsive to said induced electric signal generated by said stator core, and gauging and displaying a system parameter;

(2) a conditioning circuit coupled to said stator core for commutating and wave-filtering said induced electric signal generated thereby; and,

(3) a supplemental DC power supply coupled to said conditioning circuit responsivezing said control means responsive to said induced electric signal;

whereby said brake core is adapted to electromagnetically impart to said fly wheel a braking force for opposing the rotation thereof.

* * * * *

A.2 - Processing Source Code: PWM_Cipollina_Boost_Ac.pde

```
/*
Pulse Width Modulation Program
Created by Joseph Cipollina
*/

// Pin definitions
const int pwmouthigh = 5;    //Default at 1kHz
const int pwmoutvar = 11;    //Default to be 500 Hz
const int freqbin = 1;      //Default is 64; 8 for 4khz
const int buckonoff = 2;
const int analogpin = 0;

// Contants
const float v_boost_des = 24;
const float dcreghigh = 15;
const int mydelay = 0; //millisecs
const float dcgain = 0.39; //accuracy of PWM is 0.39
const int samplesize = 500;
const float vdivratio = (982.0+9817.0)/982.0;

// Varibles
float dcvalue = 0;
float dcbinflo = dcvalue * 256.0 / 100.0;
int dcbinary = (int)dcbinflo;
int inval;
int i;
float involt;
float involtavg;
float vratio;

void setup()
{

  pinMode(pwmouthigh, OUTPUT);
  pinMode(pwmoutvar, OUTPUT);
  pinMode(buckonoff, OUTPUT);

  Serial.begin(9600);                    // Uncomment the Serial.bla lines for debugging.
  Serial.println("Program start.");      // but feel free to comment them out after it's working
right.
  setPwmFrequency(pwmoutvar,freqbin);
}

void loop()
{

  digitalWrite(buckonoff, HIGH);
  analogWrite(pwmouthigh, dcbinary);
  analogWrite(pwmoutvar, dcbinary);
  delay(mydelay);    // in millisecs


  //Sample and Find Average
```

```
  involtavg = 0.0;
  for(i=0;i<samplesize;i++)
  {
    inval = analogRead(analogpin);
    involt = (float)inval * 5.0 / 1024.0;
    involt = involt * vdivratio;
    involtavg = involtavg + involt;
  }
  involtavg = involtavg / samplesize;

  //Solve for DC
  if (involtavg < v_boost_des)
    {
    dcvalue = dcvalue + dcgain;
    if (dcvalue >= dcreghigh)
    {
      dcvalue = dcreghigh;
    }
    }
  else
    {

    //adjustable gain to protect buck
    if (involtavg-v_boost_des > 10.0)
    {
      dcvalue = dcvalue - (15.0*dcgain);
    }
    else
    {
      dcvalue = dcvalue - dcgain;
    }

    if (dcvalue <= 0)
    {
      dcvalue = 0;
    }
    }

  //Print information
// dcvalue=35;
  Serial.println(involtavg);
  Serial.println((int)v_boost_des);
  Serial.println(dcvalue);
  dcbinflo = dcvalue * 256.0 / 100.0;
  dcbinary = (int)dcbinflo;

}

/**
 * Divides a given PWM pin frequency by a divisor.
 *
 * The resulting frequency is equal to the base frequency divided by
 * the given divisor:
 *   - Base frequencies:
 *      o The base frequency for pins 3, 9, 10, and 11 is 31250 Hz.
 *      o The base frequency for pins 5 and 6 is 62500 Hz.
```

```
 *   - Divisors:
 *      o The divisors available on pins 5, 6, 9 and 10 are: 1, 8, 64,
 *        256, and 1024.
 *      o The divisors available on pins 3 and 11 are: 1, 8, 32, 64,
 *        128, 256, and 1024.
 *
 * PWM frequencies are tied together in pairs of pins. If one in a
 * pair is changed, the other is also changed to match:
 *   - Pins 5 and 6 are paired on timer0
 *   - Pins 9 and 10 are paired on timer1
 *   - Pins 3 and 11 are paired on timer2
 *
 * Note that this function will have side effects on anything else
 * that uses timers:
 *   - Changes on pins 3, 5, 6, or 11 may cause the delay() and
 *     millis() functions to stop working. Other timing-related
 *     functions may also be affected.
 *   - Changes on pins 9 or 10 will cause the Servo library to function
 *     incorrectly.
 *
 * Thanks to macegr of the Arduino forums for his documentation of the
 * PWM frequency divisors. His post can be viewed at:
 *   http://www.arduino.cc/cgi-bin/yabb2/YaBB.pl?num=1235060559/0#4
 */
void setPwmFrequency(int pin, int divisor) {
 byte mode;
 if(pin == 5 || pin == 6 || pin == 9 || pin == 10) {
   switch(divisor) {
     case 1: mode = 0x01; break;
     case 8: mode = 0x02; break;
     case 64: mode = 0x03; break;
     case 256: mode = 0x04; break;
     case 1024: mode = 0x05; break;
     default: return;
   }
   if(pin == 5 || pin == 6) {
    TCCR0B = TCCR0B & 0b11111000 | mode;
   } else {
    TCCR1B = TCCR1B & 0b11111000 | mode;
   }
 } else if(pin == 3 || pin == 11) {
   switch(divisor) {
     case 1: mode = 0x01; break;
     case 8: mode = 0x02; break;
     case 32: mode = 0x03; break;
     case 64: mode = 0x04; break;
     case 128: mode = 0x05; break;
     case 256: mode = 0x06; break;
     case 1024: mode = 0x7; break;
     default: return;
   }
   TCCR2B = TCCR2B & 0b11111000 | mode;
 }
}
```

A.3 - Processing Source Code: PWM_Cipollina_Buck.pde

```
/*
Pulse Width Modulation Program for Buck Converter
Created by Joseph Cipollina
Version 2011.12.26.A
*/

// Pin definitions
const int pwmoutvar = 11;    //Default to be 500 Hz
const int freqbin = 1;     //Default is 64; 8 for 4khz; 1 for 31.25kHz
const int analogpin_in = 0;
const int analogpin_out = 1;

// Contants
const float v_out_des = 12.5; //12.5;
const float v_out_delta = 1.5;
const float v_des_gain = 0.1;
const float v_out_high = v_out_des + v_out_delta;
const float v_out_low = v_out_des - v_out_delta;
const float v_cutoff = 10;
const float v_in_high = 30; // bjt vce=40
const float dc_high = 98; //works through piecwise
const float dc_low = 10;//25;
const float vinoutdiff = 3.5; //found as best
const float vinoutdiff_adj = 5;
const int mydelay = 0; //millisecs
const float dcgain = 0.39; //accuracy of PWM is 0.39
const int samplesize = 100;
const float vdiv_in = (982.0+9817.0)/982.0;  //range of 0-50V
const float vdiv_out = (5000.0+14770.0)/5000.0;  //range of 0-20V

// Varibles
float v_des = v_out_des;
float v_in_low;
float v_in_low_adj;
float dcvalue = dc_low;
float dcbinflo = dcvalue * 256.0 / 100.0;
int dcbinary = (int)dcbinflo;
float onoff;
int inout;
int fromlowhigh=0;
int i;
int inval_in;
int inval_out;
float involt_in;
float involt_inavg;
float involt_out;
```

```
float involt_outavg;
float vratio;
float vdiff;

void setup()
{

  pinMode(pwmoutvar, OUTPUT);

  Serial.begin(9600);                          // Uncomment the Serial.bla lines for debugging.
  Serial.println("Program start.");            // but feel free to comment them out after it's working
right.
  setPwmFrequency(pwmoutvar,freqbin);
}

void loop()
{
  //initial set up
  delay(mydelay);    // in millisecs

  //updates
  v_in_low = v_des + vinoutdiff;
  v_in_low_adj = v_des + vinoutdiff_adj;
  inout = 1;

  //Sample and Find Average
  involt_inavg = 0.0;
  for(i=0;i<samplesize;i++)
  {
    inval_in = analogRead(analogpin_in);
    involt_in = (float)inval_in * 5.0 / 1024.0;
    involt_in = involt_in * vdiv_in;
    involt_inavg = involt_inavg + involt_in;
  }
  involt_inavg = involt_inavg / samplesize;

  involt_outavg = 0.0;
  for(i=0;i<samplesize;i++)
  {
    inval_out = analogRead(analogpin_out);
    involt_out = (float)inval_out * 5.0 / 1024.0;
    involt_out = involt_out * vdiv_out;
    involt_outavg = involt_outavg + involt_out;
  }
  involt_outavg = involt_outavg / samplesize;


  //Turn on?
  if (involt_inavg < v_cutoff)
```

```
   {
   onoff=0;
   v_des = v_out_des;
   dcvalue = dc_low; //reset
   }
 else
   {
   onoff=1;
   }

  if (involt_inavg < v_in_low)
    {
     fromlowhigh = 1;
     v_des = v_des - (v_des_gain*onoff);//onoff forces it to be 0 if 0
     if (v_des <= v_out_low)
       {
       inout = 0;
       v_des = v_out_low;
       }
    }
  else if (involt_inavg > v_in_high)
    {
     fromlowhigh = 0;
     v_des = v_des + (v_des_gain*onoff);//onoff forces it to be 0 if 0
     if (v_des >= v_out_high)
       {
       inout = 0;
       v_des = v_out_high;
       }
    }
  else if (involt_inavg > v_in_low_adj) //bring back to v_out_des
    {
     if (fromlowhigh>0)
     {
     v_des = v_des + (v_des_gain*onoff);//onoff forces it to be 0 if 0
     if (v_des >= v_out_des)
       {
       v_des = v_out_des;
       }
     }
    }

//Solve for DC
vdiff=v_des-involt_outavg;
dcvalue=(dcgain*vdiff*onoff) + dcvalue;

//Limit Checks
if (dcvalue >= dc_high)
  {
```

```
  dcvalue = dc_high;
   }
 if (dcvalue <= dc_low)
  {
  dcvalue = dc_low;
   }

 //calc binary dc
 dcbinflo = (dcvalue * 256.0) / 100.0; //onoff forces it to be 0 if 0
 dcbinary = (int)dcbinflo;
 analogWrite(pwmoutvar, dcbinary);

 //Print information
 if (inout<1)
 {
   Serial.println("Outside Param");
 }
 else
  {
    Serial.println("Inside Param");
  }

 Serial.println(involt_inavg);
 Serial.println(involt_outavg);
 Serial.println(v_des);
 Serial.println(dcvalue);

}




/**
 * Divides a given PWM pin frequency by a divisor.
 *
 * The resulting frequency is equal to the base frequency divided by
 * the given divisor:
 *   - Base frequencies:
 *     o The base frequency for pins 3, 9, 10, and 11 is 31250 Hz.
 *     o The base frequency for pins 5 and 6 is 62500 Hz.
 *   - Divisors:
 *     o The divisors available on pins 5, 6, 9 and 10 are: 1, 8, 64,
 *       256, and 1024.
 *     o The divisors available on pins 3 and 11 are: 1, 8, 32, 64,
 *       128, 256, and 1024.
 *
 * PWM frequencies are tied together in pairs of pins. If one in a
 * pair is changed, the other is also changed to match:
 *   - Pins 5 and 6 are paired on timer0
 *   - Pins 9 and 10 are paired on timer1
```

```
 *   - Pins 3 and 11 are paired on timer2
 *
 * Note that this function will have side effects on anything else
 * that uses timers:
 *   - Changes on pins 3, 5, 6, or 11 may cause the delay() and
 *     millis() functions to stop working. Other timing-related
 *     functions may also be affected.
 *   - Changes on pins 9 or 10 will cause the Servo library to function
 *     incorrectly.
 *
 * Thanks to macegr of the Arduino forums for his documentation of the
 * PWM frequency divisors. His post can be viewed at:
 *   http://www.arduino.cc/cgi-bin/yabb2/YaBB.pl?num=1235060559/0#4
 */
void setPwmFrequency(int pin, int divisor) {
 byte mode;
 if(pin == 5 || pin == 6 || pin == 9 || pin == 10) {
   switch(divisor) {
     case 1: mode = 0x01; break;
     case 8: mode = 0x02; break;
     case 64: mode = 0x03; break;
     case 256: mode = 0x04; break;
     case 1024: mode = 0x05; break;
     default: return;
   }
   if(pin == 5 || pin == 6) {
     TCCR0B = TCCR0B & 0b11111000 | mode;
   } else {
     TCCR1B = TCCR1B & 0b11111000 | mode;
   }
 } else if(pin == 3 || pin == 11) {
   switch(divisor) {
     case 1: mode = 0x01; break;
     case 8: mode = 0x02; break;
     case 32: mode = 0x03; break;
     case 64: mode = 0x04; break;
     case 128: mode = 0x05; break;
     case 256: mode = 0x06; break;
     case 1024: mode = 0x7; break;
     default: return;
   }
   TCCR2B = TCCR2B & 0b11111000 | mode;
 }
}
```

Proposed Circuit (Buck Rectifier and Buck Converter)

Part Num	Discription	Element Type	Supplier	Supplier Part Num	Price/unit	Quanity	Cost
1	4-amp; 250V;	Fuse	RadioShack	270-1010	$0.55	1	$0.55
2	2.5W @50 C;	Heat Sink	Digi-Key	HS300-ND	$1.36	4	$5.44
3	600V; 6A; No recover time; Silicon Carbide Schottky	Diode	Digi-Key	SCS106AGC-ND	$4.56	2	$9.12
4	1mH; 2.4A	Inductor	Digi-Key	M8895-ND	$3.99	1	$3.99
5	330uF; 315V	Capacitor	Digi-Key	493-1213-ND	$4.11	1	$4.11
6	MOSFET(NPN); 60 V; 52.4 A; logic level gate;	Transistor	Digi-Key	FQP50N06L-ND	$1.25	1	$1.25
8	1200uF; 65V	Capacitor	Digi-Key	P11282-ND	$2.15	1	$2.15
9	BJT(NPN); 40V; 2N3904	Transistor	Digi-Key	2N3904TFCT-ND	$0.43	2	$0.86
10	0.001uF; 50V; Ceramic	Capacitor	RadioShack	272-126	$0.95	1	$0.95
11	0.01uF; 50V; Ceramic	Capacitor	Digi-Key	478-5739-ND	$0.29	2	$0.58
12	0.1uF; 50V; Ceramic	Capacitor	RadioShack	272-0135	$0.95	2	$1.89
13	0.47uF; 100V; Ceramic	Capacitor	Digi-Key	399-4416-ND	$0.66	1	$0.66
14	45V; 6A; Schottky - Buck	Doide	Digi-Key	6TQ045PBF-ND	$2.76	1	$2.76
15	Buck Converter; 4-40V; 5A; Adjustable	Controller	Digi-Key	LM2678T-ADJ-ND	$7.43	0	$0.00
16	120uH; 5.1A	Inductor	Digi-Key	M1434-ND	$5.14	1	$5.14
17	330uF; 50V	Capacitor	Digi-Key	P11258-ND	$0.90	1	$0.90
18	Arduino Uno (Replaced Duemilanove)	Controller	Digi-Key	1050-1024-ND	$26.01	1	$26.01
19	50V; 6A; Rectifier	Diode	RadioShack	276-1661	$0.67	1	$0.67
						Total	$67.03

Boost Converter

Part Num	Discription	Element Type	Supplier	Supplier Part Num	Price/unit	Quanity	Cost
1	1mH; 2.4A	Inductor	Digi-Key	M8895-ND	$3.99	1	$3.99
2	330uF; 315V	Capacitor	Digi-Key	493-1213-ND	$4.11	1	$4.11
3	MOSFET(NPN); 60 V; 52.4 A; logic level gate;	Transistor	Digi-Key	FQP50N06L-ND	$1.25	1	$1.25
4	45V; 10A; Schottky - Boost	Doide	Digi-Key	MBR1045PBF-ND	$1.48	1	$1.48
5	1200uF; 65V	Capacitor	Digi-Key	P11282-ND	$2.15	1	$2.15
6	BJT(NPN); 40V; 2N3904	Transistor	Digi-Key	2N3904TFCT-ND	$0.43	2	$0.86
						Total	$13.84

A.5   - MATLAB m-file: Matlab_BR_BC.m

```matlab
%% Information
% Solving the Buck Rectifier (created by Michael Grant) and
% Boost Converter (created by Joseph Cipollina)
% created by Joseph Cipollina
% Averaging Proglem Solved - 7/11

clc
clear
close all

%Simulation Information
SimLinkName='Simulink_BR_BC_Rload_Feedback_2';
Stoptime=.3;
strStoptime=num2str(Stoptime);
ResRunAll=10 %10; %10 - all, 1-6 for that single run
DataLimit=2000000; %'inf'

%Component Basics
Rload=10;
Rbat=.1;
Cvalue=330e-6;
Lvalue=1e-3;
RLvalue=1;
CvalueBuck=330e-6;
LvalueBuck=120e-6;
CvalueBuckIn=1200e-6;

%Controls
V_Buck_Desired = 12.5;
SwitchFreq=31.25e3;
BuckUpdateGain=1000;
SwitchPeriod=1/SwitchFreq;

%Components Advanced
BatRvalue=4;
VfMos=1.5;
RMos=0.02;
VfdiodeBR=1.5;
VfdiodeBuck=.6;
RdiodeBuck=VfdiodeBuck/6;
VfdiodeEnd=.7;
RdiodeEnd=VfdiodeEnd/6;
Inductor_Start=0;
Cap_int=0;

% RPM=[35; 50; 60; 75; 100];
RPM=60;
legString='';
plotString2='';

for n=1:length(RPM)
```

```matlab
%Load Data
str_RPM=num2str(RPM(n));
FileName=['Data_' str_RPM 'RPM'];
FileExtension='.txt';
LoadString=['load ' FileName FileExtension];
eval(LoadString);
ResString=['ResLevel=Data_' str_RPM 'RPM(:,1);'];
eval(ResString);
ResLevel=ResLevel';
DTString=['DT=Data_' str_RPM 'RPM(:,2);'];
eval(DTString);
DT=DT';
VString=['Vmax=Data_' str_RPM 'RPM(:,3);'];
eval(VString);
Vmax=Vmax';

if ResRunAll==10;
    ResRun=1:length(ResLevel);
else
    ResRun=ResRunAll;
end

%intialize varibles to run faster
IC1avg=zeros(size(ResLevel));
IC2avg=zeros(size(ResLevel));
Iinavg=zeros(size(ResLevel));
IBuckavg=zeros(size(ResLevel));
Pinavg=zeros(size(ResLevel));
PBuckavg=zeros(size(ResLevel));
VRipple_Per=zeros(size(ResLevel));
IC1Ripple_Per=zeros(size(ResLevel));
IC2Ripple_Per=zeros(size(ResLevel));
V_Buck_avg=zeros(size(ResLevel));
V_LP_Avg=zeros(size(ResLevel));
Vcalc=zeros(size(ResLevel));

time=clock;
fprintf('Start Time: %2.0i:%2.0i\n',time(4),time(5));
for i=ResRun  %Control single level
    str_Res=num2str(ResLevel(i));
    % Set Up Individual Values
    DTvalue=DT(i);
    Vvalue=Vmax(i);
    Vavg_calc=DTvalue*Vvalue/100;
    DCvalueBuck=(V_Buck_Desired/Vavg_calc)*100;

    DC_initial_Buck=DCvalueBuck;

    %What to Simulate
    set_param(SimLinkName, 'StopTime', strStoptime)
    sim(SimLinkName)
    str_Res;
    time=clock;
    fprintf([str_Res ' done at: %2.0i:%2.0i\n'],time(4),time(5));

    int=find(Tout>(.95*Stoptime));
```

```matlab
        intfirst=int(1);
        intlast=int(length(int));

        %Find the area of each individual point because the time scale
        %is not linear and a simple mean of the set would be inaccurate

        AV_LP_Avg=0; AIC1avg=0; AIC2avg=0; AIinavg=0; AIBuckavg=0;
         AV_Buck_avg=0; APinavg=0; APBuckavg=0;
        for m=intfirst:intlast-1
            shortint=[m m+1];
            Tstep=Tout(m+1)-Tout(m);
            AV_LP_Avg=AV_LP_Avg+mean(V_LP(shortint))*Tstep;
            AIC1avg=AIC1avg+mean(I_C1(shortint))*Tstep;
            AIC2avg=AIC2avg+mean(I_C2(shortint))*Tstep;
            AIinavg=AIinavg+mean(I_in(shortint))*Tstep;
            AIBuckavg=AIBuckavg+mean(I_Buck(shortint))*Tstep;
            AV_Buck_avg=AV_Buck_avg+mean(V_Buck(shortint))*Tstep;
            APinavg=APinavg+mean(V_in(shortint).*I_in(shortint))*Tstep;

APBuckavg=APBuckavg+mean(V_Buck(shortint).*I_Buck(shortint))*Tstep;
        end

        %Divid the area by the total length
        Ttstep=Tout(intlast)-Tout(intfirst);
        V_LP_Avg(i)=AV_LP_Avg/Ttstep;
        IC1avg(i)=AIC1avg/Ttstep;
        IC2avg(i)=AIC2avg/Ttstep;
        Iinavg(i)=AIinavg/Ttstep;
        IBuckavg(i)=AIBuckavg/Ttstep;
        V_Buck_avg(i)=AV_Buck_avg/Ttstep;
        Pinavg(i)=APinavg/Ttstep;
        PBuckavg(i)=APBuckavg/Ttstep;

        Vripple=abs(max(V_LP(int))-min(V_LP(int)));
        IC1ripple=abs(max(I_C1(int))-min(I_C1(int)));
        IC2ripple=abs(max(I_C2(int))-min(I_C2(int)));
        VRipple_Per(i)=100*(Vripple/V_LP_Avg(i));
        IC1Ripple_Per(i)=100*(IC1ripple/IC1avg(i));
        IC2Ripple_Per(i)=100*(IC2ripple/IC2avg(i));
        % fprintf('V_LP_Avg= %4.2f, Ripple= %4.2f
%\n',V_LP_Avg,VRipple_Per)
        Vcalc(i)=Vavg_calc;
        str_ResLevel=num2str(ResLevel(i));
    eval(['Tout_' str_ResLevel '=Tout;'])
    eval(['V_LP_' str_ResLevel '=V_LP;'])
    eval(['V_Buck_' str_ResLevel '=V_Buck;'])
    eval(['V_in_' str_ResLevel '=V_in;'])
    eval(['I_in_' str_ResLevel '=I_in;'])
    eval(['I_Buck_' str_ResLevel '=I_Buck;'])
    eval(['I_C1_' str_ResLevel '=I_C1;'])
    eval(['I_C2_' str_ResLevel '=I_C2;'])
    eval(['P_in_' str_ResLevel '=V_in.*I_in;'])
    eval(['P_Buck_' str_ResLevel '=V_Buck.*I_Buck;'])
    eval(['I_LP_' str_ResLevel '=I_LP;'])
    end
    eval(['V_LP_Avg_' str_RPM '=V_LP_Avg;'])
```

```matlab
    eval(['Vcalc_' str_RPM '=Vcalc;'])
    eval(['ResLevel_' str_RPM '=ResLevel;'])
    eval(['V_Buck_' str_RPM '=V_Buck_avg;'])
    eval(['VRipple_Per_' str_RPM '=VRipple_Per;'])
    eval(['IC1Ripple_Per_' str_RPM '=IC1Ripple_Per;'])
    eval(['IC2Ripple_Per_' str_RPM '=IC2Ripple_Per;'])
    eval(['P_in_' str_RPM '=Pinavg;'])
    eval(['P_Buck_' str_RPM '=PBuckavg;'])
    eval(['I_in_' str_RPM '=Iinavg;'])
    eval(['I_Buck_' str_RPM '=IBuckavg;'])
    eval(['Eff_' str_RPM '=PBuckavg./Pinavg;'])
end

figure % Voltages
for i=ResRun
    str_ResLevel=num2str(ResLevel(i));
    if length(ResRun) > 1
     subplot(ceil((length(ResRun)/2)),2,i)
    subplot(3,1,i)  %ideal format for paper
    end
    %eval('xlim([' XMIN 'Tout_' str_ResLevel '])
    str=['Tout_' str_ResLevel ',V_LP_' str_ResLevel ',Tout_'
str_ResLevel ',V_Buck_' str_ResLevel];
    eval(['plot(' str ')'])
    hold on
    eval(['xmax=max(Tout_' str_ResLevel ')']); % Steady State for Paper
    xlim([.99*xmax xmax]);
    grid on
    xlabel('Time [secs]')
    ylabel('Voltage [Volts]')
    title(['VBR and VBuck for Data at ResLevel= ' str_ResLevel])
    legend('VBR','VBuck','Location','SouthEast')
    hold off
end

 figure %Currents
for i=ResRun
    str_ResLevel=num2str(ResLevel(i));
    if length(ResRun) > 1
     subplot(ceil((length(ResRun)/2)),2,i)
    subplot(3,1,i)  %ideal format for paper
    end
    str=['Tout_' str_ResLevel ',I_in_' str_ResLevel ',Tout_'
str_ResLevel ',I_LP_' str_ResLevel ',Tout_' str_ResLevel ',I_Buck_'
str_ResLevel];
    eval(['plot(' str ')'])
    hold on
    eval(['xmax=max(Tout_' str_ResLevel ')']); % Steady State for Paper
    xlim([.999*xmax xmax]);
    grid on
    xlabel('Time [secs]')
    ylabel('Current [Amps]')
    title(['Current for Data at ResLevel= ' str_ResLevel])
    legend('Iin','IBR','IBuck','Location','SouthEast')
    hold off
end
```

```matlab
 figure %Currents
for i=ResRun
    str_ResLevel=num2str(ResLevel(i));
    if length(ResRun) > 1
    subplot(ceil((length(ResRun)/2)),2,i)
    subplot(3,1,i)  %ideal format for paper
    end
    str=['Tout_' str_ResLevel ',I_C1_' str_ResLevel ',Tout_'
str_ResLevel ',I_C2_' str_ResLevel];
    eval(['plot(' str ')'])
    hold on
    grid on
    xlabel('Time [secs]')
    ylabel('Current [Amps]')
    title(['Ic1 and Ic2 for Data at ResLevel= ' str_ResLevel])
    legend('Ic1','Ic2','Location','SouthEast')
    hold off
end

figure %Avg Voltage
subplot(3,1,1)
plotString=['ResLevel_' str_RPM ',V_LP_Avg_' str_RPM ',ResLevel_'
str_RPM ',V_Buck_' str_RPM];
eval(['plot(' plotString ',''LineWidth'',2)'])
hold on
grid on
xlabel('Res Level (2-25)')
ylabel('Voltage [Volts]')
title(['Average VBR and VBuck for Data'])
legend('VBR','VBuck','Location','SouthEast')
hold off

subplot(3,1,2)  %Avg Current
plotString=['ResLevel_' str_RPM ',I_in_' str_RPM ',ResLevel_' str_RPM
',I_Buck_' str_RPM];
eval(['plot(' plotString ',''LineWidth'',2)'])
hold on
grid on
xlabel('Res Level (2-25)')
ylabel('Current [Amps]')
title(['Average Iin and IBuck for Data'])
legend('Iin','IBuck','Location','SouthEast')
hold off

subplot(3,1,3) %Avg Power
plotString=['ResLevel_' str_RPM ',P_in_' str_RPM ',ResLevel_' str_RPM
',P_Buck_' str_RPM];
eval(['plot(' plotString ',''LineWidth'',2)'])
hold on
grid on
xlabel('Res Level (2-25)')
ylabel('Power [Watts]')
title(['Pin and Pout for Data'])
legend('Pin','Pout','Location','SouthEast')
hold off
```

A.6   - Simulink_BR_BC_Rload_Feedback.mdl
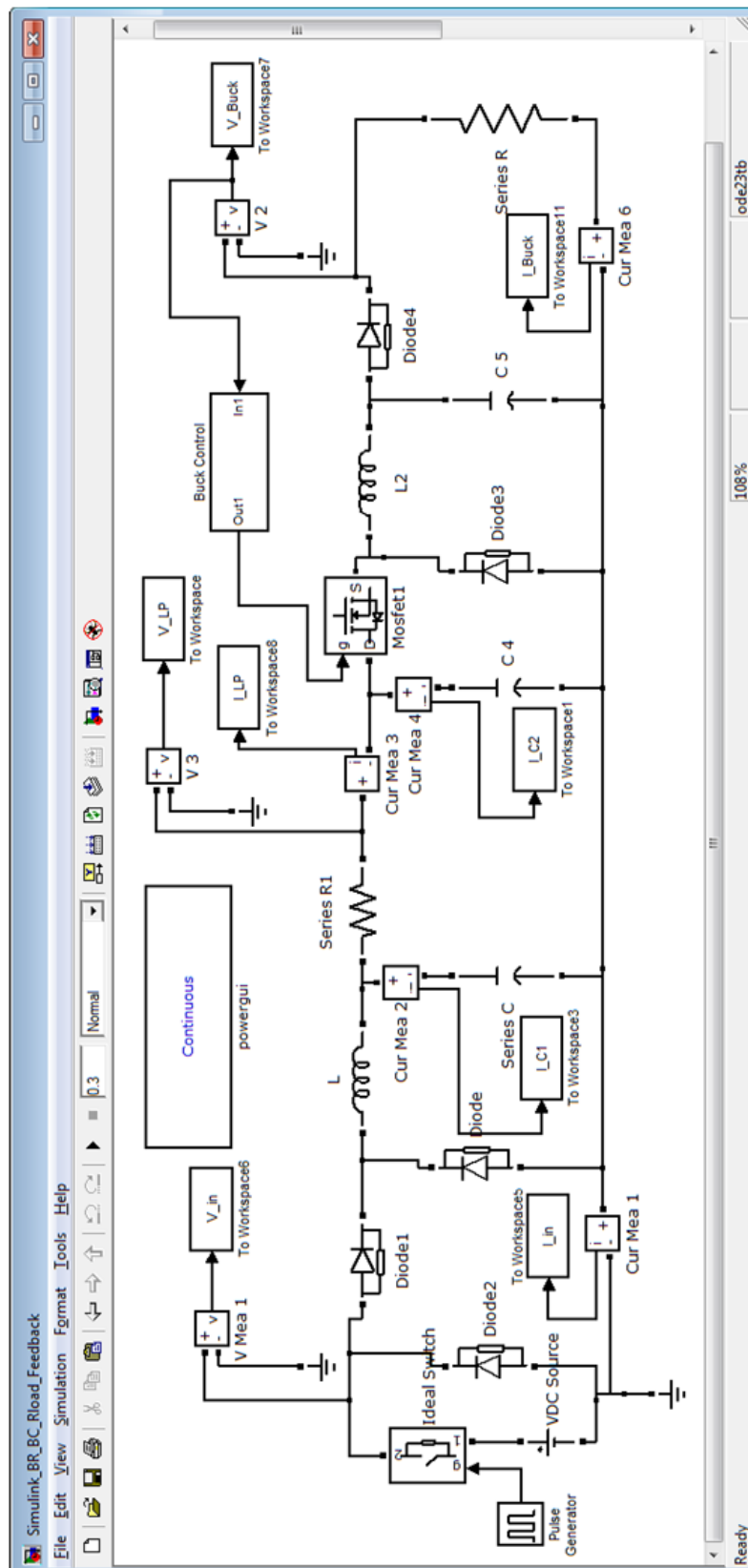
A.7   – LTSpiceIV file: BR_BC_Measurements.asc

118
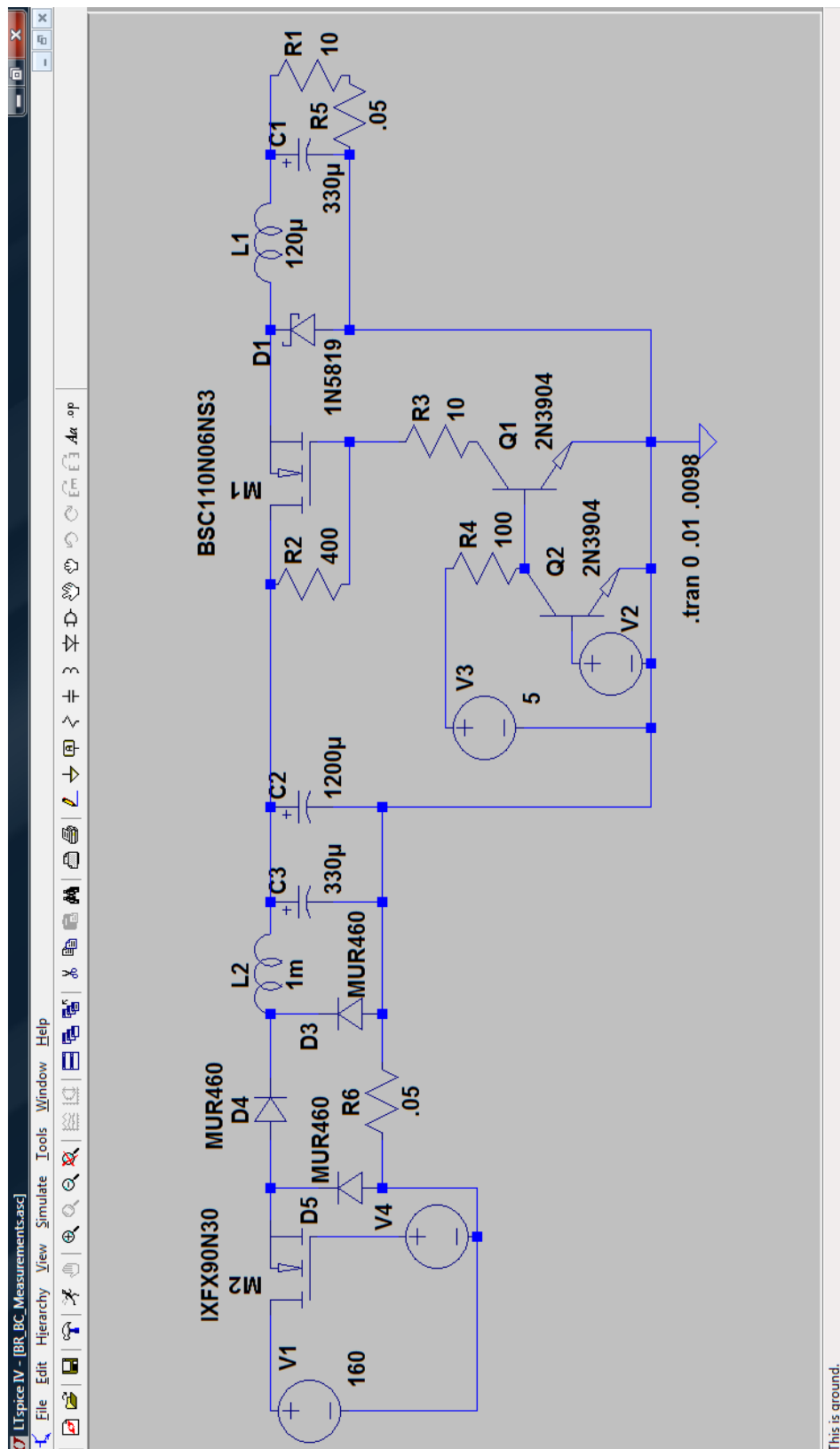
A.8 – Enphase M190 Data Sheet

[e] ENPHASE MICROINVERTER   **M190**
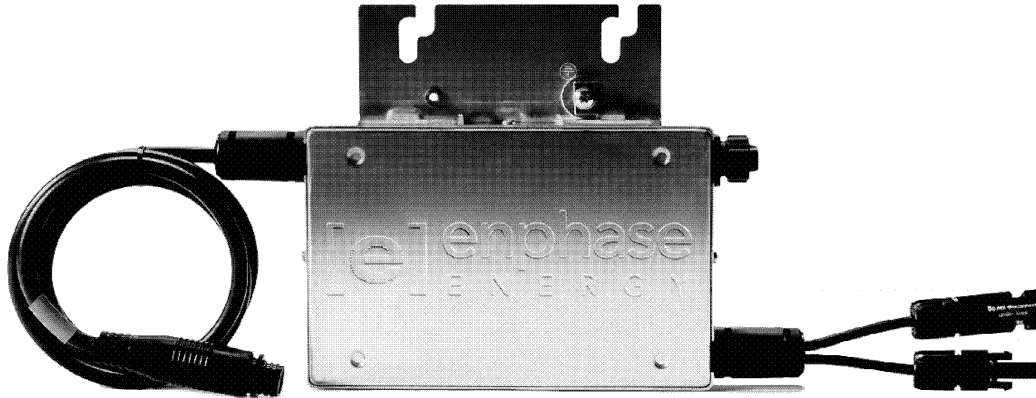
The Enphase Energy Microinverter System improves energy harvest, increases reliability, and dramatically simplifies design, installation and management of solar power systems. The Enphase System includes the microinverter, the Envoy Communications Gateway, and the web-based Enlighten monitoring and analysis website.

PRODUCTIVE
- Maximum energy production
- Resilient to dust, debris and shading
- Performance monitoring per module

RELIABLE
- MTBF of 331 years
- System availability greater than 99.8%
- No single point of system failure

SMART
- Quick & simple design, installation and management
- 24/7 monitoring and analysis

SAFE
- Low voltage DC
- Reduced fire risk

MICROINVERTER TECHNICAL DATA

60 and 72 Cell Modules		
Input Data (DC)	M190-72-208-S12/3 M190-72-208-S12/3-NA (Ontario)	M190-72-240-S12/3 M190-72-240-S12/3-NA (Ontario)
Recommended input power (STC)	230W	230W
Maximum input DC voltage	56V	56V
Peak power tracking voltage	22V – 40V	22V – 40V
Min./Max. start voltage	28V/54V	28V/54V
Max. DC short circuit current	12A	12A
Max. input current	10A	10A
Output Data (AC)		
Maximum output power	190W	190W
Nominal output current	920mA	800mA
Nominal voltage/range	208V/183V-229V	240V/211V-264V
Extended voltage/range	208V/179V-232V	240V/206V-269V
Nominal frequency/range	60.0/59.3-60.5	60.0/59.3-60.5
Extended frequency/range	60.0/59.2-60.6	60.0/59.2-60.6
Power factor	>0.95	>0.95
Maximum units per branch	21	15
Efficiency		
Peak inverter efficiency	95.5%	95.5%
CEC weighted efficiency	95.0%	95.0%
Nominal MPP tracking	99.6%	99.6%
Mechanical Data		
Operating temperature range	-40°C to +65°C	-40°C to +65°C
Night time power consumption	30mW	30mW
Dimensions (WxHxD)	8" x 5.25" x 1.25"	
Weight	4.4 lbs	
Cooling	Natural Convection – No Fans	
Enclosure environmental rating	Outdoor – NEMA 6	
Features		
Communication	Powerline	
Warranty	15 Years	
Compliance	UL1741/IEEE1547	
	FCC Part 15 Class B	

A.9 – Suggested Parts List

Part Num	Discription	Element Type	Supplier	Supplier Part Num	Price/unit	Quanity	Cost
1	Current Sensor; Hall Effect; +-5A; 180mV/A	Sensor	Digi-Key	620-1189-1-ND	$4.52	3	$13.56
2	12V; 17Ah; 5.1A max charge	SLA Battery	Batteryspace.com	LA-12V18-NB	$34.00	1	$34.00
3	MOSFET(NPN); 250 Vds; 51 A; +/- 30 Vgs;	Transistor	Digi-Key	FDPF51N25-ND	$2.41	1	$2.41
4	Micro-Inverter	Inverter	gogreensolar.com	M190-72-240-S12	$120.00	1	$120.00
5	Arduino Boost Converter	Circuit	Various	See Appendix 4	$39.85	1	$39.85
						Total	$209.82

A.10   - MATLAB m-file: Elliptical_Data.m

```matlab
%% Information
% created by Joseph Cipollina
% for use in graphing precor elliptical data

clc
clear
close all

%% Input
Vl=20;
Vh=38;
t=(1:32)*1e-6;
T=10e-6;
R=10;

%% Signal
V=Vl+(Vh-Vl).*exp(-t./T); % Single Period
t2=[t-max(t) t];
V2=[V V];
t4=[t-2*max(t) t-max(t) t t+max(t)];
V4=[V V V V];
Vavg=mean(V);
Vavg_str=['Vavg = ' num2str(Vavg) 'Volts'];
Pavg=Vavg^2/R;
Pavg_str=['Pavg = ' num2str(Pavg) 'Watts'];

plot(t4*1e6,V4,'LineWidth',2)
hold on
ylim([0,40])
xlabel('Time [microseconds]')
ylabel('Voltage [Volts]')
title('Voltage Waveform Across Load Reistor for SPM = 152 and Res Level
= 10')
grid
gtext({Vavg_str,Pavg_str},'Color','b','FontWeight','bold')
hold off
```

A.11 - MATLAB m-file: PlotOscilloscope_NormalOp.m

```matlab
%% Information
% created by Joseph Cipollina

clc
clear
close all

Rcur=.05;
Vth=10;
plotnum=3;
vdata=2;
num1=10;
num2=11;

str_n1=int2str(num1);
str_num1='0000';
numlen1=length(str_n1);
numstart1=4-numlen1+1;
str_num1(numstart1:4)=str_n1;
str_n2=int2str(num2);
str_num2='0000';
numlen2=length(str_n2);
numstart2=4-numlen2+1;
str_num2(numstart2:4)=str_n2;

if vdata==1;
    str_num=str_num1;
elseif vdata==2;
    str_num=str_num2;
end

    FileName1=['F' str_num 'CH1'];
    FileName2=['F' str_num1 'CH2'];
    FileName3=['F' str_num2 'CH2'];
    FileExtension='.CSV';
    LoadString=['load ' FileName1 FileExtension];
    eval(LoadString);
    eval(['CH1=' FileName1 ';']);
    LoadString=['load ' FileName2 FileExtension];
    eval(LoadString);
    eval(['CH2=' FileName2 ';']);
    LoadString=['load ' FileName3 FileExtension];
    eval(LoadString);
    eval(['CH2b=' FileName3 ';']);

if max(CH1(:,2))<Vth
    Vavg=mean(CH1(:,2));
else
    int=find(CH1(:,2)>Vth);
    int1=int(1);
    i=1;
    while (int(i+1)-int(i))==1;
        i=i+1;
```

```matlab
        end
        int2=int(i+1);
        int12=int(i);
        Vavg=mean(CH1(int1:int2,2));
    end

    figure
    subplot(plotnum,1,1) %ch1
    plot(CH1(:,1).*1e6,CH1(:,2),'LineWidth',2)
    hold on
    grid on
    xlabel('Time [Microseconds]')
    ylabel('V [Volts]')
    % [xv,yv]=ginput(1);
    % text(xv,yv,['Vavg = ' num2str(Vavg)]);
    title(['Voltage, Vavg = ' num2str(Vavg) ' Volts'])
    hold off

    subplot(plotnum,1,2)  %ch2
    plot(CH2(:,1).*1e6,CH2(:,2)./Rcur,'LineWidth',2)
    hold on
    grid on
    xlabel('Time [Microseconds]')
    ylabel('I [Amps]')
    xline=[min(CH2(:,1).*1e6) max(CH2(:,1).*1e6)];
    ymax=max(CH2(:,2)./Rcur);
    ymin=min(CH2(:,2)./Rcur);
    plot(xline,[ymax ymax],'k','LineWidth',2)
    plot(xline,[ymin ymin],'k','LineWidth',2)
    title(['Current, Ipk-pk = ' num2str(abs(ymax)+abs(ymin)) ' Amps'])
    % [xi1,yi1]=ginput(1);
    % text(xi1,yi1,['Ipk-pk = ' num2str(abs(y1)+abs(y2))]);
    hold off

    if plotnum>2
        subplot(plotnum,1,3)  %ch2b
        plot(CH2b(:,1).*1e6,CH2b(:,2)./Rcur,'LineWidth',2)
        hold on
        grid on
        xlabel('Time [Microseconds]')
        ylabel('I [Amps]')
        ylim([-2,4])
        [x,y1]=ginput(1);
        xline=[min(CH2b(:,1).*1e6) max(CH2b(:,1).*1e6)];
        plot(xline,[y1 y1],'k','LineWidth',2)
        [x,y2]=ginput(1);
        plot(xline,[y2 y2],'k','LineWidth',2)
        Ipeak=mean([y1 y2]);
        title(['Current, Ipeak = ' num2str(Ipeak) ' Amps'])
%        [xi2,yi2]=ginput(1);
%        text(xi2,yi2,['Iavg = ' num2str(mean([y1 y2]))]);
        hold off
    end
    Pavg=Vavg*Ipeak
```

A.12 - MATLAB m-file: PlotOscilloscope_VoltageCurves.m

```matlab
%% Information
% created by Joseph Cipollina

clc
clear
close all

num=[68;46;35;53;60];
str_num=['0000';'0000';'0000';'0000';'0000']

for i=1:5;
str_n=int2str(num(i));
numlen=length(str_n);
numstart=4-numlen+1;
str_num(i,numstart:4)=str_n;

    FileName=['F' str_num(i,:) 'CH1'];
    FileExtension='.CSV';
    LoadString=['load ' FileName FileExtension];
    eval(LoadString);
    eval(['CH' int2str(i) '=' FileName ';']);

end

figure
plot(CH1(:,1).*1e6,CH1(:,2),'k','LineWidth',2)
hold on
plot(CH2(:,1).*1e6,CH2(:,2),'b','LineWidth',2)
plot(CH3(:,1).*1e6,CH3(:,2),'m--','LineWidth',2)
plot(CH4(:,1).*1e6,CH4(:,2),'b--','LineWidth',2)
plot(CH5(:,1).*1e6,CH5(:,2),'m','LineWidth',2)
grid on
xlabel('Time [Microseconds]')
ylabel('V [Volts]')
title(['Voltage Waveforms of Constant Res Level Changing Speed'])
legend('RPM = 30','RPM = 50','RPM = 60','RPM = 70','RPM = 80')
xlim([-5,15])
hold off
```

A.13 - MATLAB m-file: PlotOscilloscope_Power.m

```matlab
%% Information
% created by Joseph Cipollina

clc
clear
close all

Power1= [2.0    15.5    30.7    36.7;
5.0 21.7    36.7    33.1;
10.0    43.4    55.6    71.2;
15.0    57.1    90.1    82.5;
20.0    57.4    114.2   94.0;
25.0    96.5    125.2   145.3];


Power2= [15.0   88.6;
18.0    88.2;
20.0    88.8;
22.0    89.1;
25.0    142.9];


% Power1= [1.0     0.0     0.0     0.0;
%          2.0     0.9     2.1     2.3;
%          5.0     2.6     4.7     4.8;
%          10.0  7.9     8.9     11.3;
%          15.0  13.1    16.7    17.2;
%          20.0  21.6    29.4    28.8;
%          25.0  36.8    45.7    45.6];
%
% Power2= [15.0 14.1;
%          18.0  17.2;
%          20.0  23.1;
%          22.0  30.1;
%          25.0  38.8];

figure
plot(Power1(:,1),Power1(:,2),'bo-','LineWidth',2)
hold on
plot(Power1(:,1),Power1(:,3),'kx-','LineWidth',2)
plot(Power2(:,1),Power2(:,2),'m*-','LineWidth',2)
plot(Power1(:,1),Power1(:,4),'bs-','LineWidth',2)
grid on
xlabel('Res Level')
ylabel('Apparent Power [VA]')
title(['Apparent Power over Res Level for Different Speeds'])
% ylabel('Power [Watts]')
% title(['Average Power over Res Level for Different Speeds'])
legend('RPM = 30','RPM = 50','RPM = 60','RPM = 70')
hold off
```

A.14 - MATLAB m-file: PlotOscilloscope_OpenVoltage.m

```matlab
%% Information
% created by Joseph Cipollina

clc
clear
close all

num=[70;73;74;75;76];
str_num=['0000';'0000';'0000';'0000';'0000'];

for i=1:5;
str_n=int2str(num(i));
numlen=length(str_n);
numstart=4-numlen+1;
str_num(i,numstart:4)=str_n;

    FileName=['F' str_num(i,:) 'CH1'];
    FileExtension='.CSV';
    LoadString=['load ' FileName FileExtension];
    eval(LoadString);
    eval(['CH' int2str(i) '=' FileName ';']);

end

figure
plot(CH1(:,1).*1e6,CH1(:,2),'k','LineWidth',2)
hold on
plot(CH2(:,1).*1e6,CH2(:,2),'b','LineWidth',2)
plot(CH3(:,1).*1e6,CH3(:,2),'m','LineWidth',2)
plot(CH4(:,1).*1e6,CH4(:,2),'g','LineWidth',2)
plot(CH5(:,1).*1e6,CH5(:,2),'r','LineWidth',2)
grid on
xlabel('Time [Microseconds]')
ylabel('V [Volts]')
title(['Voltage Waveforms of Constant Res Level Changing Speed'])
legend('RPM = 40','RPM = 50','RPM = 70','RPM = 90','RPM = 107')
hold off
```

A.15 - MATLAB m-file: PlotOscilloscope_Testing.m

```matlab
%% Information
% created by Joseph Cipollina

clc
clear
close all

Rcur=.05;
vdata=1;
num1=11;
num2=12;

str_n1=int2str(num1);
str_num1='0000';
numlen1=length(str_n1);
numstart1=4-numlen1+1;
str_num1(numstart1:4)=str_n1;
str_n2=int2str(num2);
str_num2='0000';
numlen2=length(str_n2);
numstart2=4-numlen2+1;
str_num2(numstart2:4)=str_n2;

if vdata==1;
    str_num=str_num1;
elseif vdata==2;
    str_num=str_num2;
end

    FileName1=['F' str_num 'CH1'];
    FileName2=['F' str_num1 'CH2'];
    FileName3=['F' str_num2 'CH2'];
    FileExtension='.CSV';
    LoadString=['load ' FileName1 FileExtension];
    eval(LoadString);
    eval(['CH1=' FileName1 ';']);
    LoadString=['load ' FileName2 FileExtension];
    eval(LoadString);
    eval(['CH2=' FileName2 ';']);
    LoadString=['load ' FileName3 FileExtension];
    eval(LoadString);
    eval(['CH2b=' FileName3 ';']);

Vavg=mean(CH1(:,2));

figure
subplot(3,1,1) %ch1
plot(CH1(:,1).*1e6,CH1(:,2),'LineWidth',2)
hold on
grid on
xlabel('Time [Microseconds]')
ylabel('V [Volts]')
ylim([0,ceil(max(CH1(:,2)))+1])
```

```matlab
title(['Voltage, Vavg = ' num2str(Vavg) ' Volts'])
hold off

subplot(3,1,2)  %ch2
plot(CH2(:,1).*1e6,CH2(:,2)./Rcur,'LineWidth',2)
hold on
grid on
xlabel('Time [Microseconds]')
ylabel('I [Amps]')
xline=[min(CH2(:,1).*1e6) max(CH2(:,1).*1e6)];
ymax=max(CH2(:,2)./Rcur);
ymin=min(CH2(:,2)./Rcur);
plot(xline,[ymax ymax],'k','LineWidth',2)
plot(xline,[ymin ymin],'k','LineWidth',2)
title(['Current, Ipk-pk = ' num2str(ymax-ymin) ' Amps'])
% [xi1,yi1]=ginput(1);
% text(xi1,yi1,['Ipk-pk = ' num2str(abs(y1)+abs(y2))]);
hold off

subplot(3,1,3)  %ch2b
plot(CH2b(:,1).*1e6,CH2b(:,2)./Rcur,'LineWidth',2)
hold on
grid on
xlabel('Time [Microseconds]')
ylabel('I [Amps]')
ylim([0,3])
[x,y1]=ginput(1);
xline=[min(CH2b(:,1).*1e6) max(CH2b(:,1).*1e6)];
plot(xline,[y1 y1],'k','LineWidth',2)
[x,y2]=ginput(1);
plot(xline,[y2 y2],'k','LineWidth',2)
Iavg=mean([y1 y2]);
title(['Current, Iavg = ' num2str(Iavg) ' Amps'])
%     [xi2,yi2]=ginput(1);
%     text(xi2,yi2,['Iavg = ' num2str(mean([y1 y2]))]);
hold off
Pavg=Vavg*Iavg
```

A.16   - MATLAB m-file: PlotOscilloscope_VI.m

```matlab
%% Information
% created by Joseph Cipollina

clc
clear
close all

P1=14.1;
P2=38.8;
R=1:50;

VI= [5.10    6.03    1.06    10.61   1.84;
     9.70    10.04   1.04    17.06   1.77;
     20.80   16.22   0.79    26.96   1.34;
     30.10   18.85   0.61    29.92   1.02;
     40.50   21.72   0.59    34.64   0.87;
     49.10   23.99   0.51    37.16   0.79];

V1=sqrt(P1.*R);
I1=sqrt(P1./R);
V2=sqrt(P2.*R);
I2=sqrt(P2./R);

str_1=['Ideal Power Curve at P = ' num2str(P1) ' Watts'];
str_2=['Ideal Power Curve at P = ' num2str(P2) ' Watts'];
str_3='Measured Resistance Level = 15';
str_4='Measured Resistance Level = 25';

figure
plot(V1,I1,'b','LineWidth',2)
hold on
plot(V2,I2,'m','LineWidth',2)
plot(VI(:,2),VI(:,3),'b*','LineWidth',2)
plot(VI(:,4),VI(:,5),'m*','LineWidth',2)
grid on
xlabel('Voltage [Volts]')
ylabel('Current [Amps]')
title('Voltage-Current Data Compared to Ideal Curves')
legend(str_1,str_2,str_3,str_4)
hold off
```

A.17   - MATLAB m-file: PlotOscilloscope_2plots.m

```matlab
%% Information
% created by Joseph Cipollina

clc
clear
close all

Rcur=.05;
timescale=1e-6;
vdata=1;
num1=67;

str_n1=int2str(num1);
str_num1='0000';
numlen1=length(str_n1);
numstart1=4-numlen1+1;
str_num1(numstart1:4)=str_n1;

    FileName1=['F' str_num1 'CH1'];
    FileName2=['F' str_num1 'CH2'];
    FileExtension='.CSV';
    LoadString=['load ' FileName1 FileExtension];
    eval(LoadString);
    eval(['CH1=' FileName1 ';']);
    LoadString=['load ' FileName2 FileExtension];
    eval(LoadString);
    eval(['CH2=' FileName2 ';']);



Vavg=mean(CH1(:,2));
Iavg=mean(CH2(:,2))/Rcur;

figure
subplot(2,1,1) %ch1
plot(CH1(:,1)./timescale,CH1(:,2),'LineWidth',2)
hold on
grid on
xlabel(['Time [seconds x' num2str(timescale) ']'])
ylabel('V [Volts]')
ymax=max(CH1(:,2));
ymin=min(CH1(:,2));
Vrip=num2str(ymax-ymin);
title(['Voltage, Vavg = ' num2str(Vavg) ' Volts, Vpk-pk = ' Vrip '
Volts'])
ylim([0,ceil(max(CH1(:,2)))+1])
hold off

subplot(2,1,2)   %ch2
plot(CH2(:,1)./timescale,CH2(:,2)./Rcur,'LineWidth',2)
hold on
grid on
xlabel(['Time [seconds x' num2str(timescale) ']'])
```

```
ylabel('I [Amps]')
ymax=max(CH2(:,2)./Rcur);
ymin=min(CH2(:,2)./Rcur);
Irip=num2str(ymax-ymin);
title(['Current, Iavg = ' num2str(Iavg) ' Amps, Ipk-pk = ' Irip '
Amps'])
ylim([0,1.5])
hold off
```

A.18 - MATLAB m-file: PlotOscilloscope_PWM.m

```matlab
%% Information
% created by Joseph Cipollina

clc
clear
close all

Rcur=.05;
num1=69;
num2=69;

str_n1=int2str(num1);
str_num1='0000';
numlen1=length(str_n1);
numstart1=4-numlen1+1;
str_num1(numstart1:4)=str_n1;
str_n2=int2str(num2);
str_num2='0000';
numlen2=length(str_n2);
numstart2=4-numlen2+1;
str_num2(numstart2:4)=str_n2;


    FileName1=['F' str_num1 'CH1'];
    FileName2=['F' str_num2 'CH2'];
    FileExtension='.CSV';
    LoadString=['load ' FileName1 FileExtension];
    eval(LoadString);
    eval(['CH1=' FileName1 ';']);
    LoadString=['load ' FileName2 FileExtension];
    eval(LoadString);
    eval(['CH2=' FileName2 ';']);

Vavg=mean(CH1(:,2));

figure
plot(CH1(:,1).*1e6,CH1(:,2),'b','LineWidth',2)
hold on
plot(CH2(:,1).*1e6,CH2(:,2),'m','LineWidth',2)
grid on
xlabel('Time [Microseconds]')
ylabel('V [Volts]')
title('Voltage')
legend('Digital PWM','Driving PWM')
hold off
```

A.19 - MATLAB m-file: PlotOscilloscope_Boost.m

```matlab
%% Information
% created by Joseph Cipollina

clc
clear
close all

Rcur=.05;
num1=4;
num2=4;

str_n1=int2str(num1);
str_num1='0000';
numlen1=length(str_n1);
numstart1=4-numlen1+1;
str_num1(numstart1:4)=str_n1;
str_n2=int2str(num2);
str_num2='0000';
numlen2=length(str_n2);
numstart2=4-numlen2+1;
str_num2(numstart2:4)=str_n2;

    FileName1=['F' str_num1 'CH1'];
    FileName2=['F' str_num2 'CH2'];
    FileExtension='.CSV';
    LoadString=['load ' FileName1 FileExtension];
    eval(LoadString);
    eval(['CH1=' FileName1 ';']);
    LoadString=['load ' FileName2 FileExtension];
    eval(LoadString);
    eval(['CH2=' FileName2 ';']);
Vavg=mean(CH2(:,2));

figure
subplot(2,1,1)
plot(CH1(:,1).*1e6,CH1(:,2),'LineWidth',2)
hold on
grid on
xlabel('Time [Microseconds]')
ylabel('V [Volts]')
title('Voltage of MOSFET Driver')
hold off

subplot(2,1,2)
plot(CH2(:,1).*1e6,CH2(:,2),'LineWidth',2)
hold on
grid on
xlabel('Time [Microseconds]')
ylabel('V [Volts]')
str_title='Voltage between Buck Rectifier and Boost Converter';
title([str_title ' Vavg = ' num2str(Vavg) ' Volts'])
hold off
```

134

A.20 - MATLAB m-file: PlotOscilloscope_2Volts.m

```matlab
%% Information
% created by Joseph Cipollina

clc
clear
close all

Rcur=.05;
num1=9;
num2=10;

str_n1=int2str(num1);
str_num1='0000';
numlen1=length(str_n1);
numstart1=4-numlen1+1;
str_num1(numstart1:4)=str_n1;
str_n2=int2str(num2);
str_num2='0000';
numlen2=length(str_n2);
numstart2=4-numlen2+1;
str_num2(numstart2:4)=str_n2;


    FileName1=['F' str_num1 'CH1'];
    FileName2=['F' str_num2 'CH1'];
    FileExtension='.CSV';
    LoadString=['load ' FileName1 FileExtension];
    eval(LoadString);
    eval(['CH1=' FileName1 ';']);
    LoadString=['load ' FileName2 FileExtension];
    eval(LoadString);
    eval(['CH2=' FileName2 ';']);

Vavg1=mean(CH1(:,2));
Vavg2=mean(CH2(:,2));

figure
plot(CH1(:,1).*1e6,CH1(:,2),'b','LineWidth',2)
hold on
plot(CH2(:,1).*1e6,CH2(:,2),'m','LineWidth',2)
grid on
xlabel('Time [Microseconds]')
ylabel('V [Volts]')
title('Voltage')
str_1=['Buck Converter Output Voltage, Vavg=' num2str(Vavg1) 'Volts'];
str_2=['Buck Rectifier Output Voltage, Vavg=' num2str(Vavg2) 'Volts'];
legend(str_1,str_2)
hold off
```

References

[1] Krahenbuhl, E. (1901). *Patent No. US685685.* San Rafael, California.

[2] Johansen, G. (2010, September 29). ReRev Process. (J. D. Cipollina, Interviewer)

[3] Woodway USA, Inc. (n.d.). *All Green Treadmill Requires Zero Electricity and Manual Power.* Retrieved September 30, 2010, from Woodway: http://www.woodway.com/productliterature/Commercial_Fitness_Treadmills_Specs.pdf

[4] ReRev. (2011). *Facilities*. Retrieved January 13, 2012, from ReRev. A Renewable Energy: http://www.rerev.com/facilities.html

[5] Gibson, T. (2011, July). Turning Sweat Into Watts. *IEEE Spectrum* , pp. 50-55.

[6] Human Dynamo. (n.d.). *Team Dynamo*. Retrieved September 8, 2010, from Human Dynamo: http://www.humandynamo.com/teamdynamo.html

[7] Huessner, K. M. (2008, September 8). *ABC News: Power-aid? Sweat Fuels Electricity at Gym.* Retrieved September 28, 2010, from ReRev.com: http://www.rerev.com/downloads/Articles/Power_Aid.pdf

[8] Rosenow, C. (2011, Feburary 23). Query on Resistance Control Prinicple. (J. D. Cipollina, Interviewer)

[9] Hsu, C.-C. (2000). *Patent No. US006084325A.* Taipei City, Taiwan.

[10] *Energy-Efficient Lighting*. (2010). Retrieved September 28, 2010, from Eartheasy: http://eartheasy.com/live_energyeff_lighting.htm

[11] Cybex International. (2011). *Commerical Arc Trainer 750AT Non Elliptical.* Retrieved November 21, 2011, from Cybex: http://www.cybexintl.com/products/cardio/750A/specs.aspx

[12] Interactive Fitness Holdings LL. (2011). *s3_novo_el_spec.* Retrieved November 22, 2011, from Expresso Interactive Cardio System: http://www.expresso.com/pdf/product_services/s3_novo_el_spec.pdf

[13] Mohan, N. (2003). *Electric Drives: an intergrative approach.* Minneapolis, MN: MNPERE.

[14] Mohan, N., Undeland, T. M., & Robbins, W. P. (2006). *Power Electronics: Converters, Applications, and Design.* Manhattan, NY, United States of America: Wiley.

[15]   Adrio Communications Ltd. (n.d.). *LC Low Pass Filter Circuit*. Retrieved
         November 7, 2011, from Radio-Electronics: http://www.radio-
         electronics.com/info/rf-technology-design/rf-filters/simple-lc-lowpass-filter-
         design.php

[16]   National Semiconductor Corporation. (2008). *LM2678 - SIMPLE SWITCHER
         High Efficiency 5A Step-Down Voltage Regulator*. Retrieved July 28, 2011, from
         National Semiconductor:
         http://www.national.com/pf/LM/LM2678.html#Overview

[17]   Mohan, N. (2009). *First Course On Power Electronics* (2009 ed.). Minneapolis,
         NM, United States of America: MNPERE.

[18]   GoGreenSolar. (n.d.). *Enphase Micro Inverter M190-72-240-S12 MC4*. Retrieved
         May 3, 2012, from Go Green Solar:
         http://www.gogreensolar.com/products/enphase-micro-inverter-m190-72-240-
         s12-mc4